NASA TECHNICAL MEMORANDUM 101591

O-RING SEALING VERIFICATION FOR THE SPACE SHUTTLE REDSIGN SOLID ROCKET MOTOR

Cynthia L. Lach

May 1989

NASA

National Aeronautics and
Space Administration

Langley Research Center
Hampton, Virginia 23665-5225

SUMMARY

As a part of the redesign of the Space Shuttle Solid Rocket Motor, the field and nozzle-to-case joints were redesigned to minimize the dynamic flexure caused by internal motor pressurization during ignition. The O-ring seals and glands for these joints were designed to accommodate both structural deflections and to promote pressure assistance. A test program was conducted to determine if a fluorocarbon elastomeric O-ring (V747-75) could meet this criteria in the redesigned gland. Resiliency tests were used to investigate the O-ring response to gap motion while static seal tests were used to verify design criteria of pressure assistance for sealing. All tests were conducted in face seal fixtures mounted in servo-hydraulic test machines.

The resiliency of the O-ring was found to be extremely sensitive to the effects of temperature. The External Tank/Solid Rocket Booster attach strut loads had a negligible affect on the ability of the O-ring to track the simulated SRB field joint deflection. In the static pressure-assisted seal tests, as long as physical contact was maintained between the O-ring and the gland sealing surface, pressure assistance induced instantaneous sealing.

I. INTRODUCTION

The Space Shuttle Solid Rocket Booster (SRB) is composed of separate steel segments that are twelve-foot diameter cylindrical shells. Before the Challenger accident the adjoining case segments were mechanically fastened using a clevis-tang joint, each joint having two twelve-foot diameter continuous O-ring seals. An investigation by the Presidential Commission on the Challenger accident concluded that "the cause of the Challenger accident was the failure of the pressure seal in the aft field joint of the Solid Rocket Motor."[1] As a result, the Solid Rocket Motor (SRM) was redesigned in accordance to the Prime Equipment Contract End Item Detail Specification.[2] In particular, the primary requirements for the seals in the field and nozzle-to-case joints are that: the seal must operate within a specified temperature range; any structural deflections must be accommodated; the O-ring seal must be capable of tracking twice the maximum expected gap opening without pressure assistance; and the use of pressure assistance for sealing must be possible but not required.

The current investigation was undertaken to examine the resiliency and sealing characteristics of an O-ring (V747-75) in the redesigned gland. Three types of tests were conducted:

1. Resiliency Characterization Tests. - The Commission stated that the elastomeric seals were severely affected by the cold temperatures which rendered the material unresponsive to the joint flexing caused by dynamic conditions at launch. Thus, resiliency characterization tests were conducted to examine the resilient behavior of the O-ring at various gap opening rates for different temperatures.

2. Simulated SRB Field Joint Deflection Tests. - The two main sources of case structural deflections are the dynamic External Tank/SRB attach strut

loads during liftoff and the internal pressurization of the SRB during ignition. The simulated SRB field joint deflection tests were conducted to verify the ability of the O-ring to track the prescribed gap opening without pressure assistance.

3. Static pressure-assisted seal tests - As stated above, one of the requirements for the redesigned gland is to accommodate pressure assistance. However, the minimum residual load that was necessary for pressure-assisted sealing was unknown. Therefore, the static pressure-assisted seal tests were conducted to determine the minimum amount of residual load on the O-ring that would maintain a seal against the specified pressure transient.

II. TEST EQUIPMENT AND PROCEDURES

This investigation was conducted with two different face seal fixtures mounted in servo-hydraulic test machines. (A face seal fixture squeezes the O-ring in an axial direction.) Figures 1 and 2 display both face seal fixtures which had glands that were fabricated according to the cross-sectional dimensions of the redesigned field joint gland. During each test, normal forces on the O-rings were measured with a load cell while a direct current displacement transducer (DCDT) measured the separation distance between the fixture halves. Thermocouples were used to verify that thermal equilibrium of the test fixture halves was maintained at the desired test temperature.

After the O-rings and the fixture glands were lightly greased, the room temperature O-rings were placed in the fixture halves and compressed to an initial gap separating the fixture halves which related to a given percent squeeze (the amount of diametral compression) of the O-ring. The fixture

halves were held at this initial gap for approximately 30 minutes to allow for viscoelastic relaxation. The O-rings relax to relieve the peak load resulting from the initial compression. This relaxation process is possible in the redesigned gland because, when compressed, the O-rings are unconstrained by the sidewalls of the widened gland. The minimum load calculated at the end of the relaxation period is referred to as the "relaxed" load. During this period, the fixture halves were also brought to the desired test temperature. In order to expedite the testing when consecutive tests required new O-rings, they were placed in the fixture halves that were already at the specified test temperature. The room temperature O-rings were immediately compressed to allow for viscoelastic relaxation effects before thermal equilibrium was established between the O-ring and the fixture.

Viscoelastic relaxation effects are shown in figure 3 for some of the test squeezes at 75°F and 120°F. Although the O-rings were statically compressed for approximately 30 minutes, the majority of the relaxation process had occurred in four minutes with the O-ring retaining 72% of its original load while the load was reduced only a further 5% by the end of the relaxation period. Therefore, any changes in the load state cannot be assumed to be caused by thermal effects because most of the viscoelastic relaxation occurs before thermal equilibrium between O-rings and fixture is established.

Resiliency Characterization Test

The resiliency chracteristics of the O-ring were examined in a face seal fixture with a single gland (see figure 1). The test O-ring had a 4.477 inch inner diameter with a nominal cross-sectional diameter of 0.280 inch.

The viscoelastic relaxation period for these tests did not induce the permanent compression set effects that SRB O-rings would experience during

storage after assembly. Compression set is the unrecovered deformation (as a fraction of the original squeeze) that the O-ring experiences after being held in compression for an extended period of time. Although compression set alters the O-ring resiliency, these short term tests revealed the basic effect of temperature on the resiliency of the elastomer.

During the test preparations, the O-ring was compressed so that the initial gap separating the fixture halves was 0.005 inch. The lower fixture half was then cyclically displaced at various frequencies to produce a load versus displacement hysteresis. A delta gap was chosen of sufficient amplitude such that the O-ring would eventually lose contact, or liftoff, from the sealing surface. The cyclical displacements were converted to gap opening rates to determine the response of the O-ring in relation to specified gap opening rates. Figure 4 shows the liftoff gap as the difference between the initial gap separating the fixture halves and the gap opening where the O-ring is no longer in contact with the sealing surface. These tests were conducted at several constant temperatures between 20°F and 120°F. The cyclical displacements followed a prescribed sine wave at frequencies ranging from 0.01 Hz to 50 Hz.

Simulated SRB Field Joint Deflection Tests

These tests used the same face seal fixture (see figure 1) as the resiliency characterization studies but used a servo-hydraulic test machine that provided better displacement response times. The test O-ring had a 4.477 inch inner diameter with a nominal cross-sectional diameter of 0.290 inch. These tests were conducted to examine the effects of simulated SRB field joint deflections on the O-ring tracking ability.

The two main sources of case structural deflections are the dynamic External Tank/SRB attach strut loads during liftoff and the internal pressurization of the SRB during ignition. The first source of structural deflections occurs during the launch sequence when the Shuttle assembly experiences unique dynamic loads caused by the constraint of the SRB during Shuttle main motor ignition. These dynamic loads are stored within the assembled structure and released immediately after liftoff. An analysis of previous flight data conducted by F. Bugg of NASA Marshall Space Flight Center in January, 1987, revealed that the structural vibrations caused by the attach strut loads are three hertz with a maximum deflection of 0.001 inch. The second source of deflection is caused by the internal motor pressurization of the SRB. The 3-sigma case of the head end SRB motor pressure would result in a maximum pressure of 1015 psi. This pressure will cause a maximum gap opening (delta gap) of 0.009 inch between the clevis and the tang of the redesigned field joint.[3] For this investigation, these structural deflections were simulated to verify the resiliency response for twice the maximum expected gap opening (0.018 inch) as shown in figure 5.

During these test preparations, the O-ring was initially compressed to one of the required percent squeezes, 16.2% and 23.3%. These squeezes were provided by reference 4 and incorporated various factors such as stretch, thermal expansion and estimated long term compression set effects.

For these tests, a computer applied a non-linear displacement ramp that simulated twice the maximum gap opening curve, resulting from the 3-sigma pressurization of the SRB field joint. Figure 5 shows the displacment curve and the pressure rise; the gap opening was 0.018 inch within the prescribed 600 msec interval. Preliminary tests indicated that the computer simulation followed the projected non-linear displacement ramp very closely with a

maximum deviation in delta gap opening of 0.001 inch. To determine the effect of the vibrations due to the External Tank/ SRB attach strut loads, the vibrations were added onto the end of the computer-generated displacement ramp. The minimum residual load, calculated for these tests, is the load per unit length acting on the O-ring that occurs during the maximum gap opening. The two temperatures tested, 75°F and 120°F, bracketed the specified operating range of the O-ring seal.[2] Six tests were conducted at each temperature; three for the delta gap only and three with the added vibrations.

Static Pressure-Assisted Seal Tests

The static pressure-assisted seal tests were conducted in the face seal fixture that contained a primary and a secondary O-ring gland as shown in Figure 2. This fixture was specially fabricated to allow for simulation of a leak check procedure to preseat the O-rings and monitor for pressure blow-by (see figure 6). A fixture chamber O-ring ensured proper sealing between fixture halves and prevented any atmospheric leakage during testing. The primary and secondary O-rings had inner diameters of 6.052 inch and 8.022 inch, respectively. Both test O-rings had nominal cross-sectional diameters of 0.290 inch.

Preliminary testing determined the initial percent squeezes that would best simulate the actual resiliency behavior of the O-ring after long term compression set. This testing involved applying various amounts of static compression on the primary O-ring, holding the the displacement constant for the relaxation period, and then calculating the load per unit length which is referred to as the relaxed load. To avoid measuring frictional loads from the chamber O-ring, it was omitted during this preliminary examination. Results from this testing show that the relaxed load was essentially zero for the

initial percent squeezes of 1.7% and 3.5% while a 5.2% squeeze corresponded to a relaxed load of 3.12 lbf/in. The worst possible case for sealing occurs when the O-ring is essentially unloaded (i.e. zero load) after long term compression set. Therefore, since this investigation sought to examine the worst possible sealing conditions, initial percent squeezes of 5.2%, 3.5%, 1.7% and 0.0%. Though the percent squeeze of 0.0% did not correspond to a compressed state, it was tested to observe the dynamic sealing characteristics of an O-ring through pressure assistance.

The static seal tests consisted of initially compressing the primary and secondary O-rings to various initial percent squeezes (5.2%, 3.5%, 1.7% and 0.0%) as determined from preliminary testing. Then the leak check procedure was conducted with the gaps between the fixture halves held constant. This procedure involved first applying a 250 psi pressure in the secondary chamber between the two test O-rings while the pressure in the primary chamber (see figure 6) was monitored to detect leaks. The pressure in the secondary chamber was vented and then a 250 psi pressure was applied to the primary chamber while the secondary chamber was monitored for leaks. After the leak check procedure was completed, the pressure-assisted seal tests were conducted by applying a 1015 psi pressure transient in the primary chamber for two minutes which is the flight duration of the SRBs prior to separation from the Shuttle system. This 1015 psi pressure transient is the simulation of the 3-sigma case of the head end SRB motor pressure. For the prescribed two minute interval, pressure in the secondary chamber was monitored to detect pressure leaks (blow-by). Pressure blow-by during leak checks and seal tests indicate improper or "unsuccessful" sealing. The static seal studies consisted of three tests at each initial percent squeeze and were conducted at the minimum operating temperature of the O-ring, 75°F.

III. DISCUSSION OF RESULTS

Resiliency Characterization Tests

Figures 7 through 10 show that the resiliency of the fluorocarbon elastomeric O-ring (V747-75) was adversely affected by cold temperatures. As the glass transition temperature of this O-ring was approached (7°F to 12°F from reference 5), the O-ring became unresponsive to changes in the gap opening, regardless of the gap opening rate (frequency). In general, the ability of the O-ring to track the gap decreased as the gap opening rate increased. The results from figures 7 through 10 are tabulated in Table I.

As a side note, this investigation also confirms the Presidential Commission findings of the Challenger accident.[1] Various structural analyses of the original SRB field joint showed that the average gap or relative displacement between tang and inner clevis arm was ranged from 0.018 inch to 0.037 inch.[1,6] For the original SRB field joint, the estimated maximum gap opening rate of 0.23 inch/sec was calculated from data provided by reference 7. At the coldest test temperature of 20°F which is closest to the minimum launch temperature of the Challenger SRB joint (23°F), figure 9 shows that the O-ring cannot track any gap opening at any rate. For the redesigned SRB field joint, this investigation has determined that the minimum operating temperature of the O-ring begins at 70°F where the O-ring easily can track the maximum displacement requirement of 0.018 inch at the required gap opening rate of 0.19 inch/sec (see figure 10).

Simulated SRB Field Joint Deflection Tests

Figures 11 through 14 show the results of the tests simulating structural deflections of the SRB field joint. For all initial percent squeezes and temperatures tested, the O-ring tracked the required gap opening of 0.018 inch

without pressure assistance during the critical 600 msec interval. The load curves in figures 11 and 13 are similar to the displacement curve in figure 5 which indicates that the O-ring maintained contact with the sealing surface throughout the non-linear gap opening ramp.

The resulting relaxed loads and minimum residual loads for the simulated SRB field joint deflection tests conducted for 16.2% and 23.3% squeezes at 75°F and 120°F are shown in figures 12 and 14. These tests were conducted for the delta gap only and the delta gap with the added vibrations. For the delta gap only tests, the 16.2% and the 23.3% squeezes produced relaxed loads of -24.2 lbf/in and -44.2 lbf/in at 120°F as compared to -21.4 lbf/in and -40.1 lbf/in, respectively, at 75°F. The corresponding residual loads for the 16.2% and the 23.3% squeezes were -7.5 lbf/in and -18.2 lbf/in at 120°F and -4.0 lbf/in and -13.1 lbf/in at 75°F, respectively. The higher residual loads for both squeezes at 120°F , in comparison to those at 75°F, are most probably caused by thermal expansion.

The minimum residual loads obtained in these short term tests were higher than the 3.12 lbf/in value determined in long term tests conducted by R. G. Clinton of NASA Marshall Space Flight Center in January, 1988. The long term test value was obtained for tests conducted at room temperature (75°F) with the same O-ring material, gland dimensions, and prescribed delta gap opening as in the current short term tests.

In an effort to better simulate the residual loads resulting from long term compression, the squeezes of 14.7% and 15.0% were examined. The squeezes resulted in minimum residual loads of 2.8 lbf/in and 3.0 lbf/in, respectively, after the delta gap opening as compared to the long term data of 3.12 lbf/in. However, larger scatter was observed during testing for the 14.7% squeeze.

The effect of added vibrations on the ability of the O-ring to track the gap opening was evaluated for the initial squeezes of 14.7%, 16.2% and 23.3% with the 14.7% squeeze tested only at 75°F. Comparing the percent loss between the original relaxed load state to the final residual load state after the gap opening, it was observed that all of the tests conducted with the added vibrations had higher load losses than the tests conducted with the delta gap only with the exception of the 23.3% squeeze at 75°F. However, the magnitude of the additional load loss was small, and therefore, the vibrations never caused the O-ring to lose contact with the sealing surface.

Thus, the design requirements of maintaining contact through any structural deflection and tracking twice the maximum expected gap opening without pressure assistance was verified for the minimum SRB O-ring seal operating temperature of 75°F. The additional cyclic gap opening of ±0.0005 inch at three hertz due to the External Tank/SRB strut loads had a negligible effect on the ability of the O-ring to track the gap opening of 0.018 inch. It was determined that a 15.0% squeeze best simulated the long term compression set effects on the resilient behavior of the O-ring.

Static Pressure-Assisted Seal Tests

Figures 15 through 23 show that for the percent squeezes of 1.7%, 3.5%, and 5.2%, the leak checks were successful and the O-rings instantly sealed upon application of the 1015 psi pressure (3-sigma pressure transient). For example, figure 23 displays typical chamber pressure and displacement curves for a successful seal for the 1.7% squeeze case. In figures 23a, no pressure blow-by was observed in the primary chamber due to the 250 psi pressure applied to the secondary chamber. Figure 23c indicates that a very slight pressure rise in the secondary chamber was caused by the 250 psi applied to

-11-

the primary O-ring. However, this slight pressure increase can be attributed to the translation of the primary O-ring toward the secondary O-ring which reduces the secondary chamber volume, and thus, increased the pressure in that chamber. Finally, instantaneous sealing upon the 1015 psi pressure application is verified in figure 23e which shows no pressure blow-by. The test data for all the squeezes tested are presented in Table IV.

For the zero percent squeeze, the three tests conducted resulted in one successful seal and two delayed seals. The successful seal is shown in figure 24 and two delayed seals are shown in figures 25 and 26. Figure 25 displays a typical delayed seal where slight pressure blow-bys occurred prior to sealing for each pressure application. After each 250 psi pressure applied during the leak check procedure, slight pressure blow-bys were observed (see figures 25a and 25c) in the primary and secondary chamber, respectively. However, the 1015 psi pressure transient caused a noticeable pressure increase as seen in figure 25e. The delayed seal in this case can be attributed to the tolerance range in gland depth and O-ring cross-sectional diameter. The deviations in these two dimensions are combined such that the actual initial gap separating the fixture halves could vary around the O-ring circumferences. Therefore, the O-rings may not have had complete contact with the sealing surface, allowing slight pressure blow-bys to occur.

Therefore, a specific amount of residual load is not necessary for successful sealing. This investigation showed that if the O-ring merely remained in contact with the sealing surface (essentially zero load), pressure assistance provided by the 1015 psi pressure transient would induce instantaneous sealing.

IV. CONCLUSIONS

Static and dynamic tests were conducted to assess O-ring sealing response for the revised SRB seal requirements. In the resiliency characterization tests, the resilient behavior of the fluorocarbon elastomeric O-ring (V747-75) was examined by studying the effects of temperature and gap opening rates. Additional resiliency tests were used to investigate the O-ring response to simulated SRB field joint deflections while static pressure-assisted seal tests were used to verify the design criteria of pressure-assisted sealing. Resiliency was gauged by load and displacement measurements. During static seal tests, chamber pressures were monitored to confirm successful sealing. All tests were conducted in face seal fixtures that were mounted in servo-hydraulic test machines.

The resiliency of the O-ring was adversely affected by cold temperatures. At 20°F, the O-ring was unresponsive to any gap opening rate, resulting in immediate separation (liftoff) from the sealing surface. The minimum operating temperature was determined to be 70°F, above which the O-ring could easily track the required delta gap of 0.018 inch at the gap opening rate of 0.19 inch/sec.

For the simulated SRB field joint deflection tests conducted at 75°F and 120°F, the O-ring maintained contact throughout the delta gap opening of 0.018 inch. The External Tank/SRB attach strut load vibrations had a negligible effect on the ability of the O-ring to track the gap opening. These tests also determined that a 15.0% squeeze best simulated the effects of long term material compression set on the resilient behavior of the O-ring.

The design requirement for pressure-assisted sealing was verified for the redesigned gland. As long as physical contact was maintained between the O-ring and the gland sealing surface, the simulated 3-sigma case of the SRB motor pressure transient induced instantaneous sealing.

REFERENCES

[1] "Report of the Presidential Committee on the Space Shuttle Accident," Washington, D. C., June 1986.

[2] "Prime Equipment Contract End Item Detail Specification," Morton Thiokol, Inc., Wasatch Operations, Specification Number CPW-3600A, August 1987.

[3] "RSRM CDR Summary Report: Seal Design," Morton Thiokol, Inc., Wasatch Operations, Document Number TWR-17082, December 1987.

[4] St. Aubin, B. K., "O-ring Squeeze Calculations for the RSRM," Morton Thiokol, Inc., Wasatch Operations, Document Number TWR-16682 Rev. A, September 1987.

[5] Morris, D. E., "Thermal Characterization of SRM Joint Seal Materials," NASA Test Report Number EH33/86-1, NASA Marshall Space Flight Center, December 1986.

[6] Greene, W. H., Knight, N. F., and Stockwell, A. E., "Structural Behavior of the Space Shuttle SRM Tang-Clevis Joint," NASA TM-89018, September 1986.

[7] Turner, J. E., "Evaluation of the Sealing Capabilities of Several O-ring Materials in Subscale, Cold-Gas, Pressurization Tests," NASA TM-86586, January 1987.

THIS PAGE INTENTIONALLY LEFT BLANK

Table I. Resiliency characterization test (full recovery is 0.063 inch).

Vibration, Hz	Gap opening rate, in/sec	Delta gap opening at liftoff, in						
		20°F	30°F	40°F	50°F	60°F	70°F	120°F
0.01	0.002	0.002	0.011	0.025	0.034	0.041	0.042	0.052
0.05	0.010	0.002	0.006	0.019	0.028	0.036	0.039	0.049
0.10	0.019	0.001	0.004	0.014	0.025	0.034	0.038	0.047
0.20	0.038	0.001	0.002	0.010	0.020	0.029	0.035	0.045
0.30	0.057	0.000	0.002	0.008	0.018	0.027	0.033	0.043
0.50	0.095	0.000	0.001	0.005	0.014	0.024	0.029	0.042
1.00	0.190	0.000	0.001	0.003	0.009	0.018	0.024	0.040
2.00	0.380	0.000	0.001	0.002	0.005	0.012	0.021	0.036
5.00	0.950	0.000	0.000	0.001	0.002	0.006	0.012	0.032
10.00	1.900	0.000	0.000	0.001	0.001	0.003	0.006	0.028
14.50	2.755	0.000	0.000	0.000	0.001	0.002	0.004	0.023
20.00	3.800	0.000	0.000	0.000	0.001	0.002	0.003	0.021
29.00	5.510	0.000	0.000	0.000	0.000	0.001	0.002	0.018
50.00	9.500	0.000	0.000	0.000	0.000	0.001	0.001	0.012

Table II. Static pressure-assisted seal test.

Percent squeeze	Peak pressure, psi primary (secondary)		
	Leakcheck procedures		Seal test
	250 psi applied to secondary	250 psi applied to primary	1015 psi applied to primary
5.2%	2 (259) 1 (255) 1 (256)	239 (4) 240 (4) 242 (4)	1051 (2) 1038 (1) 1042 (2)
3.5%	1 (254) 1 (255) 2 (256)	239 (4) 241 (4) 242 (4)	1037 (2) 1038 (2) 1042 (3)
1.7%	1 (254) 2 (255) 2 (255)	240 (3) 242 (3) 242 (2)	1036 (2) 1042 (2) 1040 (0)
0%	3 (254) 3 (254) DS 2 (256)	241 (1) 242 (5) DS 243 (0)	1040 (5) DS 1040 (15) DS

(Successful seal unless otherwise indicated)
DS - delayed seal
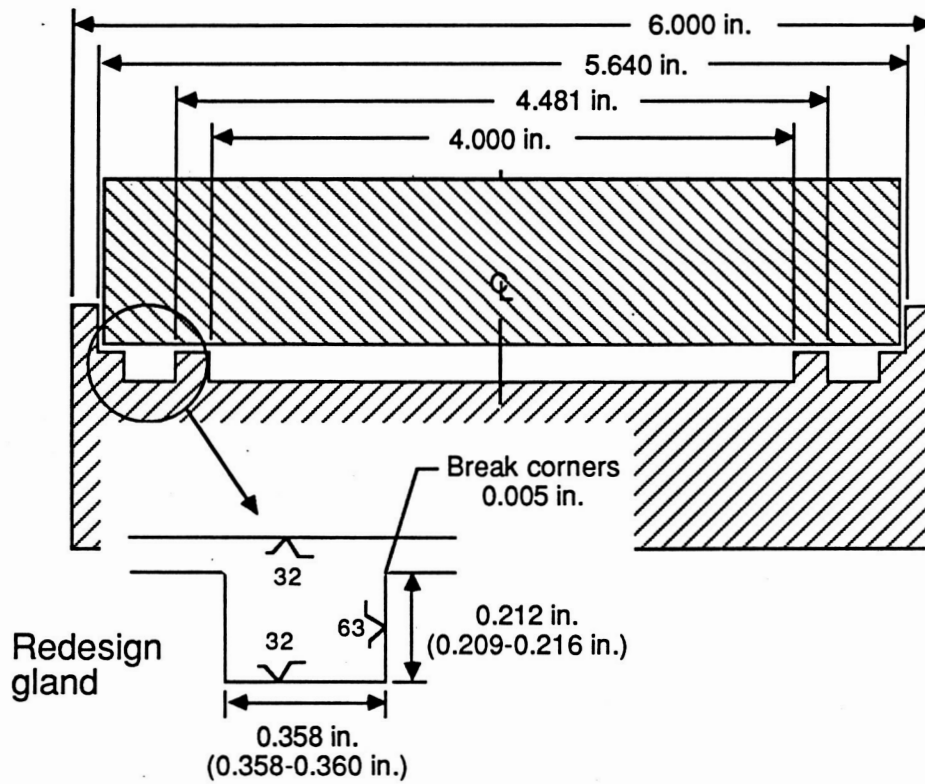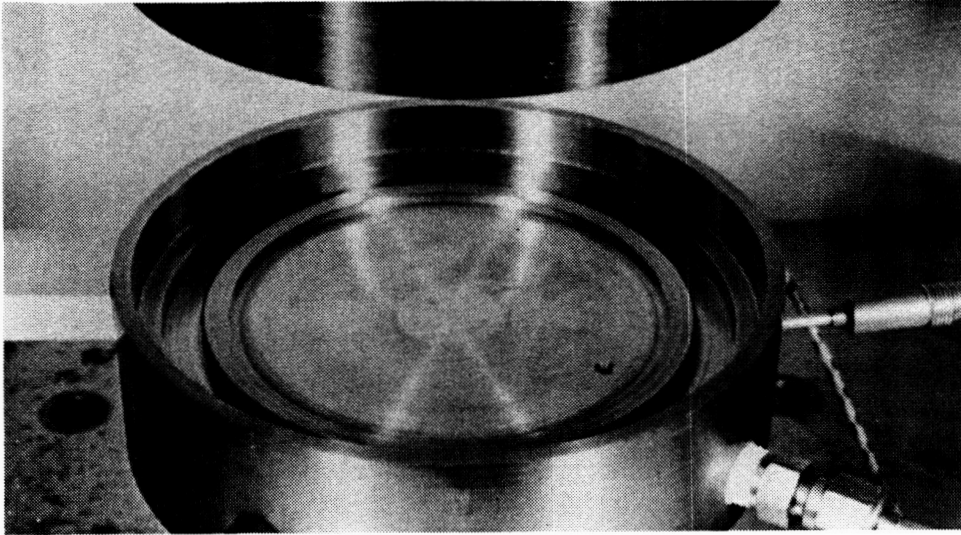
Figure 1. Resiliency face seal fixture.

19
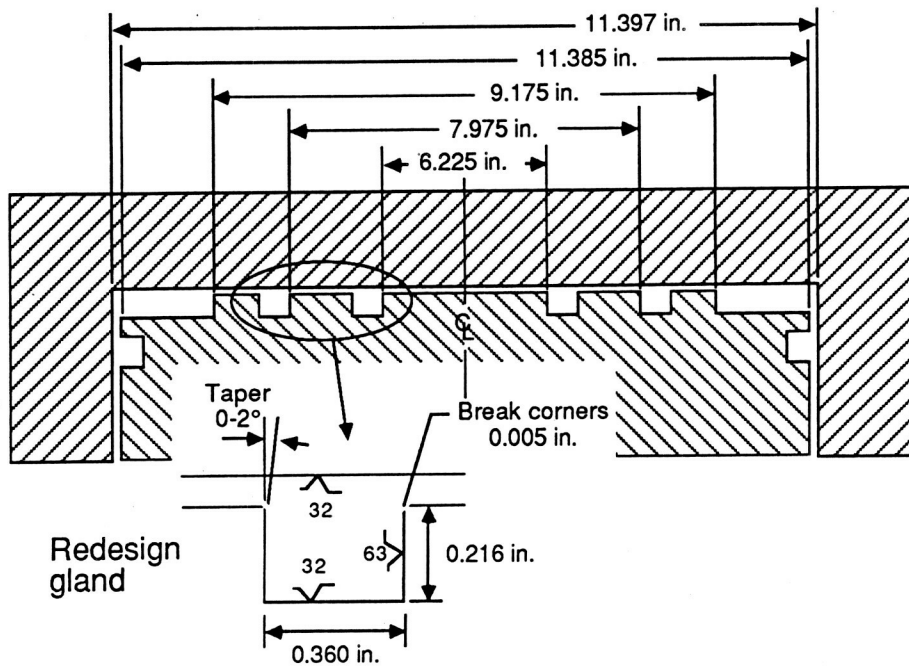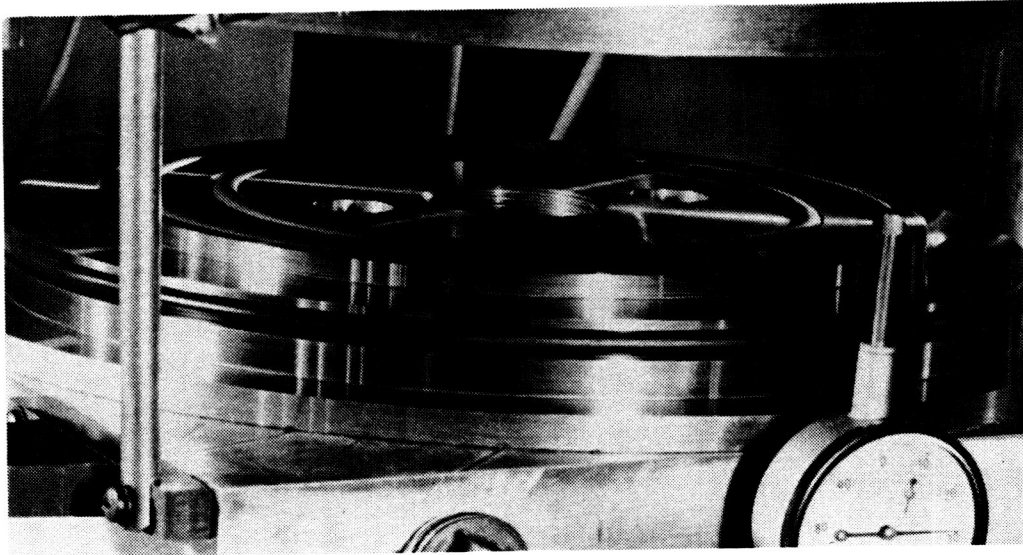
Figure 2. Static face seal fixture.
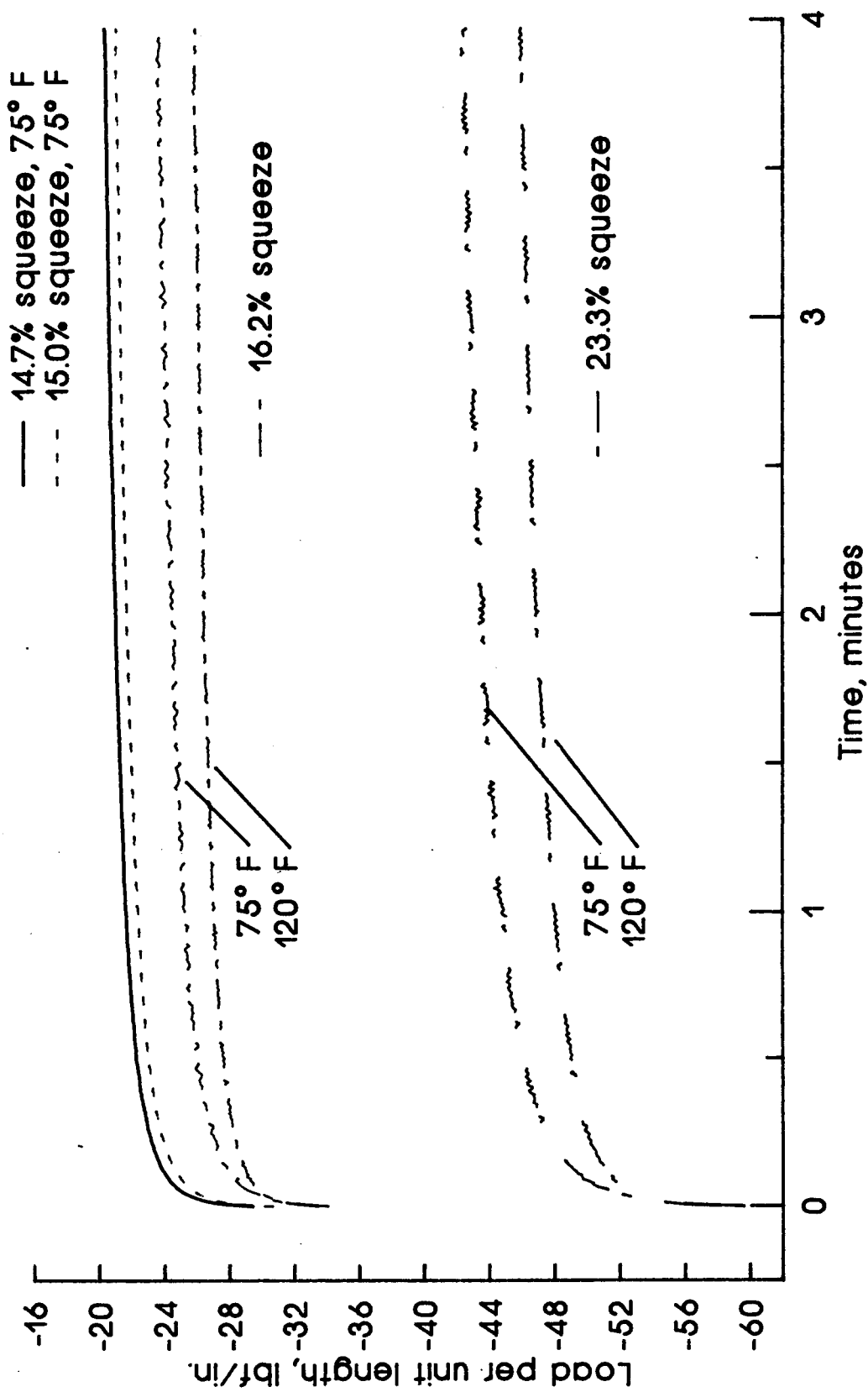
Figure 3. Initial critical interval of the viscoelastic load relaxation period.

21
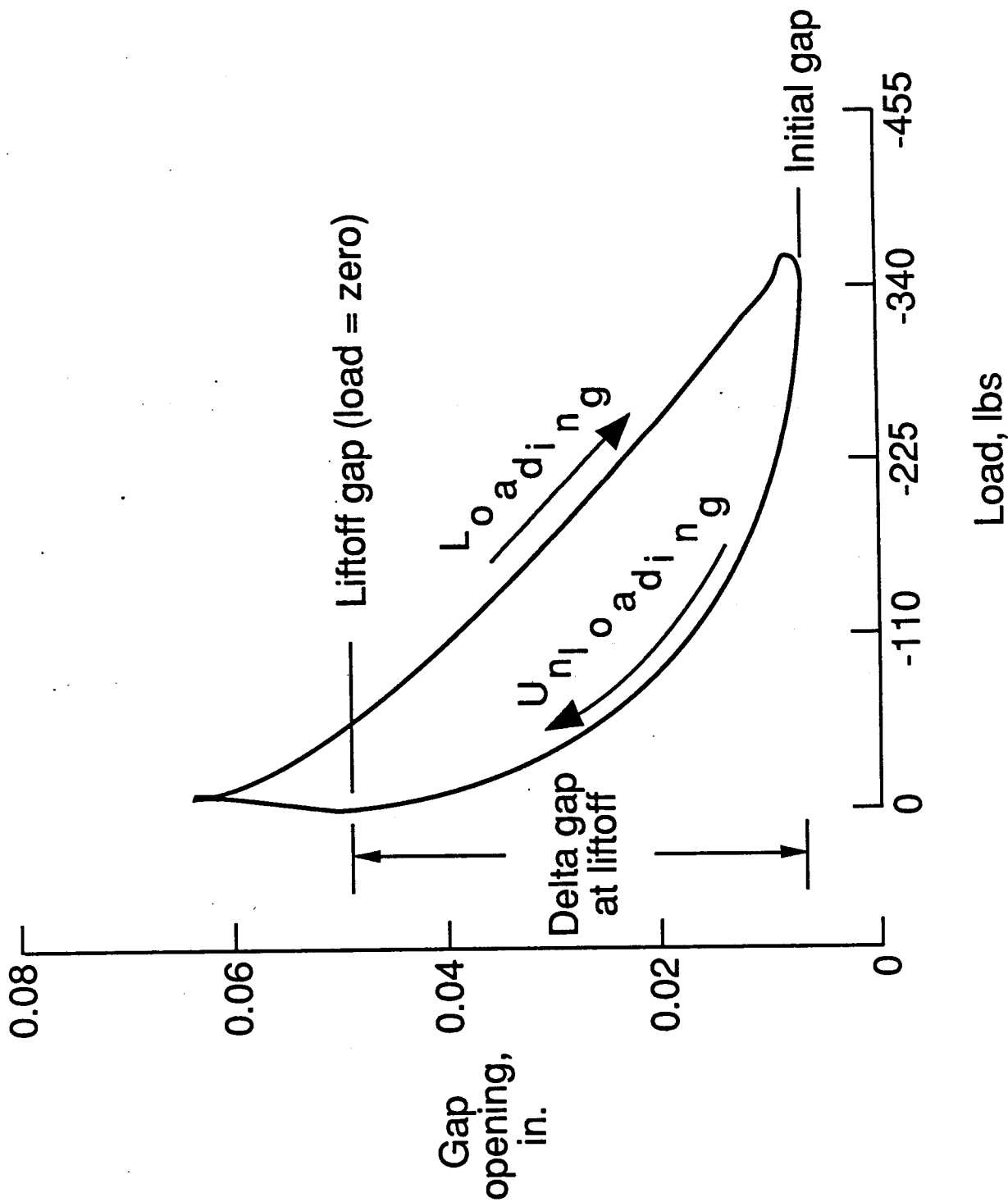
Figure 4. Gap opening versus load in the resiliency test.
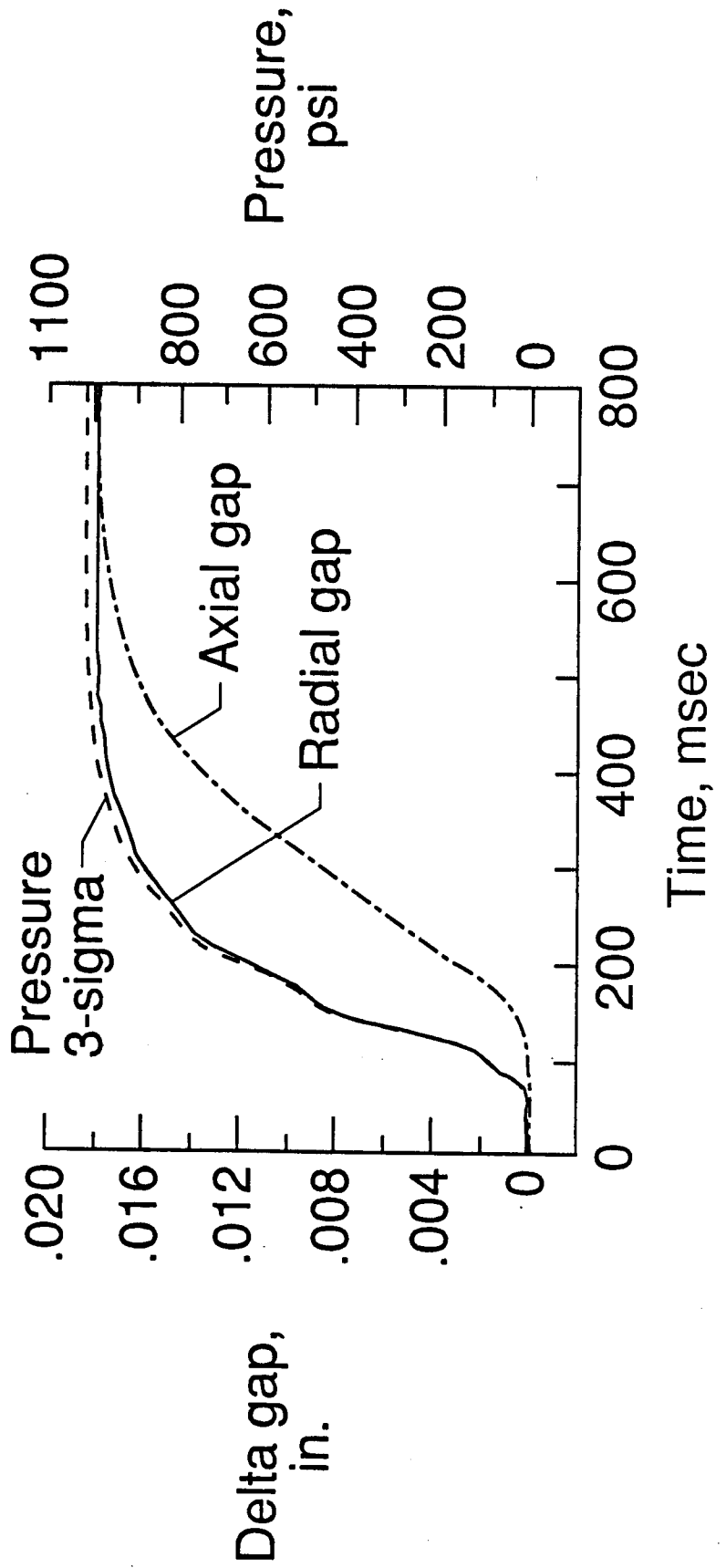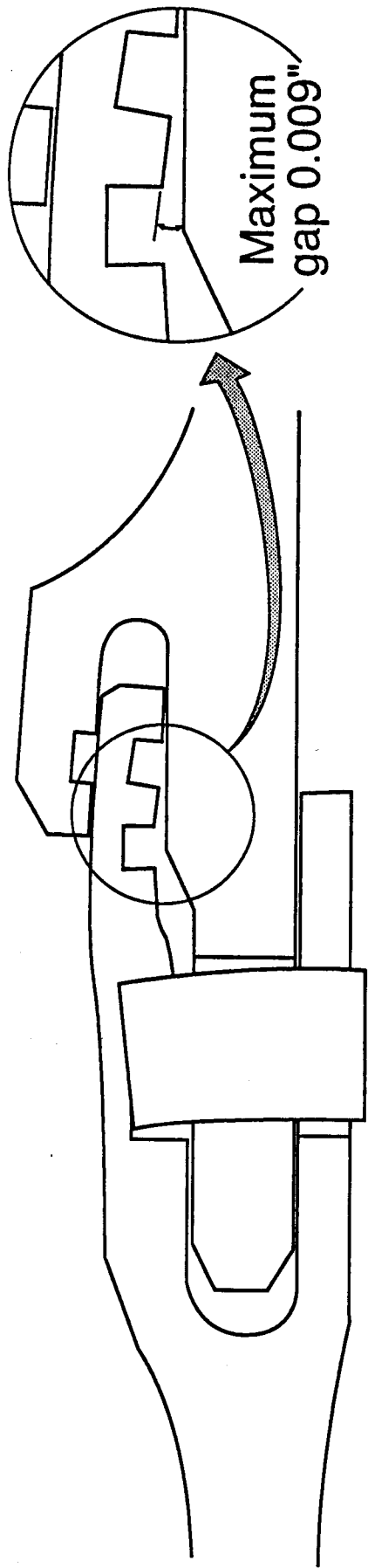
Figure 5. Delta gap history for the SRB field joint deflection test.
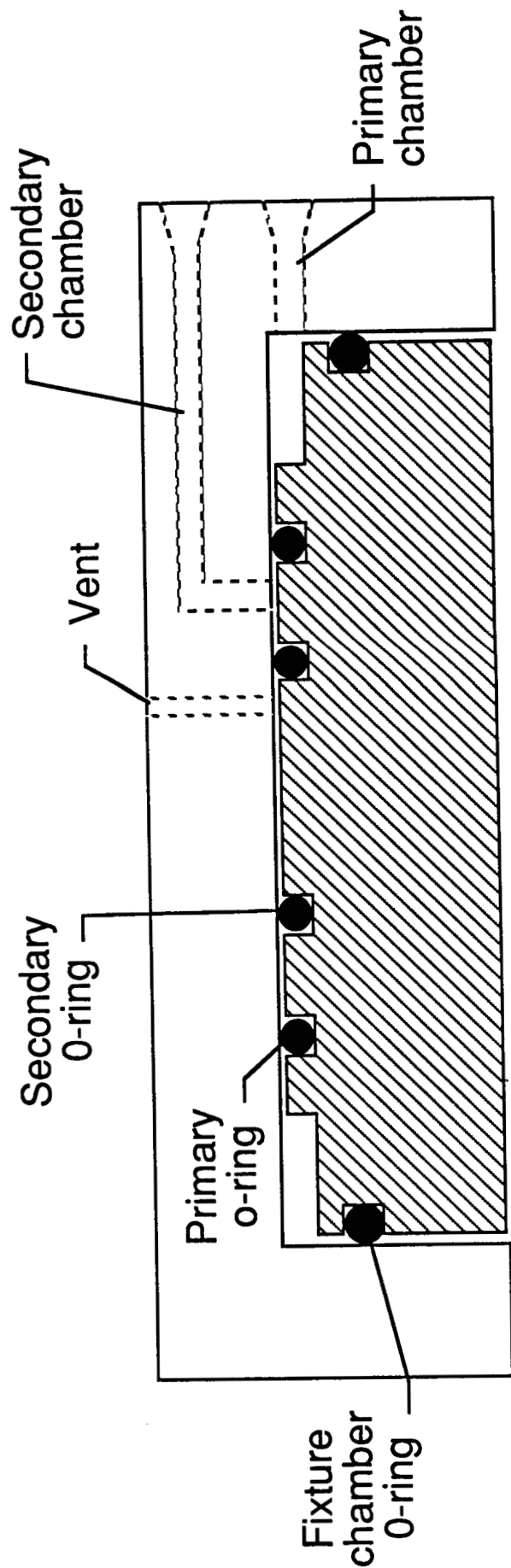
Figure 6. Static face seal fixture schematic.

24
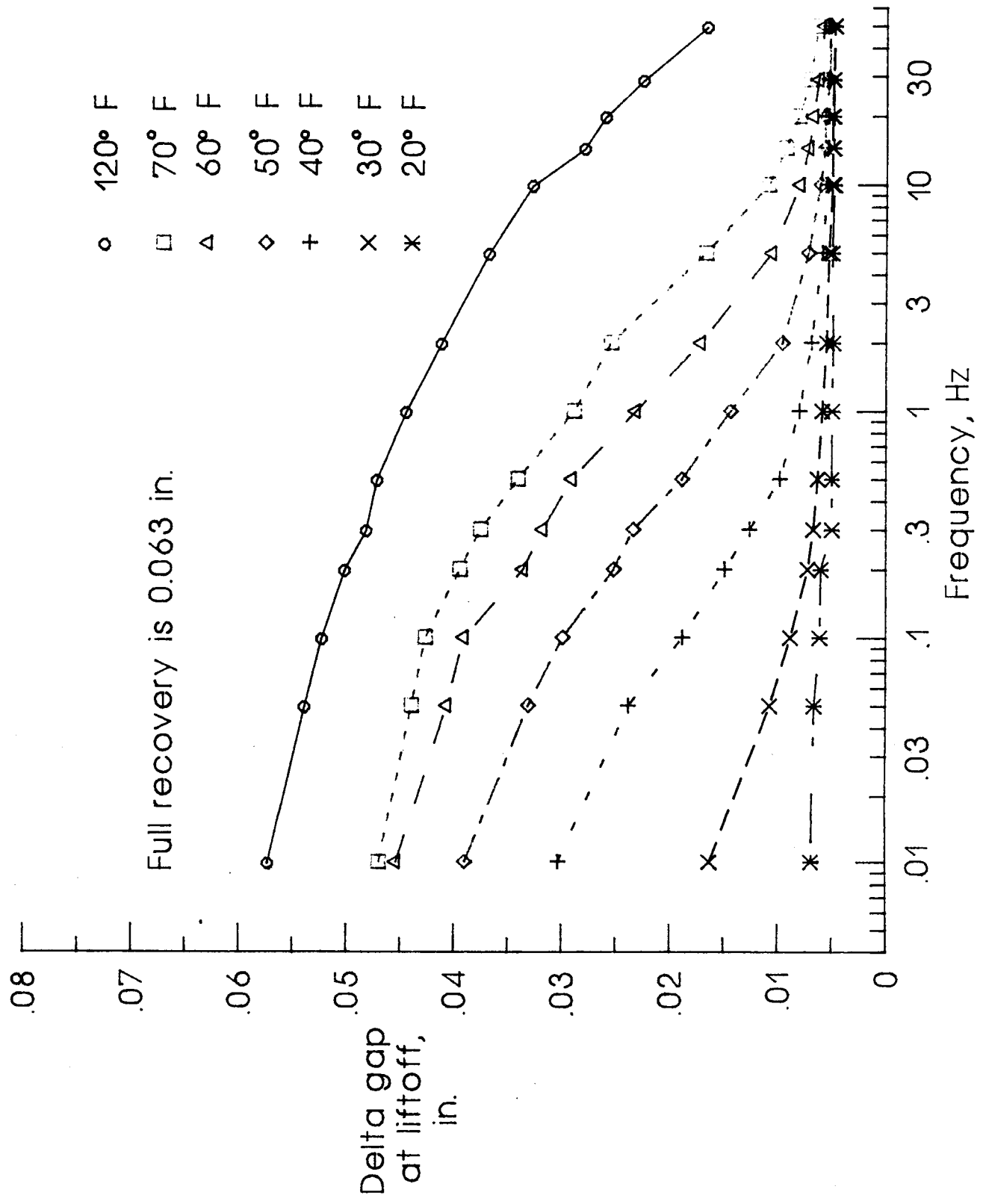
Figure 7. Temperature and frequency effects on delta gap at liftoff.

RES*1-D.TM
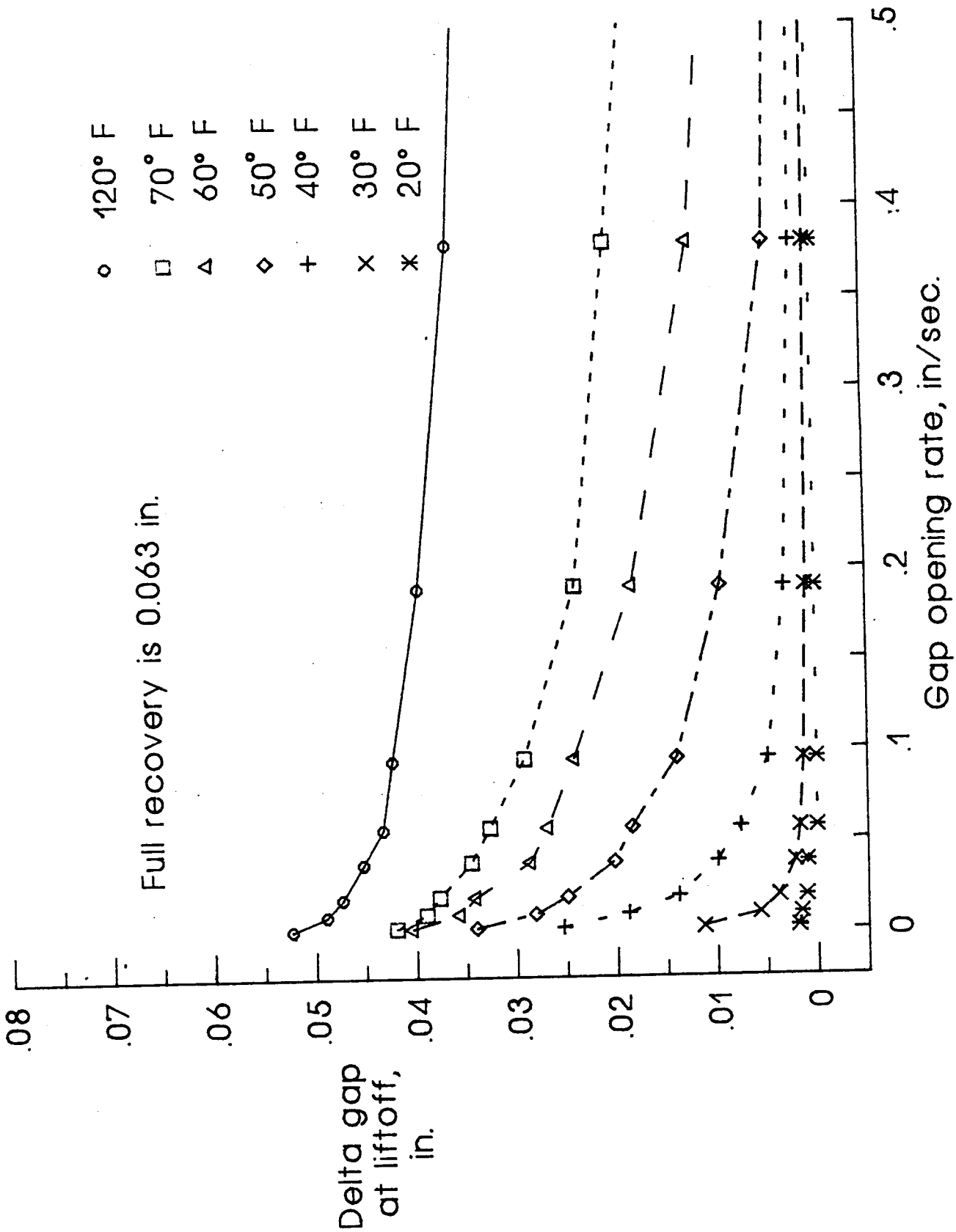
Figure 8. Temperature and gap opening rate effects on delta gap at liftoff.

RES*4-C.TM

26
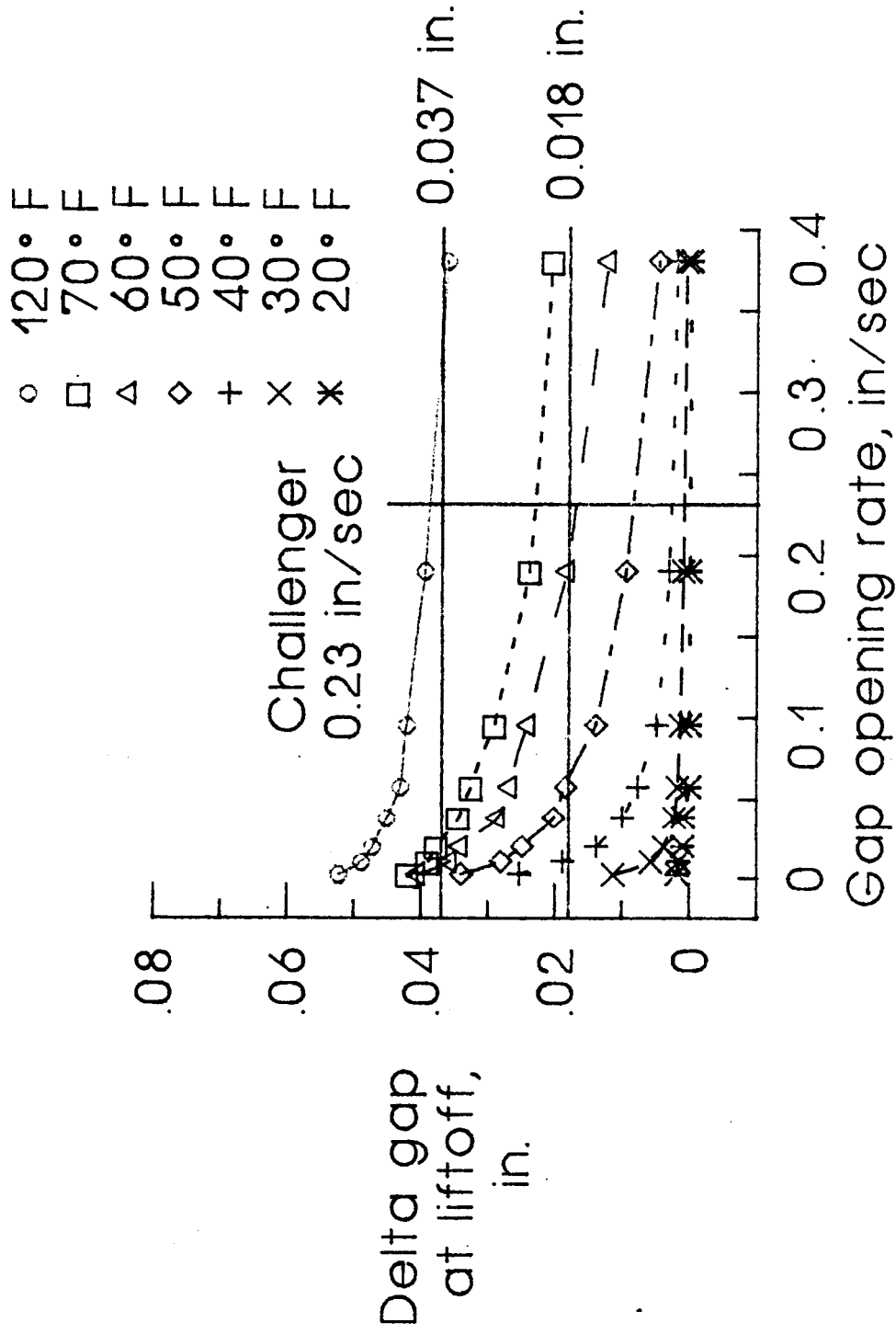
Figure 9. Resiliency response compared to the Challengers' joint deflection and gap opening rate.

27

Figure 10. Resilency response compared to the Redesign joint deflection and gap opening rate.

28

RES✱4-C3.TMM
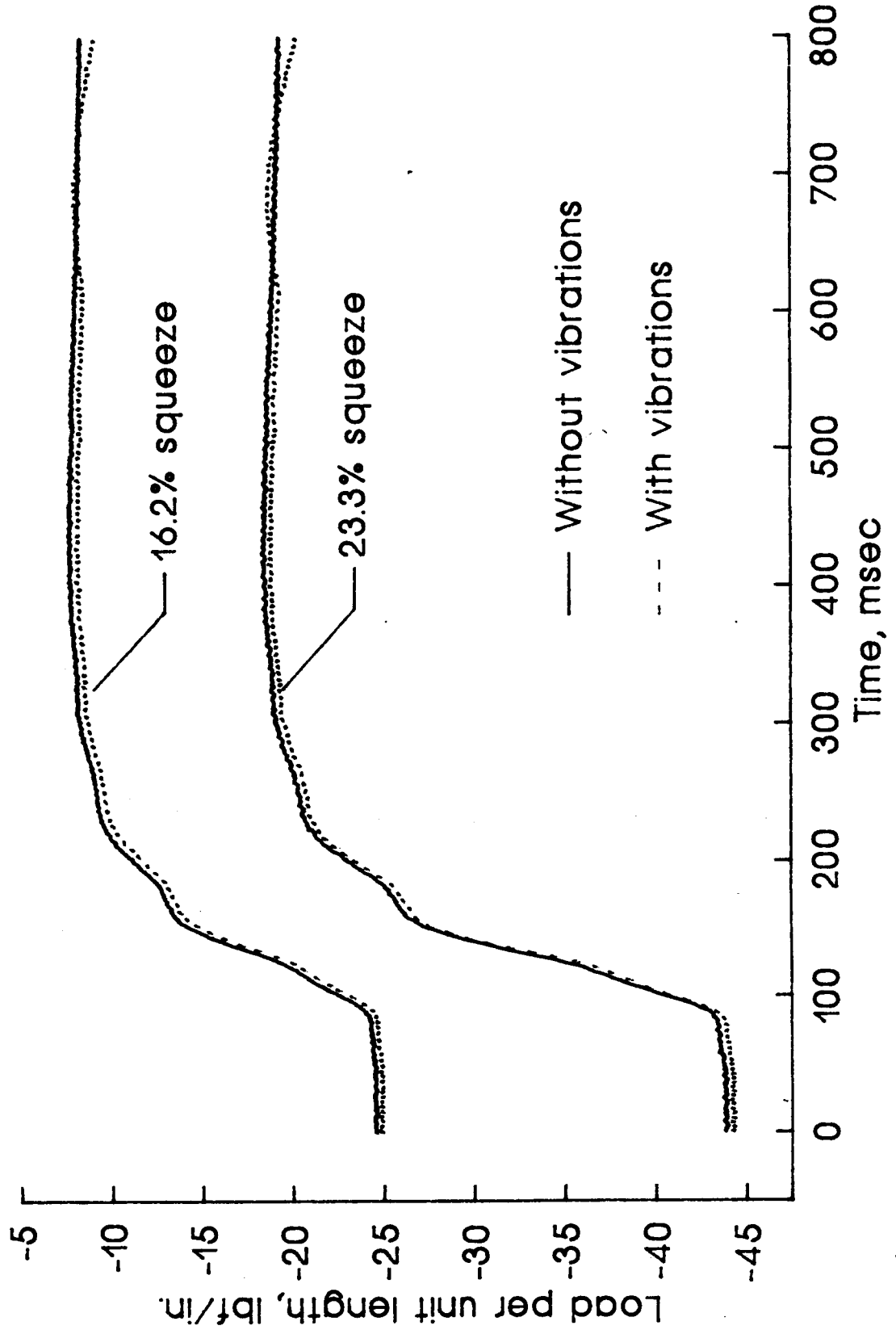
Figure 11. O-ring resiliency (load tracking curve) for the simulated SRB field joint deflections at 120 degrees F.

R-rmp120.gtc
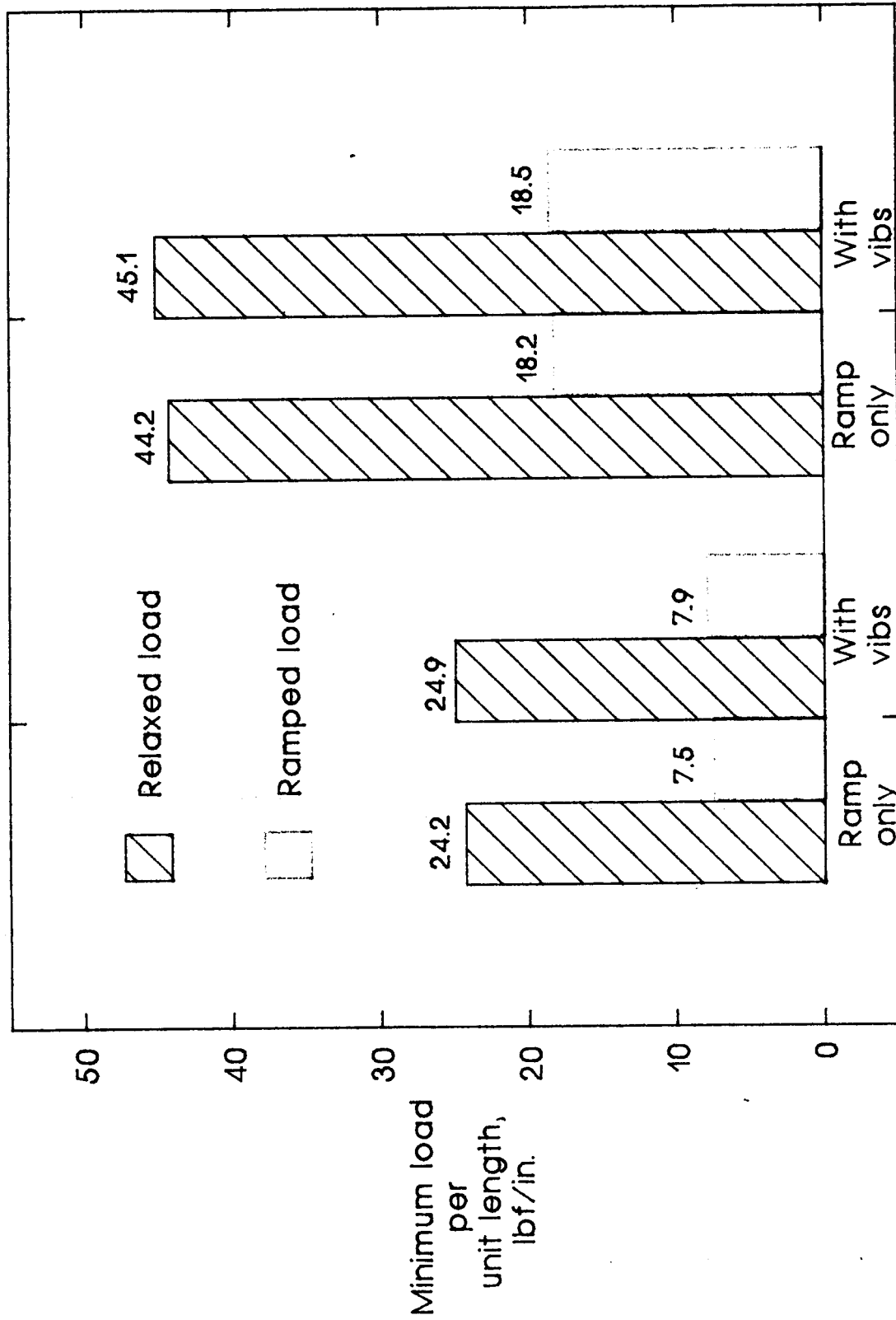
Figure 12. Relaxed and residual loads for the simulated SRB field joint deflection tests at 120 degrees F.

BAR+4.TM
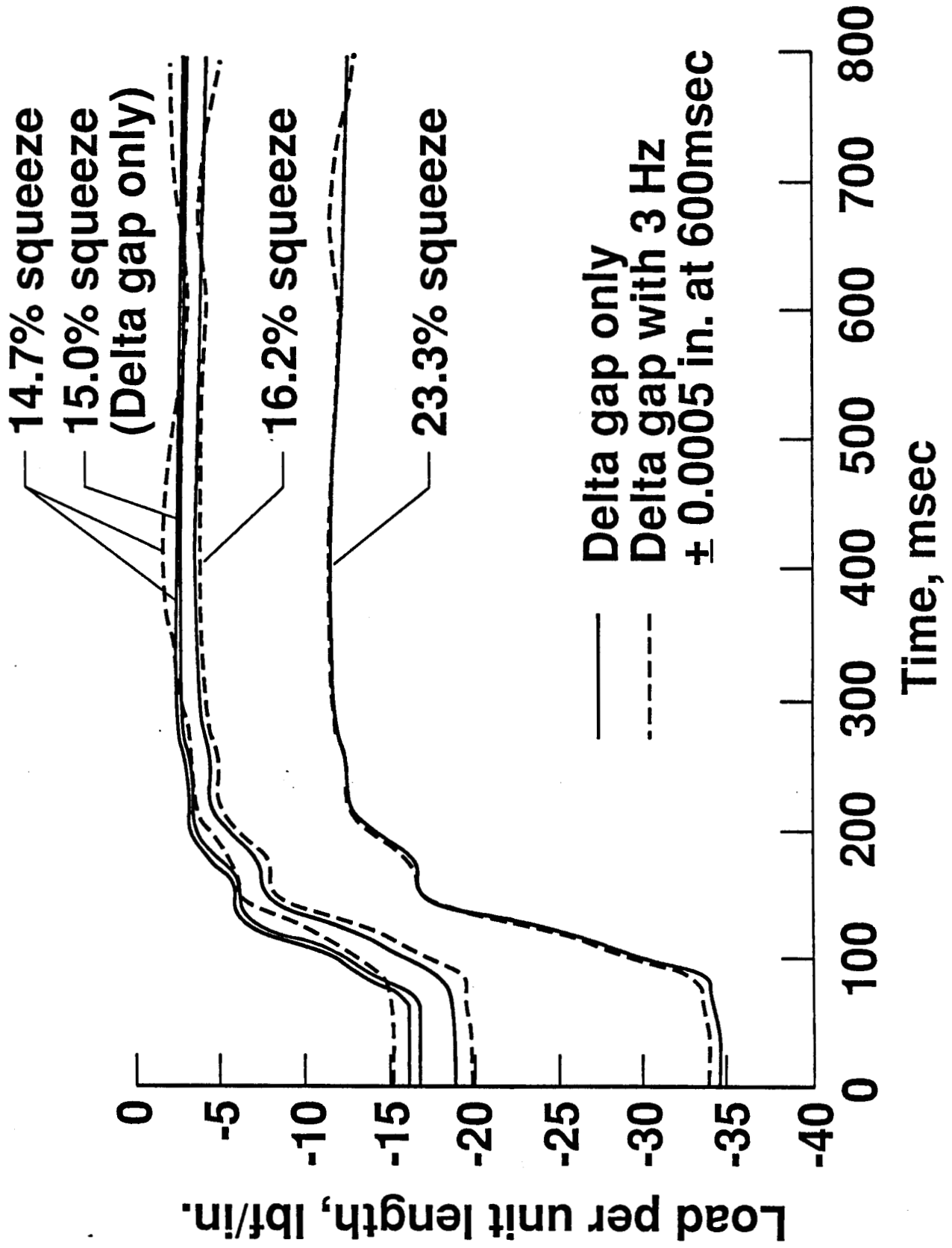
Figure 13. O-ring resiliency (load tracking curve) for the simulated SRB field joint deflections at 75 degrees F.
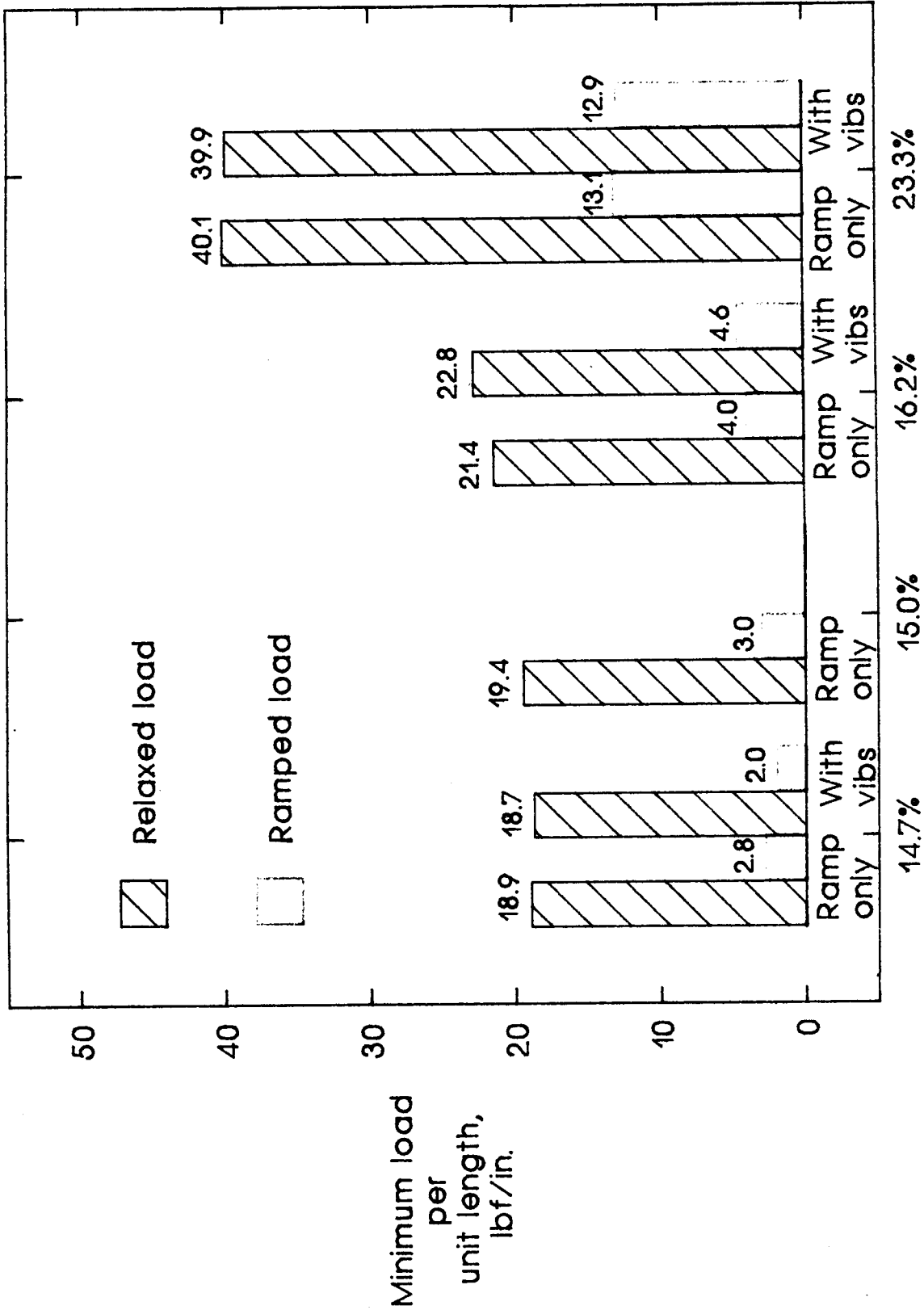
Figure 14. Relaxed and residual load values for the simulated SRB field joint deflections at 75 degrees F.

BAR*3.TM
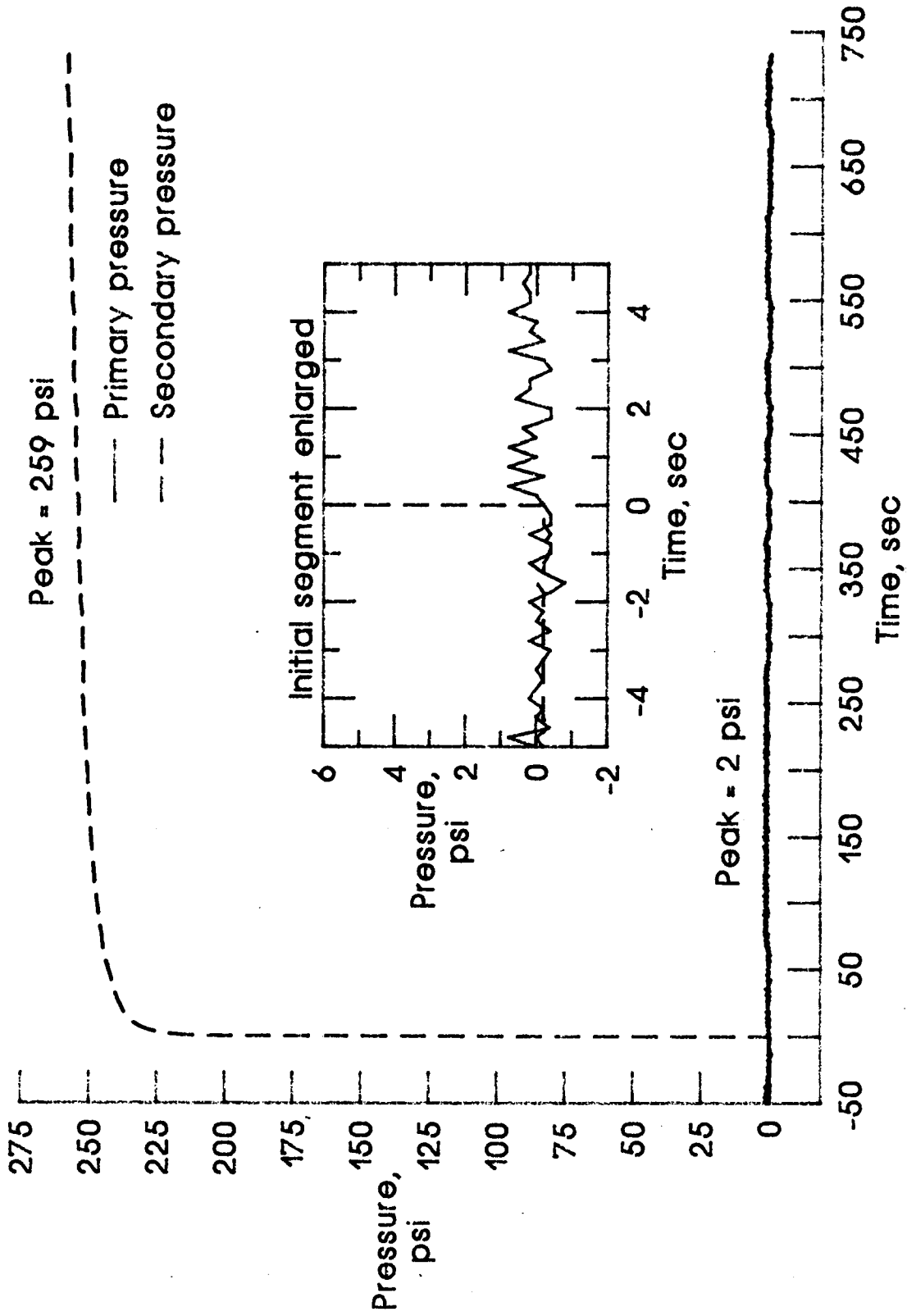
Figure 15a. 250 psi applied to the secondary chamber.

Figure 15. Pressure and displacement curves for the leak check and seal test for a successful seal at an initial squeeze of 5.2%.

MIN1-4,P/P

33
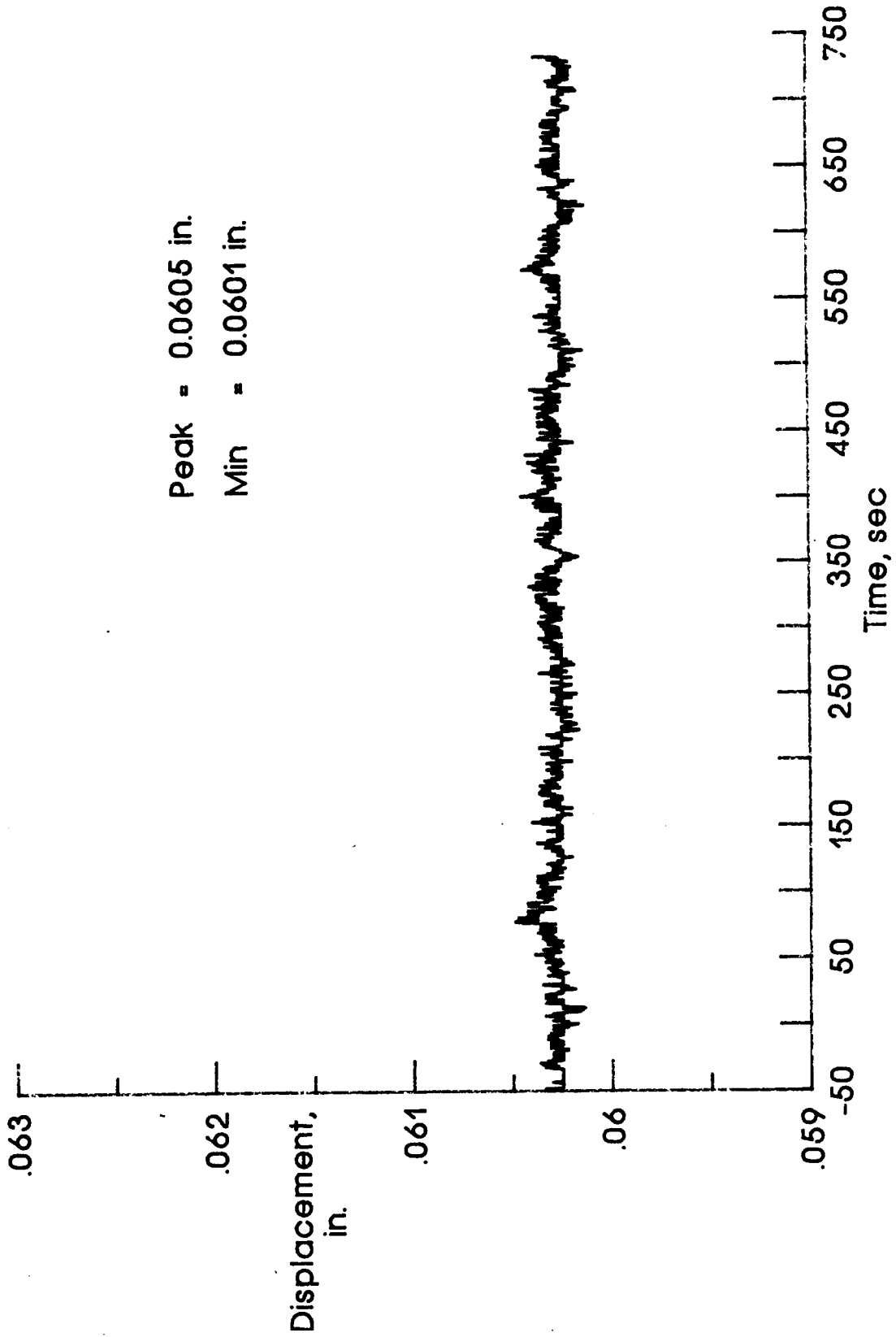
Figure 15b.. 250 psi applied to the secondary chamber.

MIN1-4, Disp

34
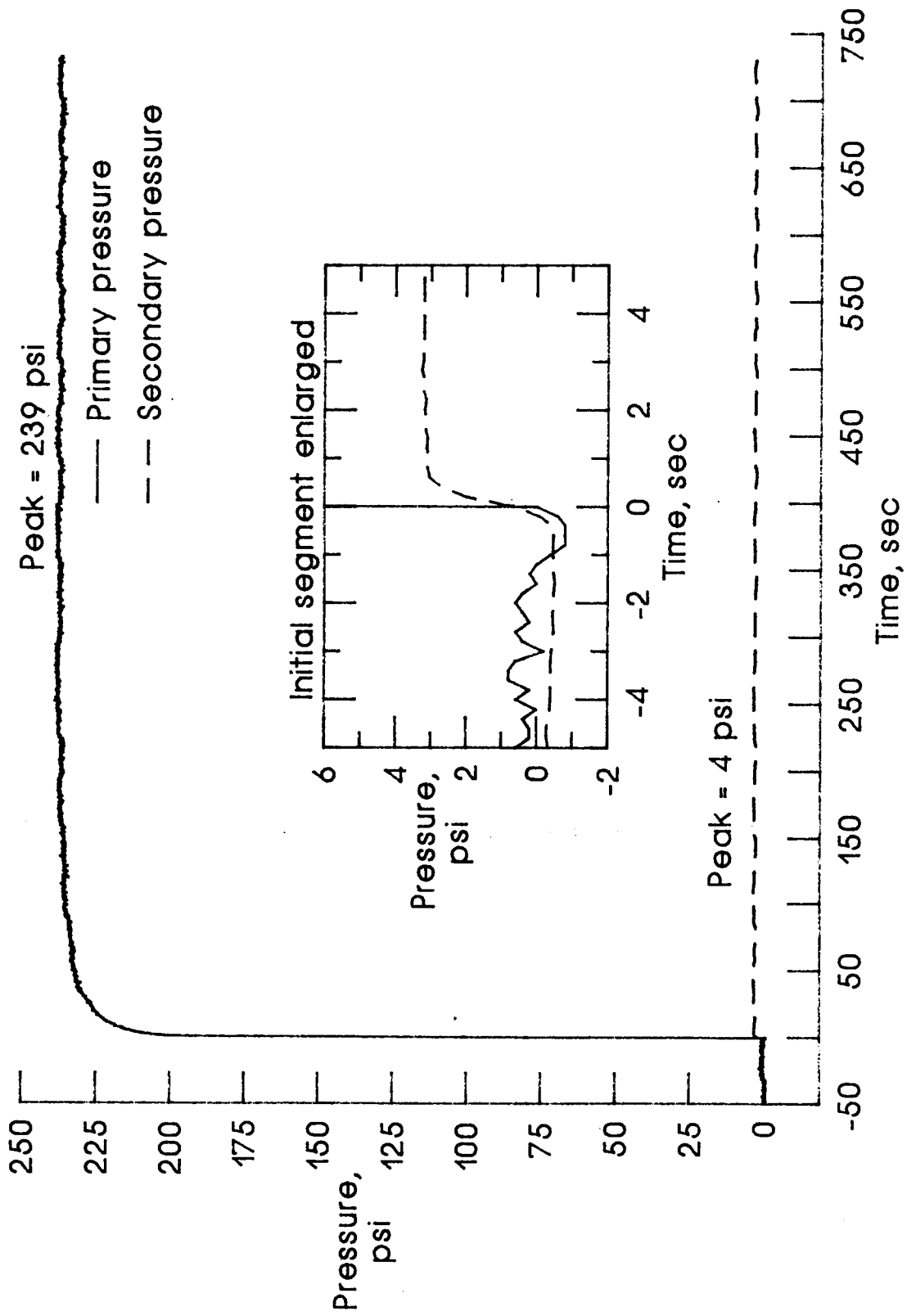
Figure 15c. 250 psi applied to the primary chamber.

MIN1-5,P/P

35

Peak = 0.0604 in.

Min = 0.0600 in.
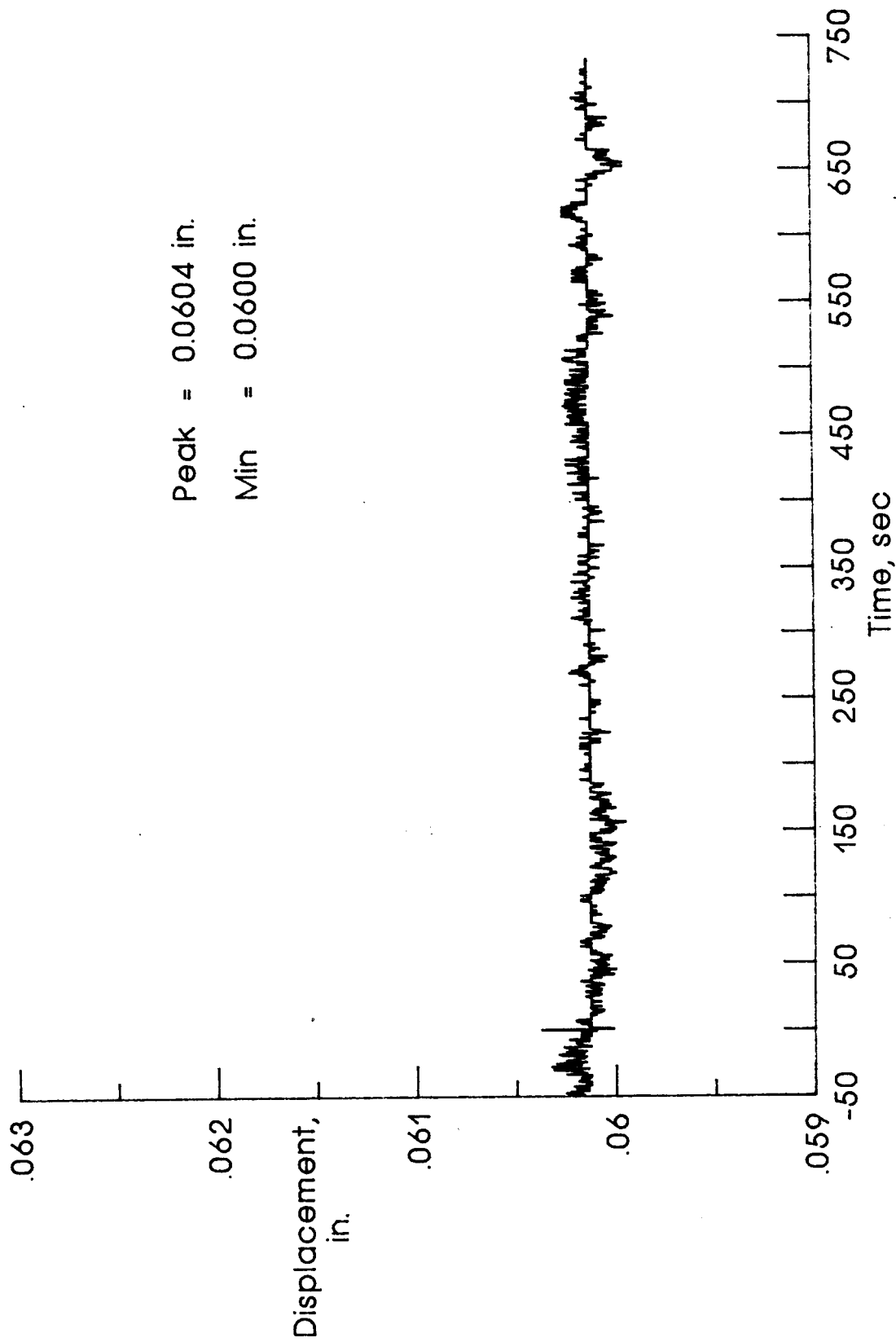
Figure 15d. 250 psi applied to the primary chamber.

MIN1-5, Disp

36
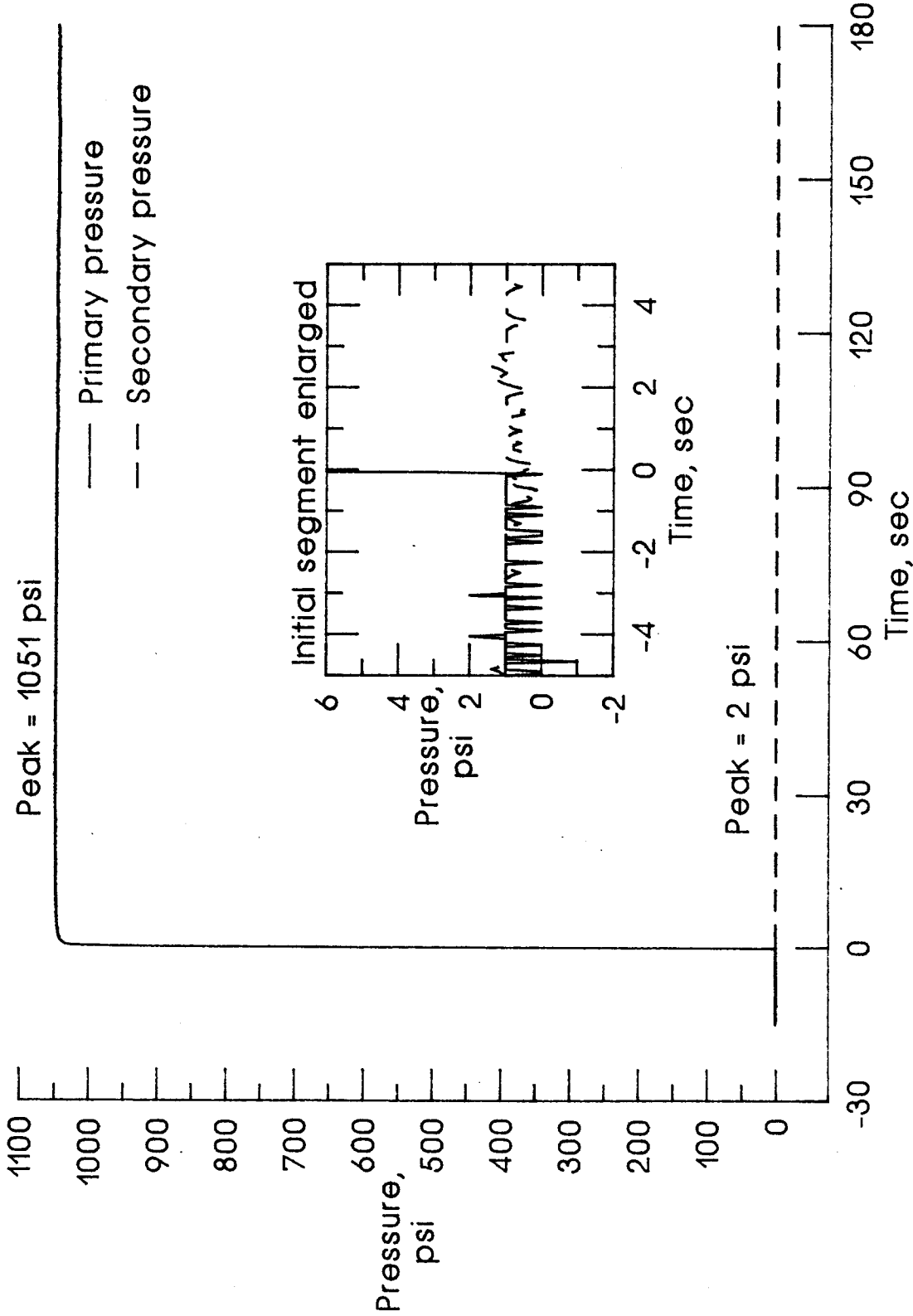
Figure 15e. 1015 psi applied to the primary chamber.

MIN1-6,P/P

37
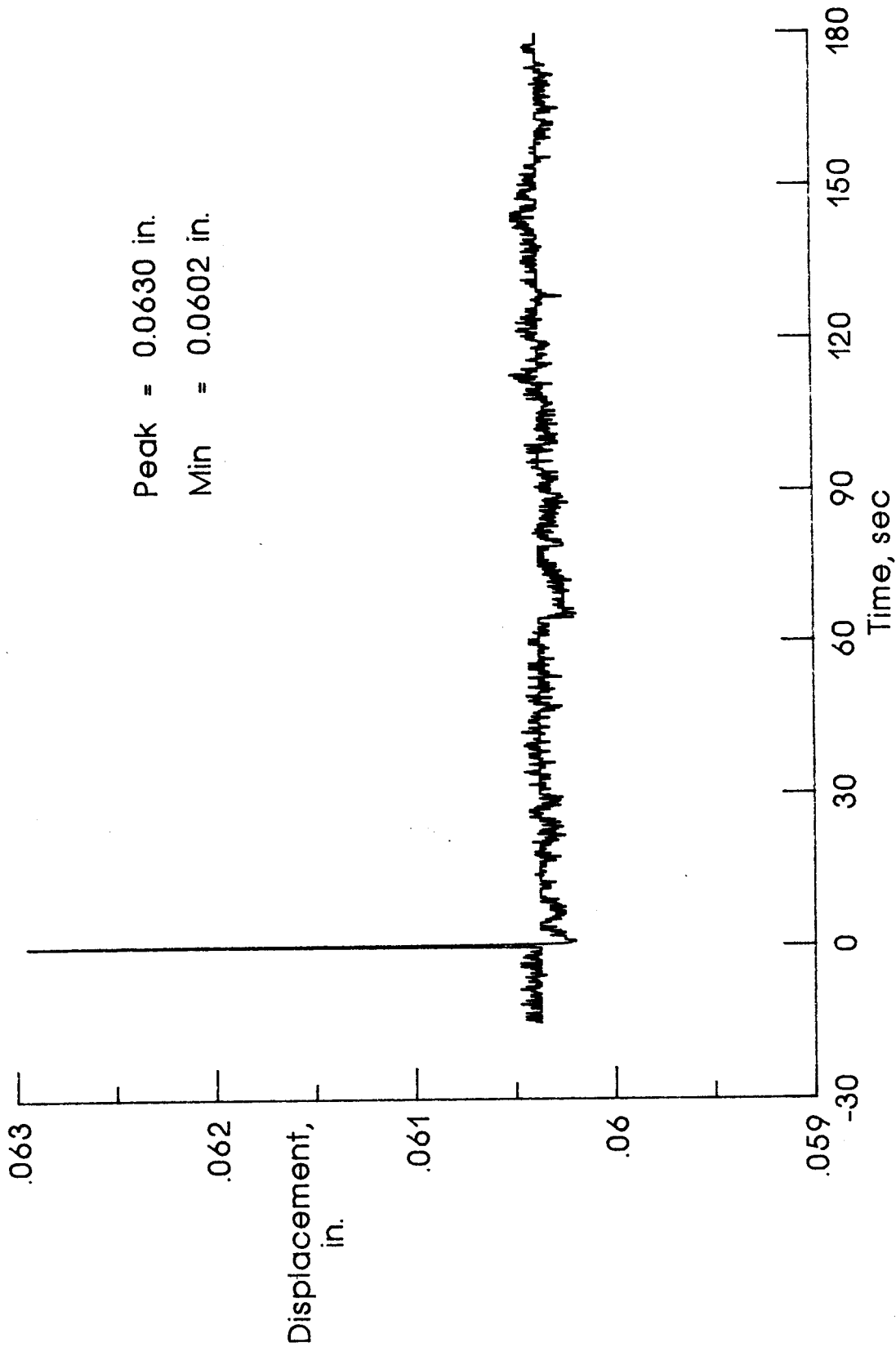
Figure 15f. 1015 psi applied to the primary chamber.

MIN1-6,Disp

Peak = 2 psi

Min = 0 psi

Secondary pressure, psi

Time, sec
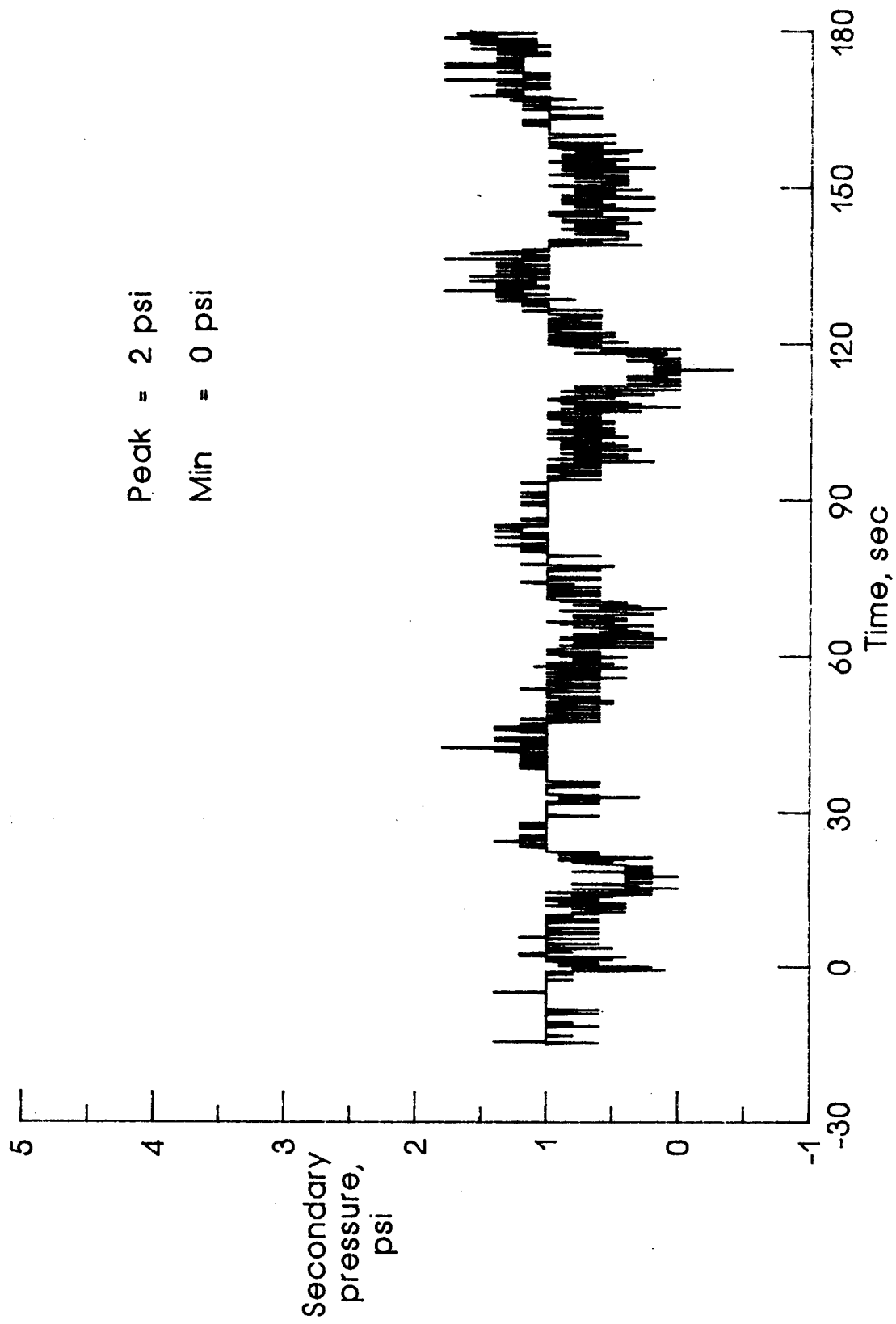
Figure 15g. 1015 psi applied to the primary chamber.

39

MIN1-6,SecPr
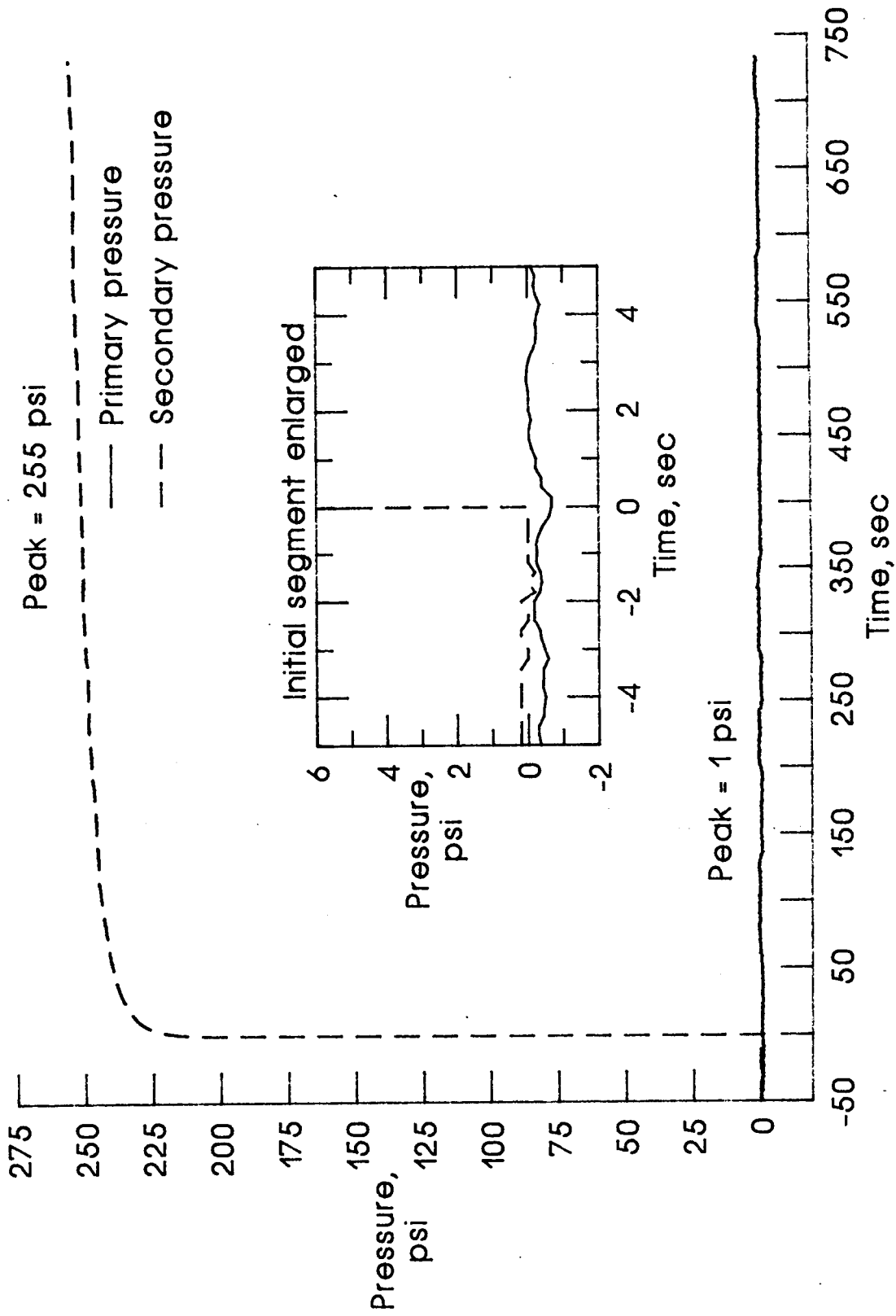
Figure 16a. 250 psi applied to the secondary chamber.

Figure 16. Pressure and displacement curves for the leak check and seal test for a successful seal at an initial squeeze of 5.2%.

MIN2-16, P/P
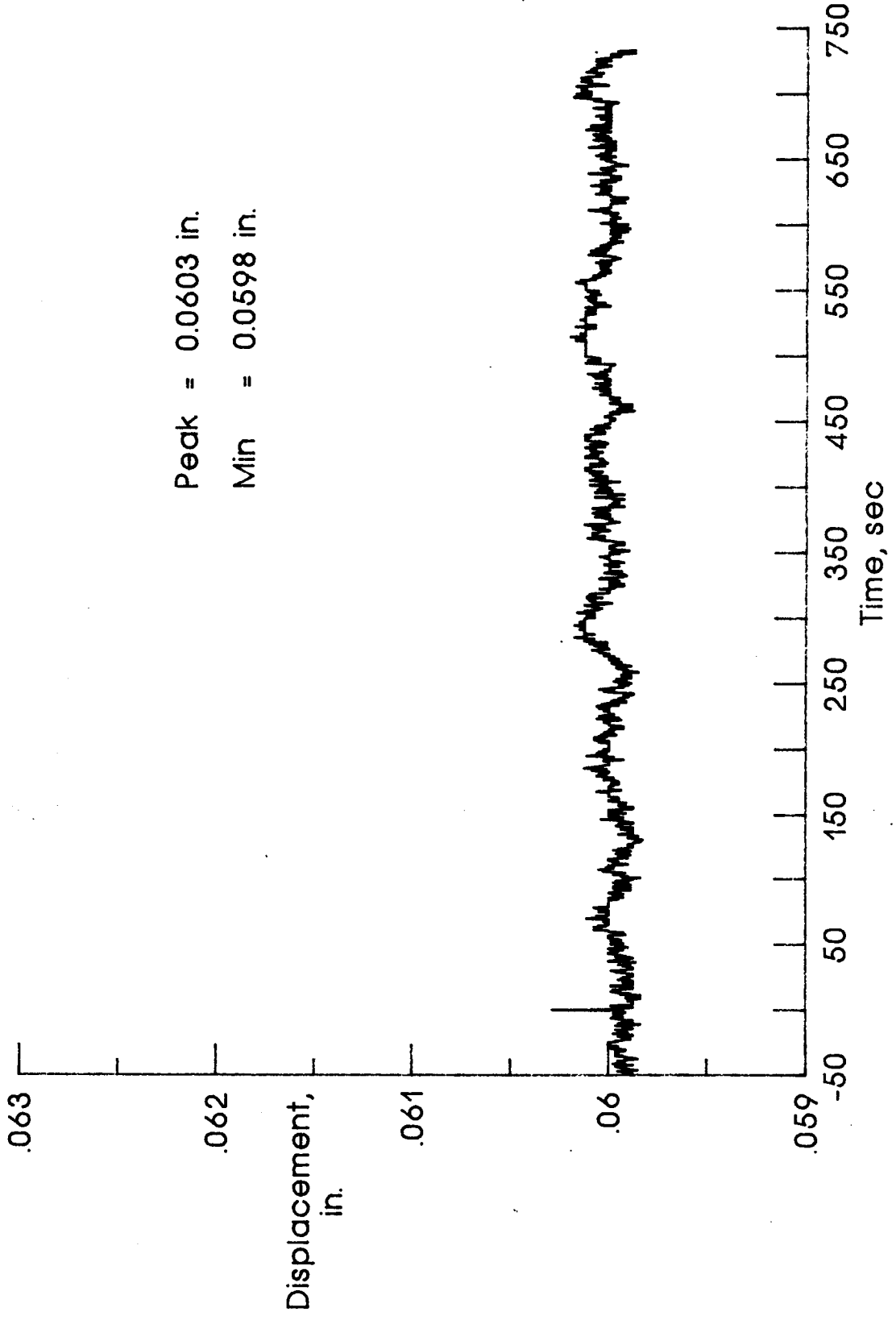
Figure 16b. 250 psi applied to the secondary chamber.

MIN2-16, Disp

41
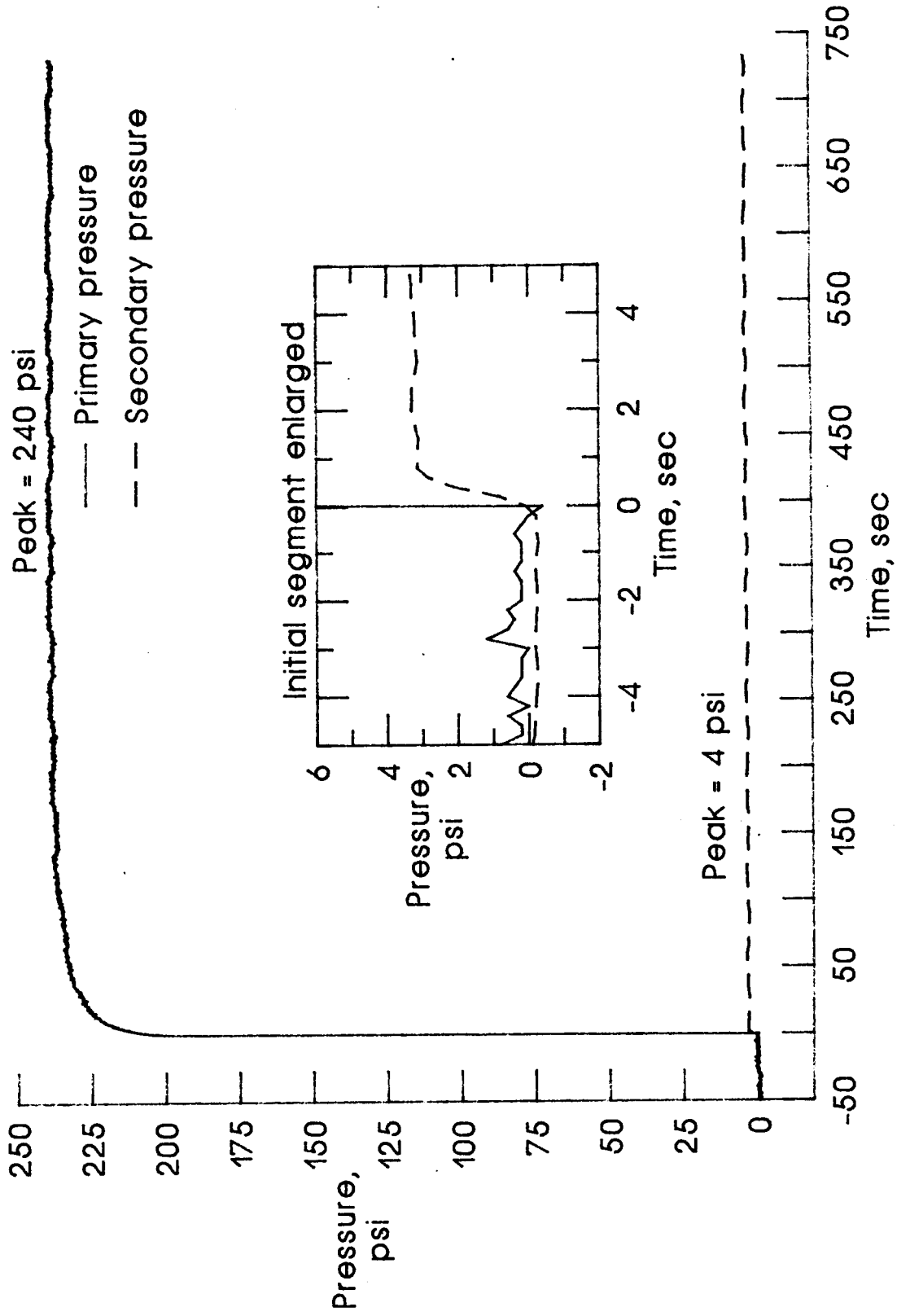
Figure 16c. 250 psi applied to the primary chamber.

42

MIN2-17,P/P

Peak = 0.0600 in.

Min = 0.0596 in.
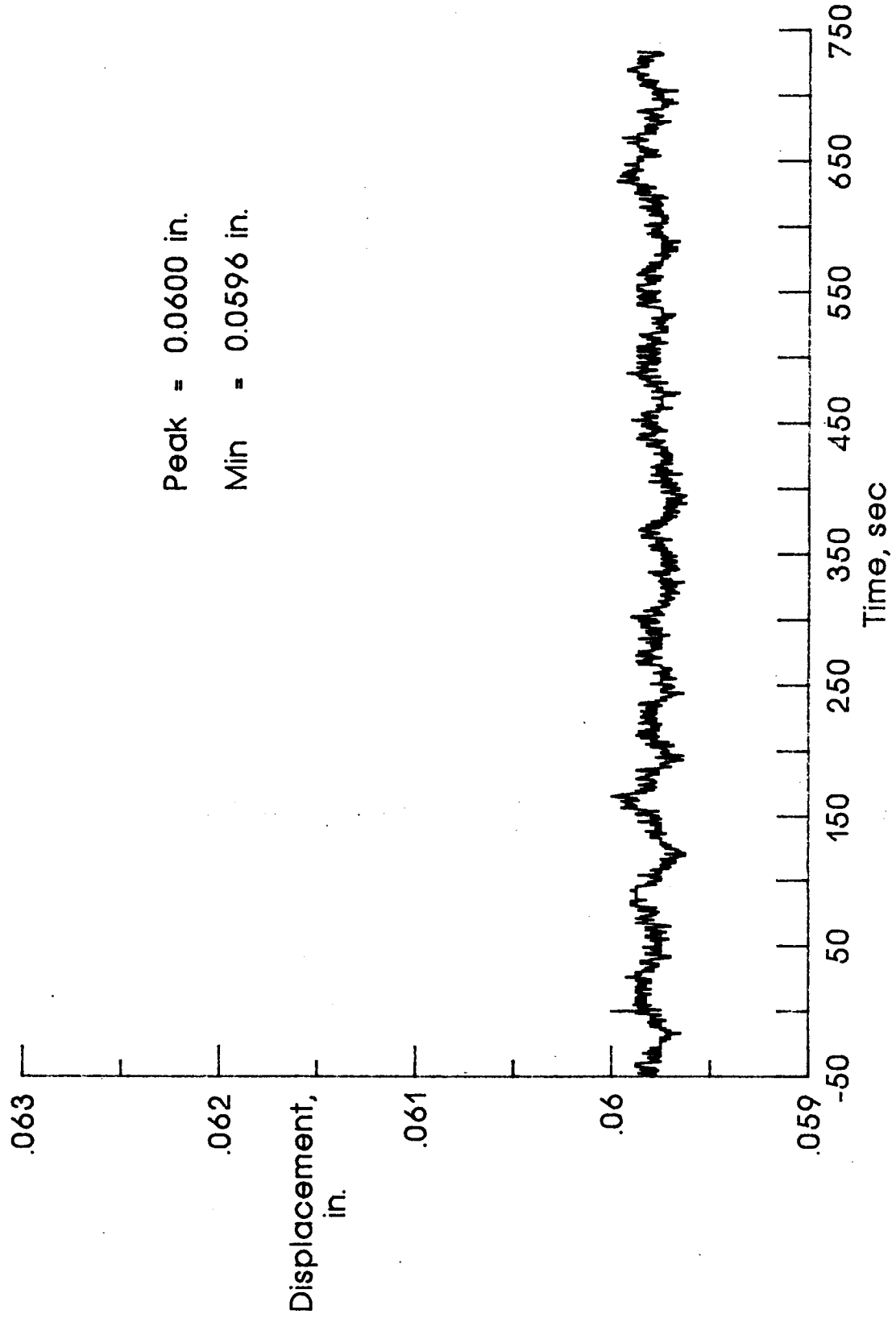
Figure 16d. 250 psi applied to the primary chamber.

MIN2-17, Disp
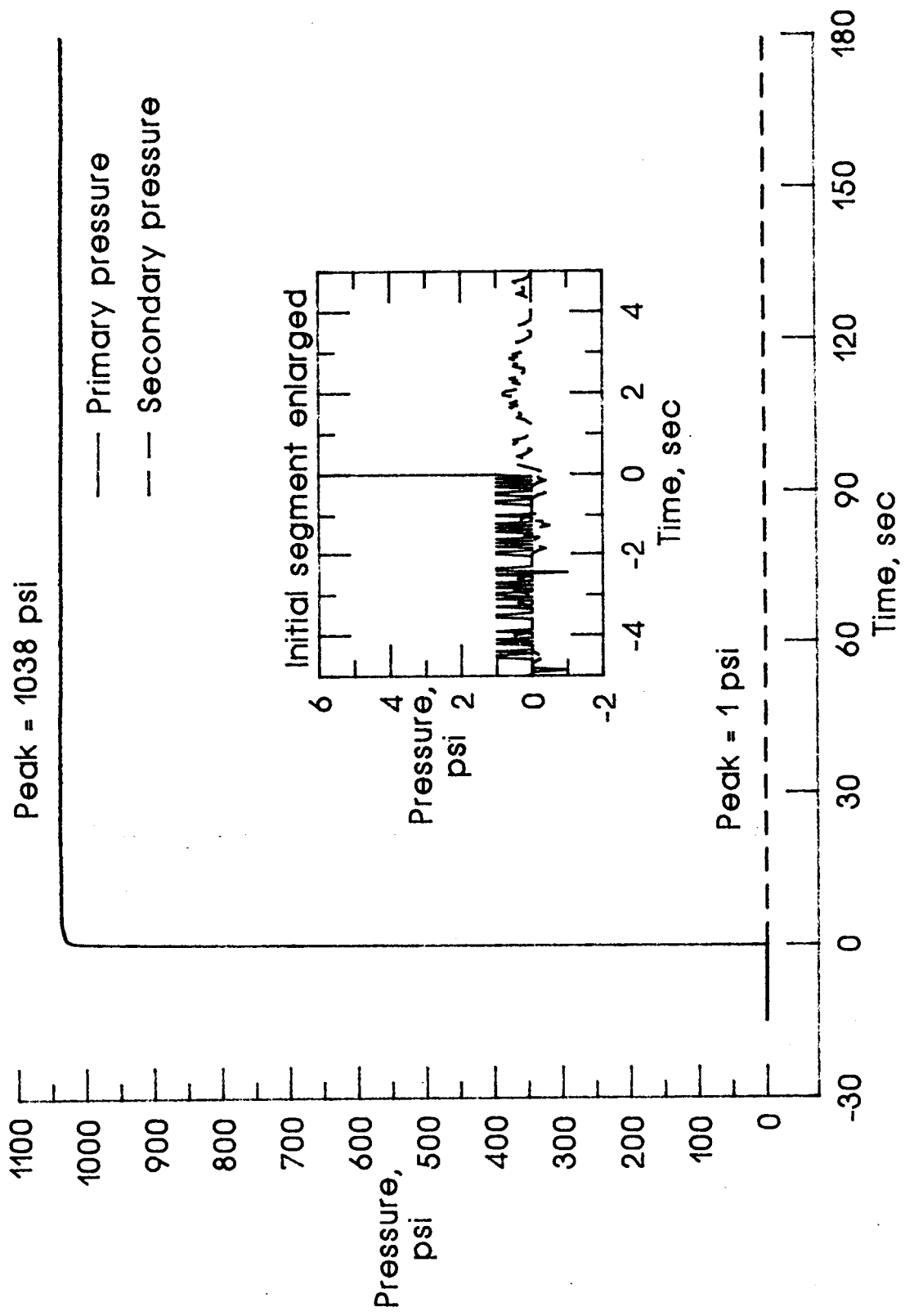
Figure 16e. 1015 psi applied to the primary chamber.

44

MIN2-18,P/P

Peak = 0.0623 in.

Min = 0.0598 in.
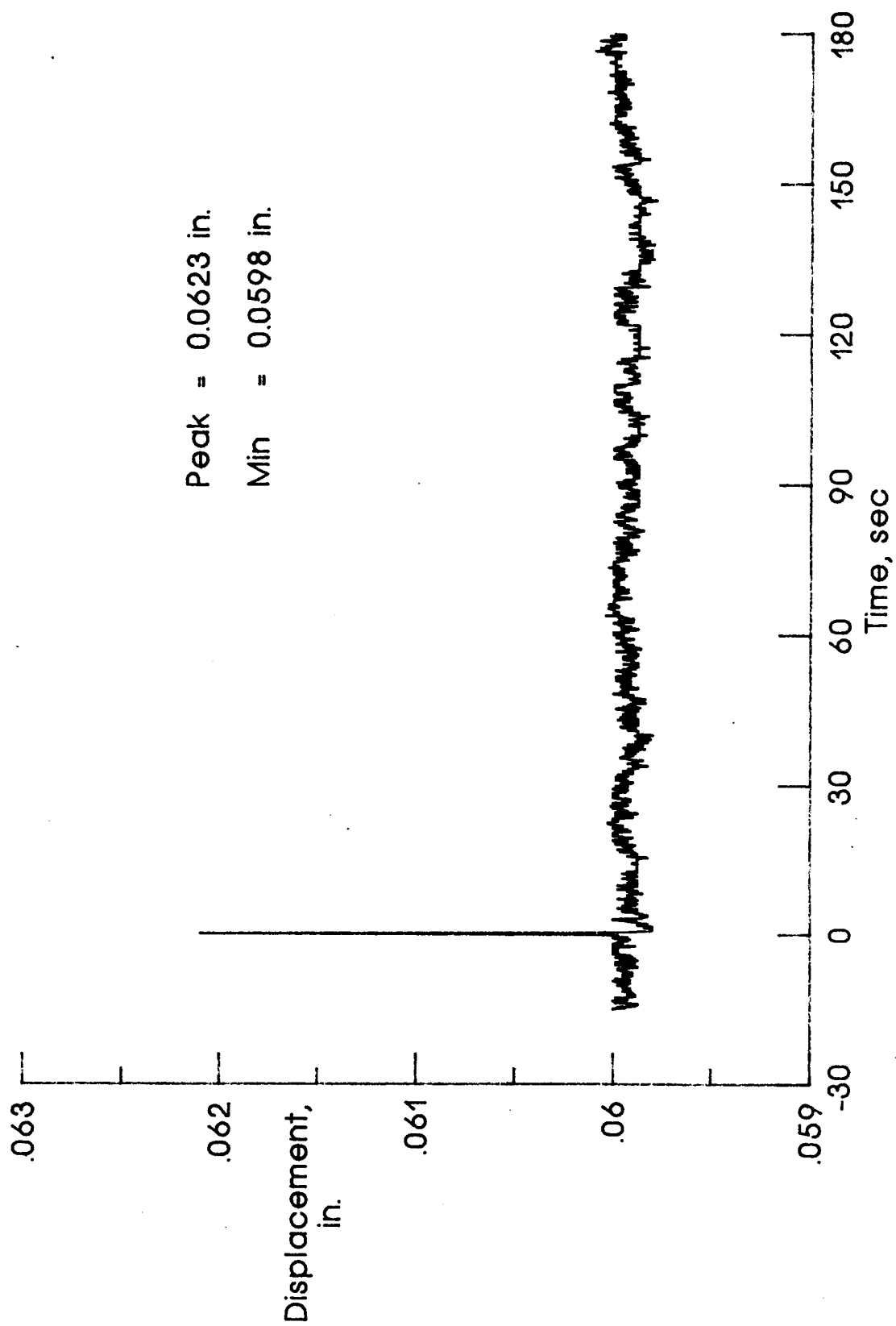
Figure 16f. 1015 psi applied to the primary chamber.

MIN2-18,Disp

45
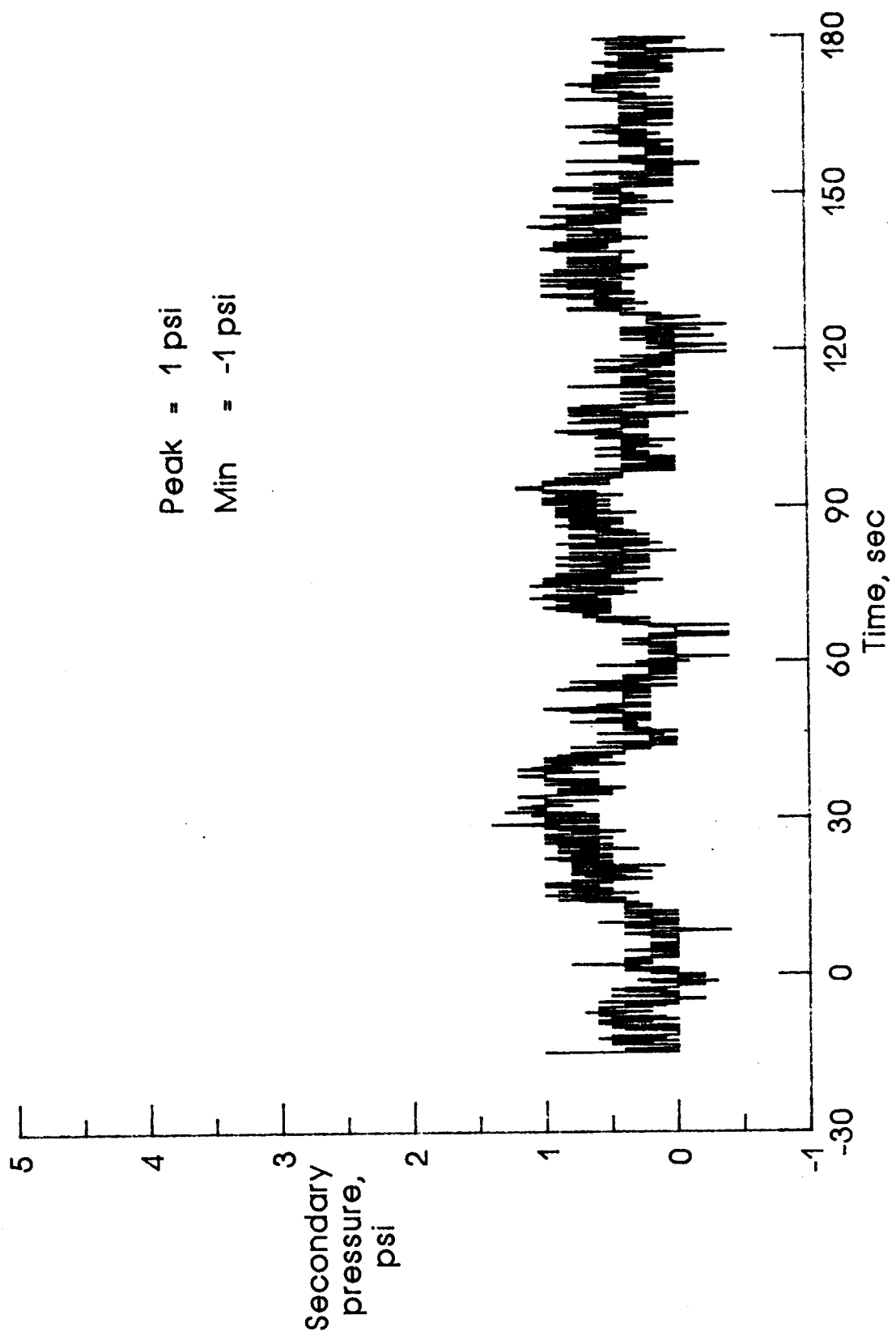
Figure 16g.   1015 psi applied to the primary chamber.

MIN2-18,SecPr
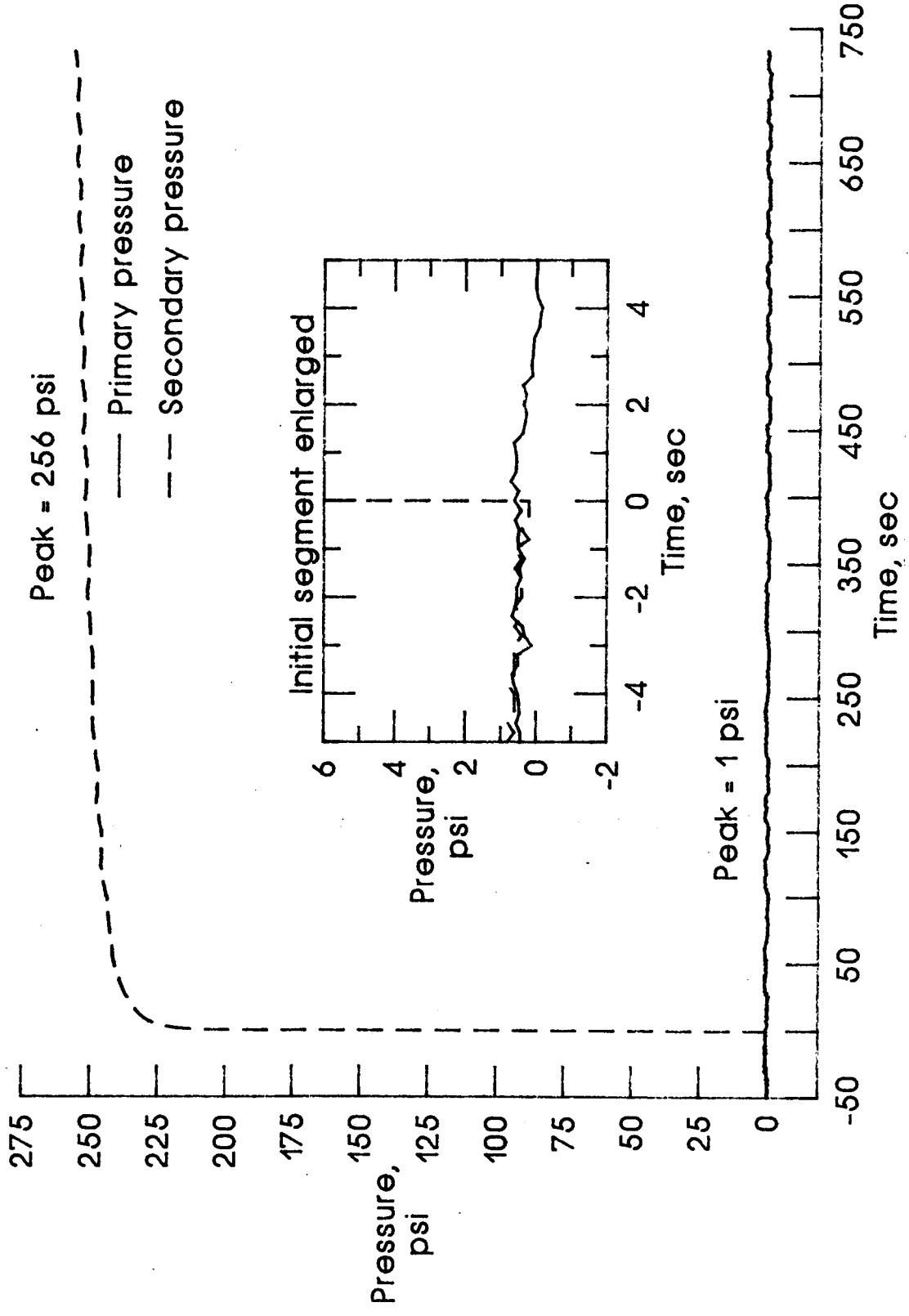
Figure 17a.   250 psi applied to the secondary chamber.

Figure 17.   Pressure and displacement curves for the leak check and seal test
for a successful seal at an initial squeeze of 5.2%.

MIN4-10,P/P

47
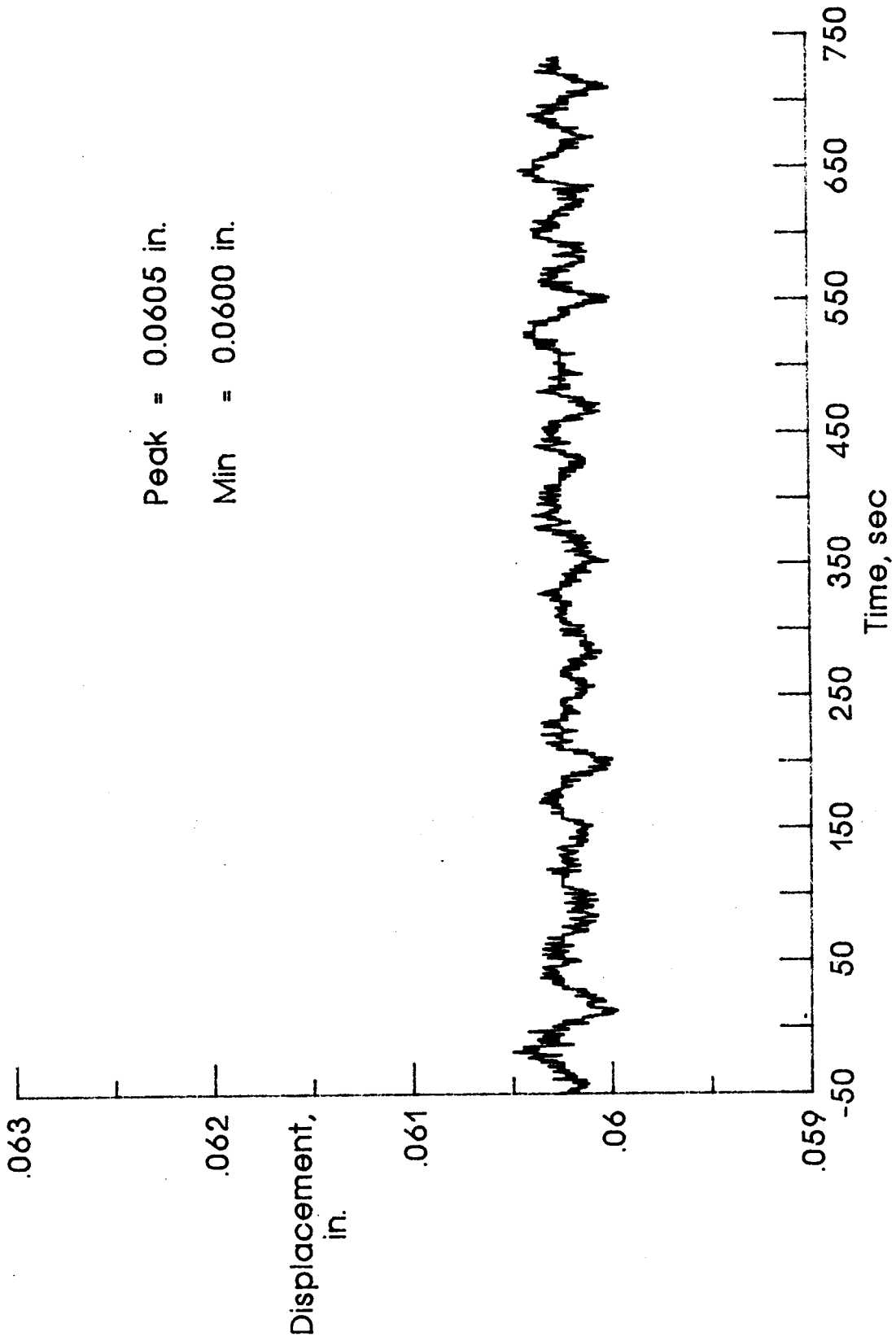
Figure 17b. 250 psi applied to the secondary chamber.

MIN4-10, Disp

48
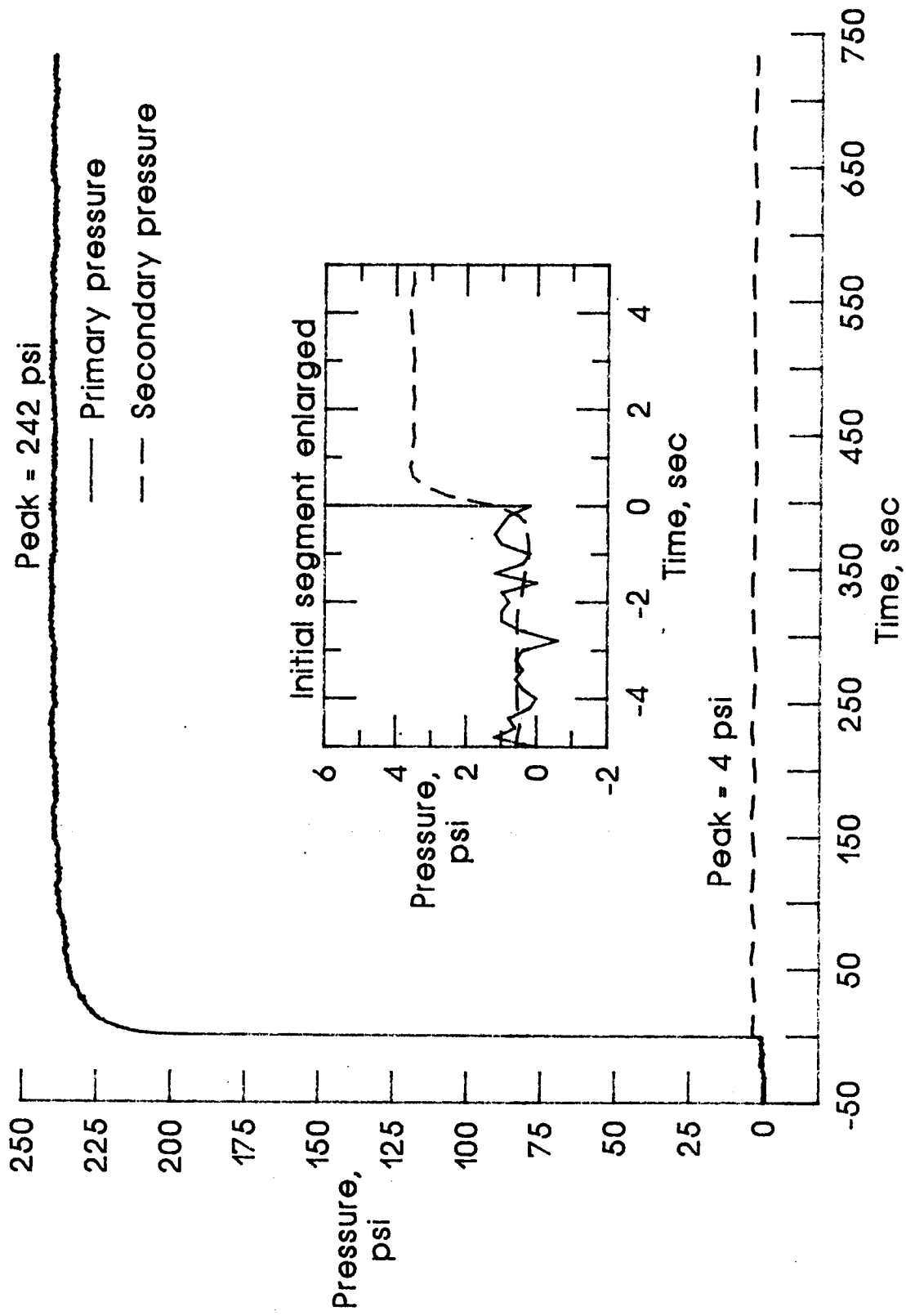
Figure 17c. 250 psi applied to the primary chamber.

49

MIN4-11,P/P
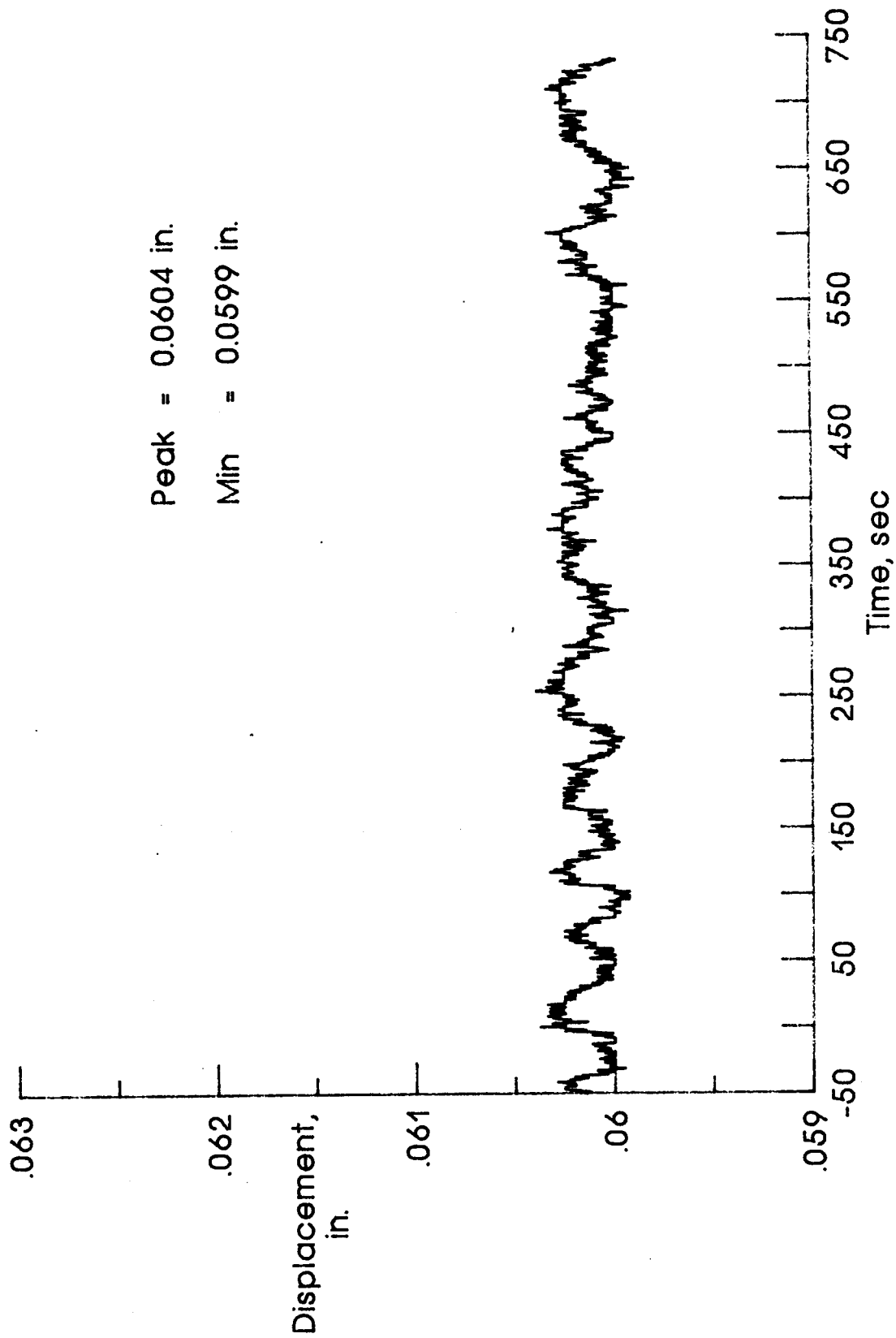
Figure 17d. 250 psi applied to the primary chamber.

MIN4-11, Disp
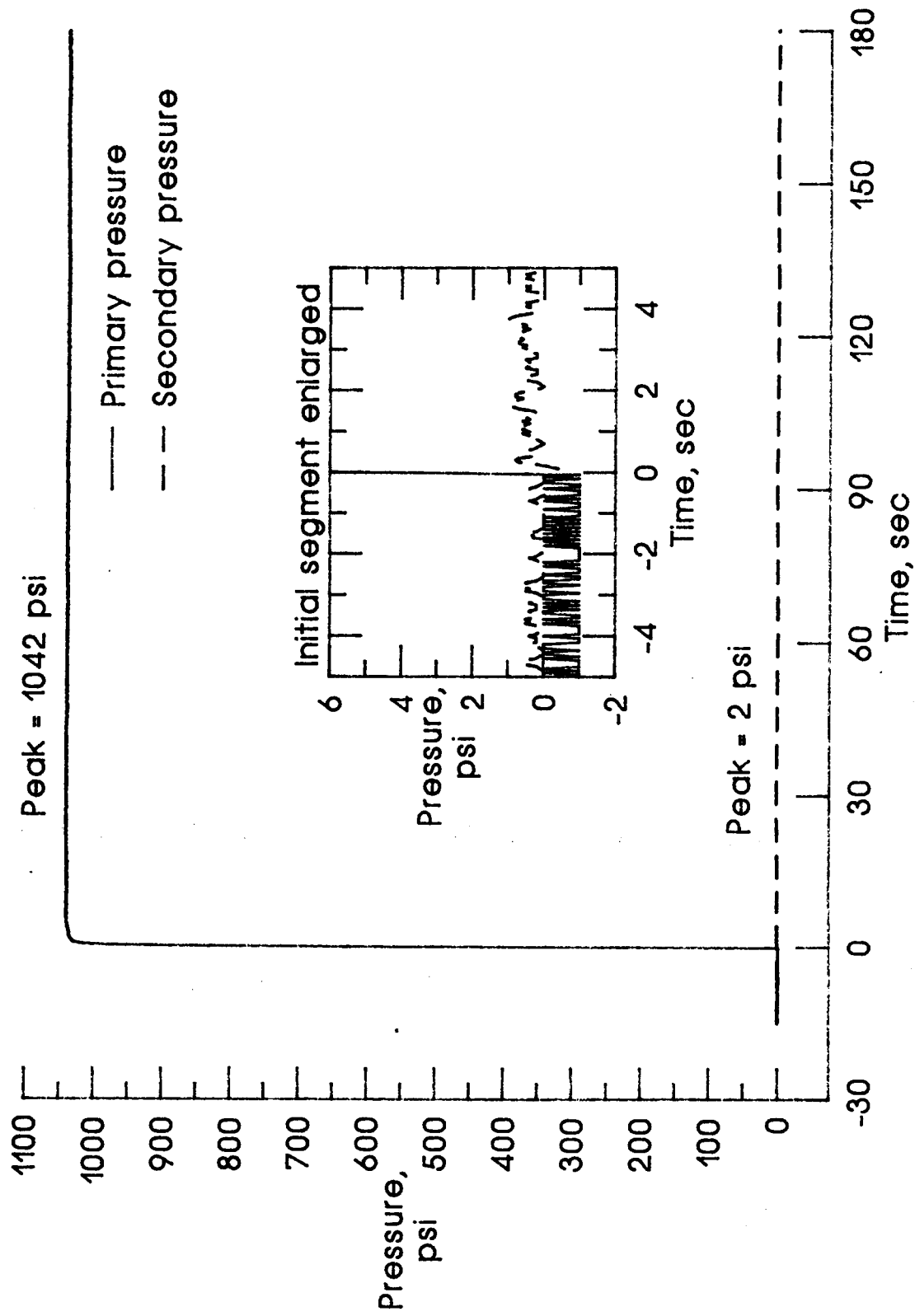
Figure 17f. 1015 psi applied to the primary chamber.

Peak = 1042 psi

Peak = 2 psi

— Primary pressure
— — Secondary pressure

Pressure, psi

Time, sec

Initial segment enlarged

Pressure, psi

Time, sec

MIN4-12,P/P

51

Peak = 0.0626 in.

Min = 0.0600 in.

Displacement, in.

Time, sec

MIN4-12,Disp
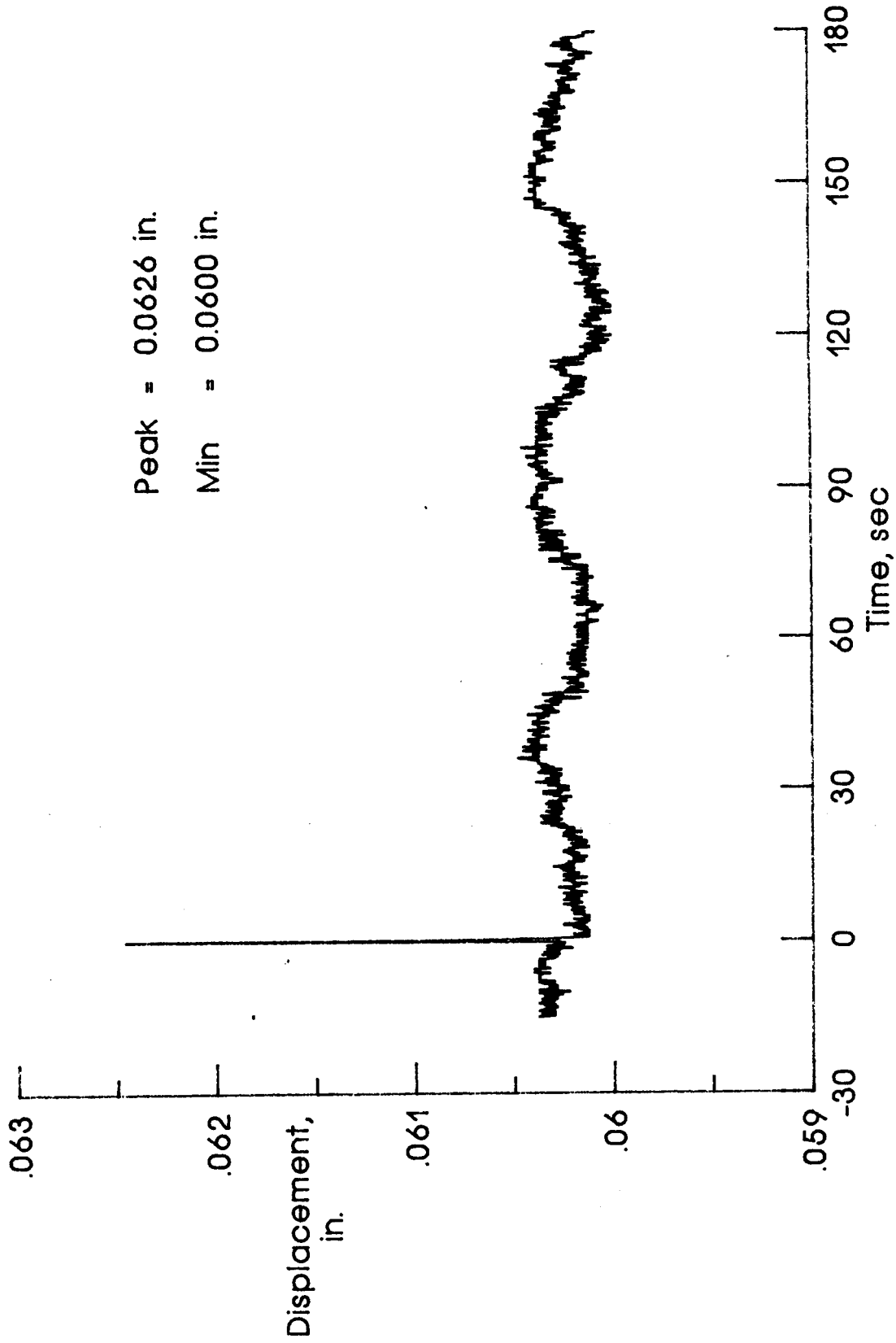
Figure 17e. 1015 psi applied to the primary chamber.

52
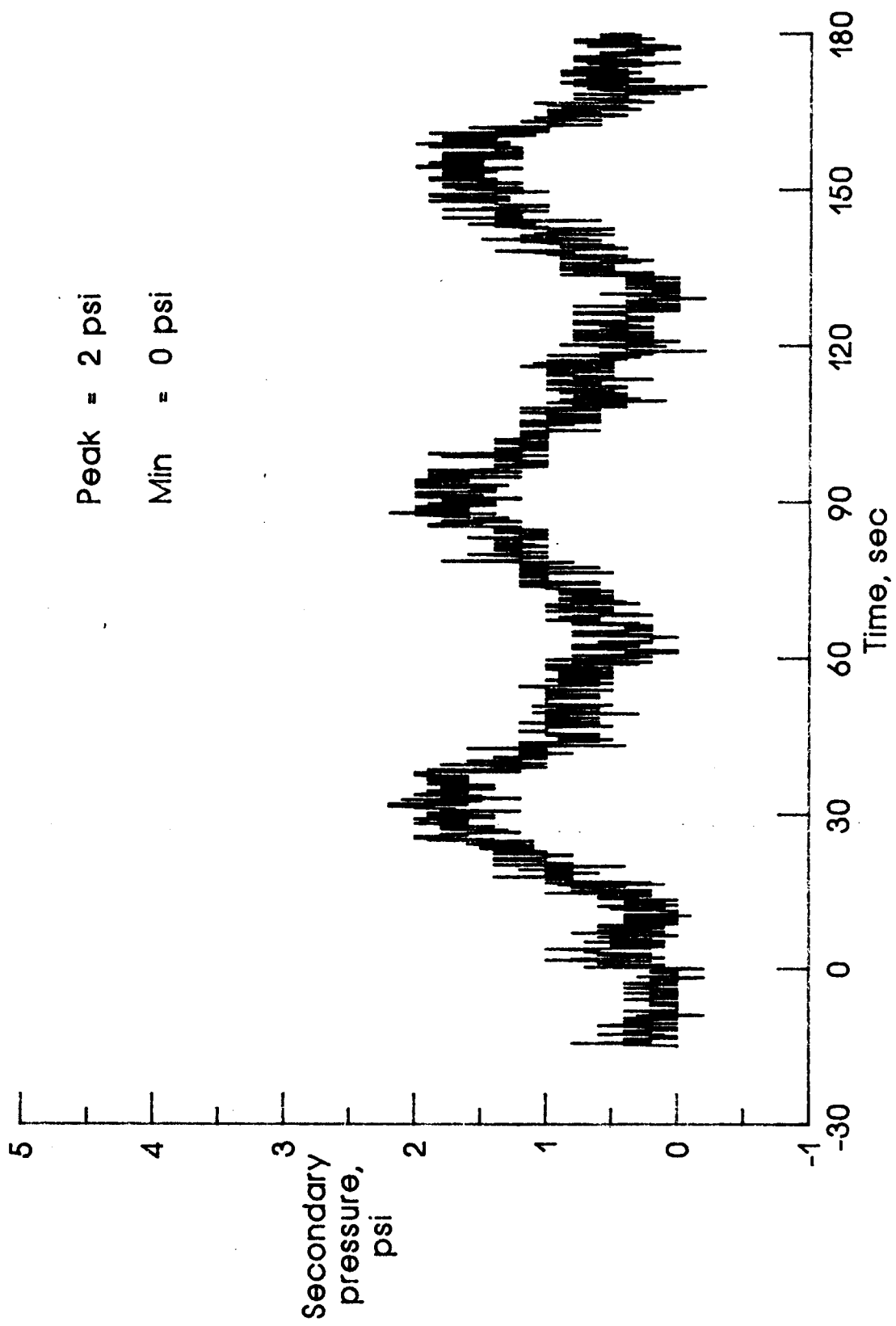
Figure 17g. 1015 psi applied to the primary chamber.

Peak = 2 psi

Min = 0 psi

MIN4-12,SecPr

53
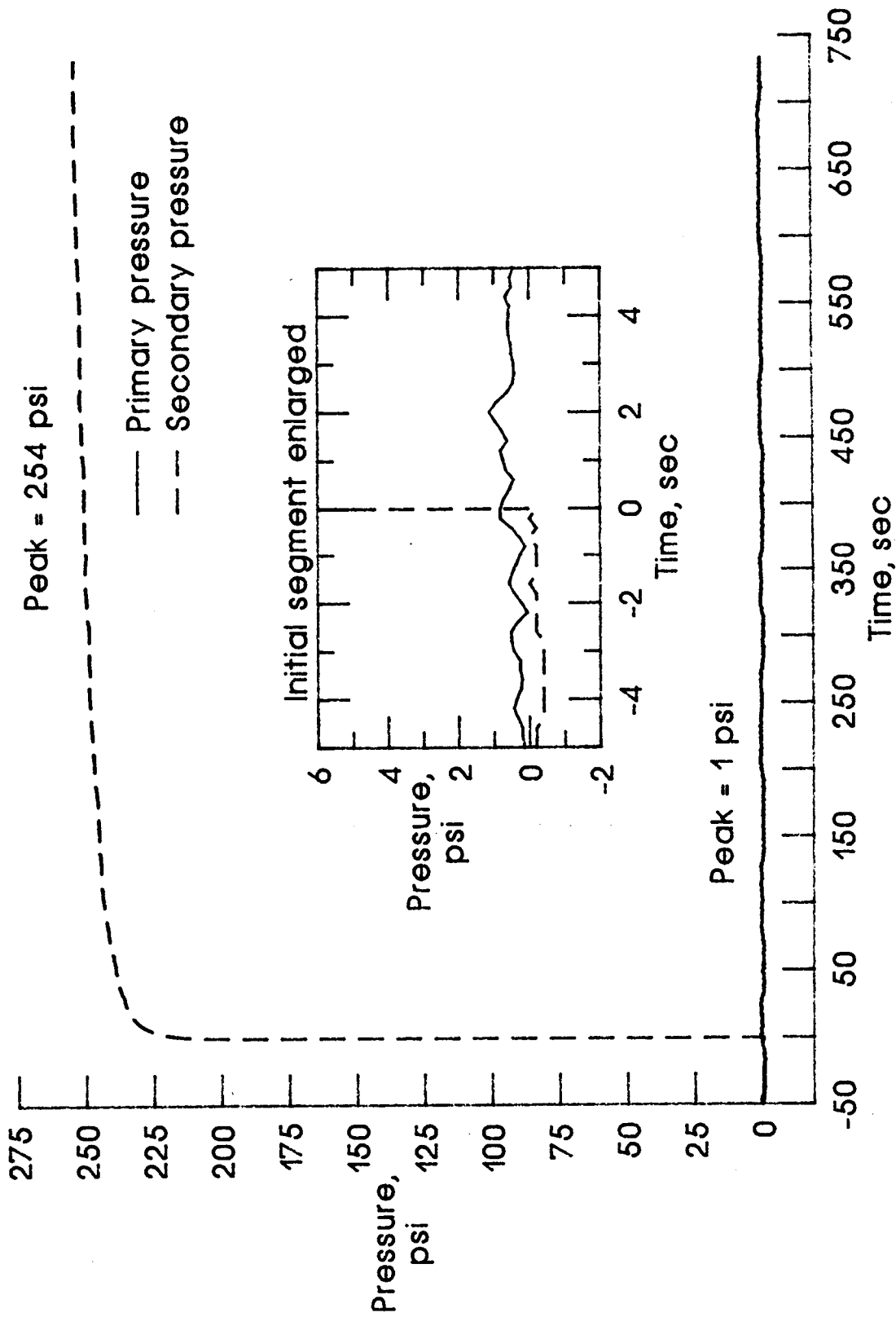
Figure 18a. 250 psi applied to the secondary chamber.

Figure 18. Pressure and displacement curves for the leak check and seal test for a successful seal at an initial squeeze of 3.5%.

MIN1-10,P/P

54
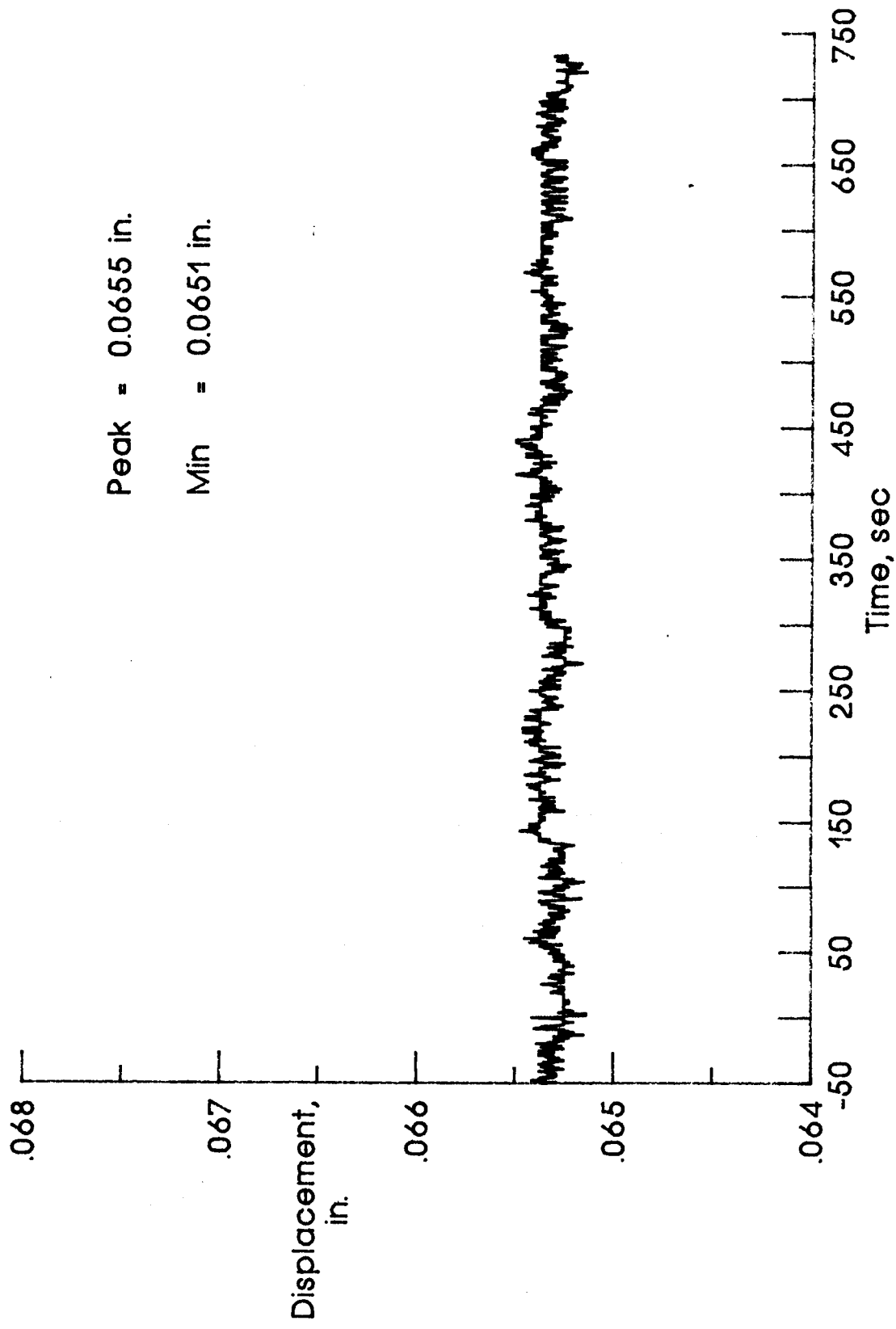
Figure 18b. 250 psi applied to the secondary chamber.

MIN1-10, Disp

55
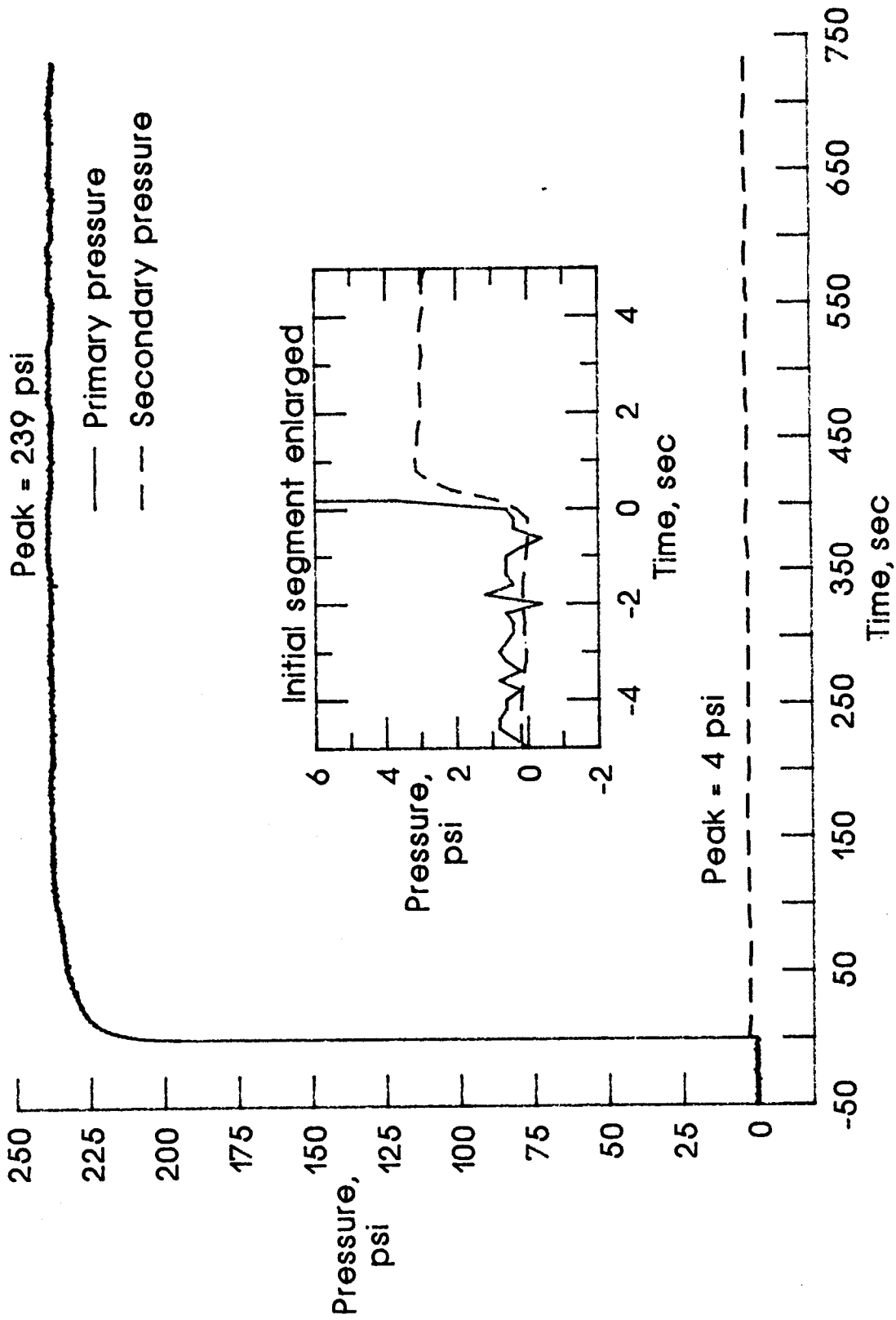
Figure 18c.   250 psi applied to the primary chamber.

MIN1-11, P/P

56
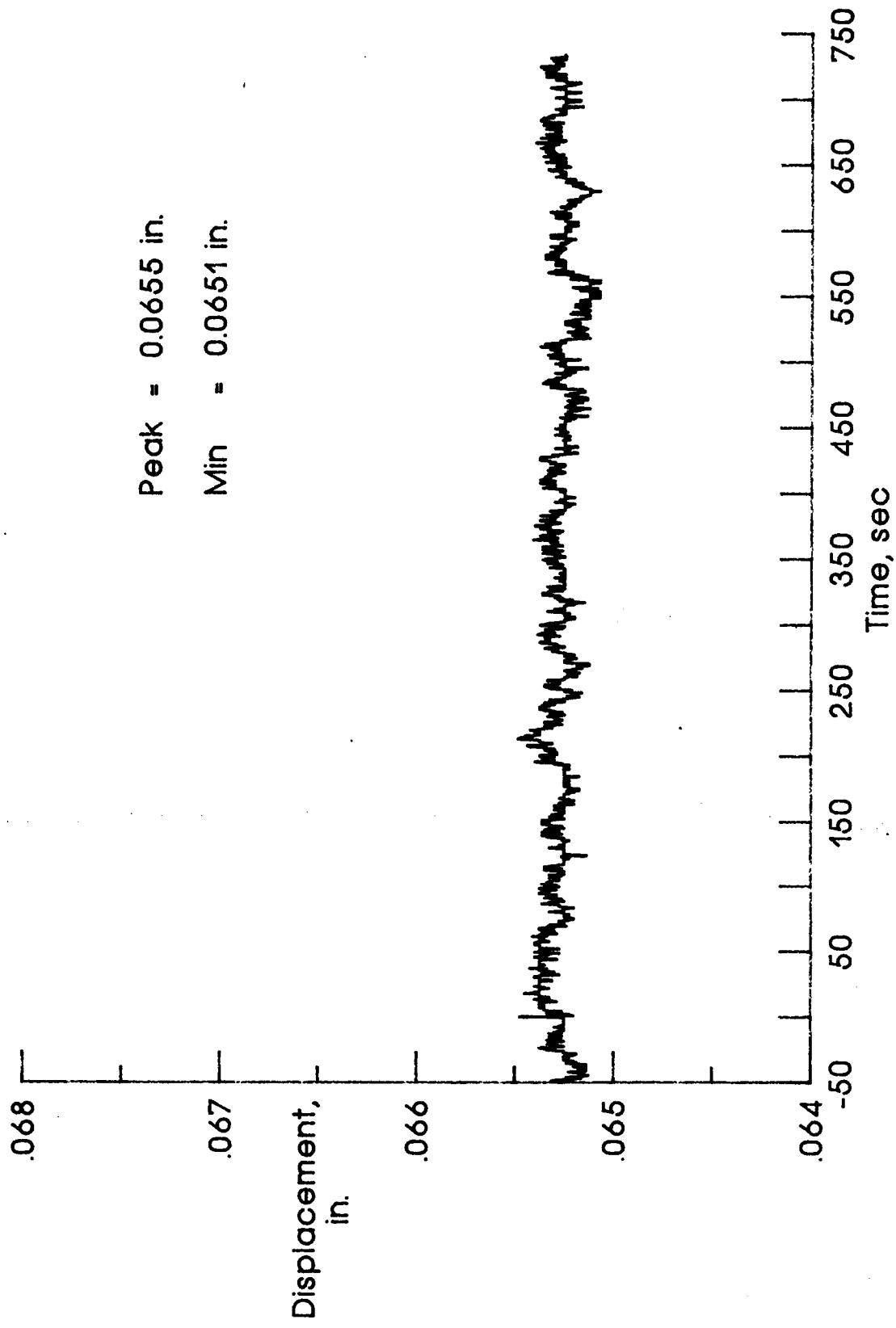
Figure 18d. 250 psi applied to the primary chamber.

MIN1-11, Disp

57
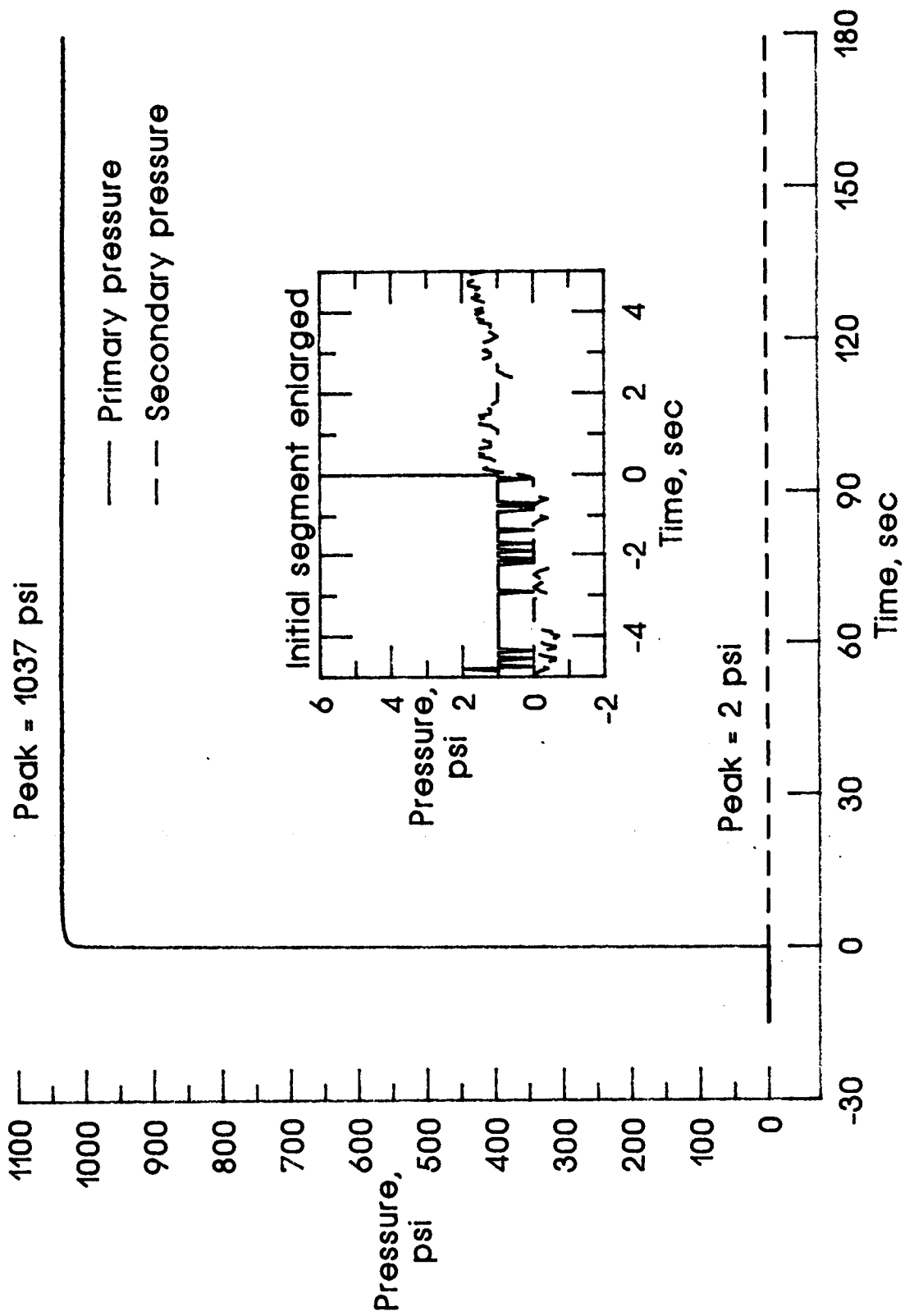
Figure 18e. 1015 psi applied to the primary chamber.

MIN1-12,P/P

Peak = 0.0678 in.

Min = 0.0651 in.
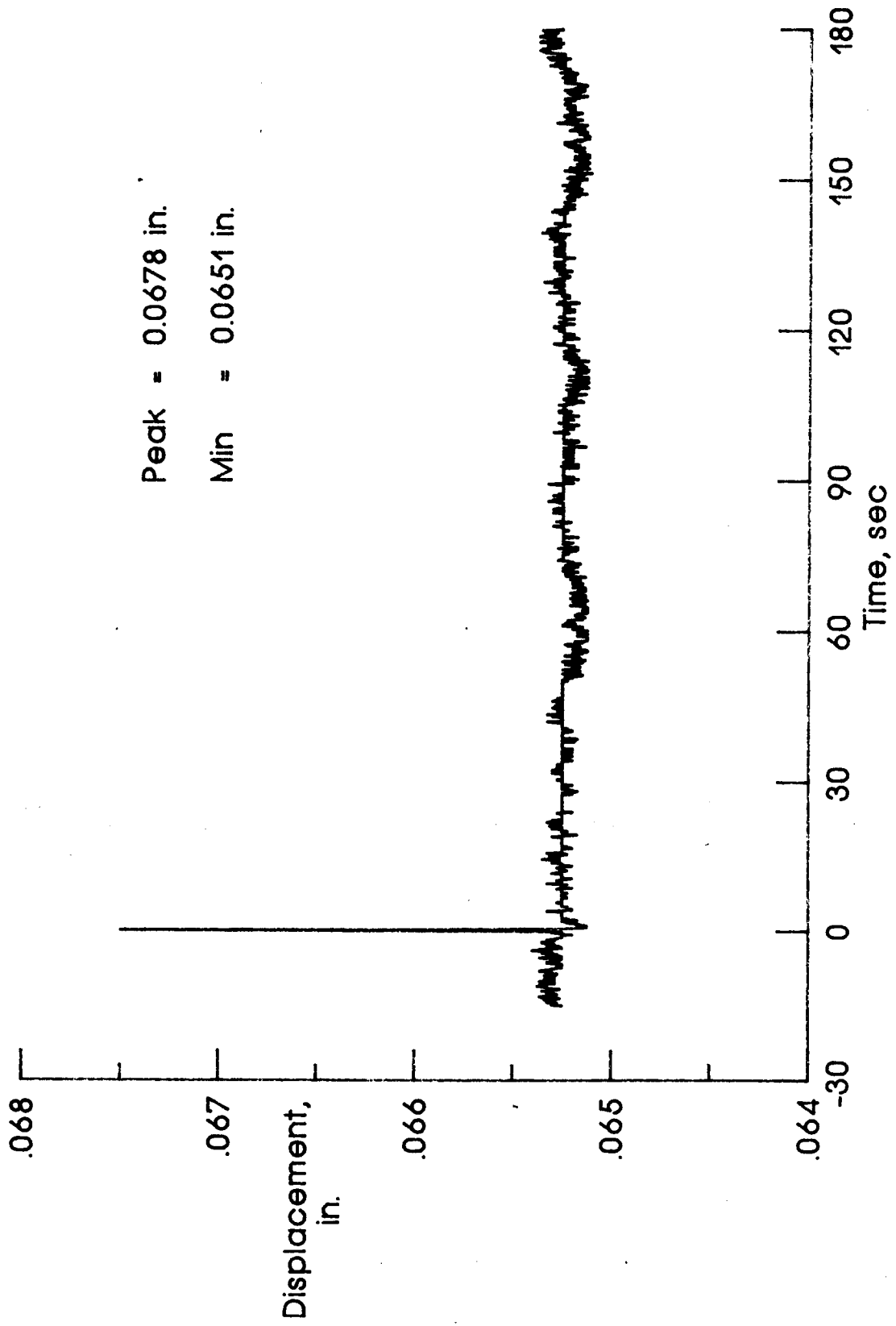
Figure 18f. 1015 psi applied to the primary chamber.

MIN1-12,Disp

59

Peak = 2 psi

Min = -1 psi

Secondary pressure, psi

Time, sec

Figure 13g.   1015 psi applied to the primary chamber.

MIN1-12,SecPr

60
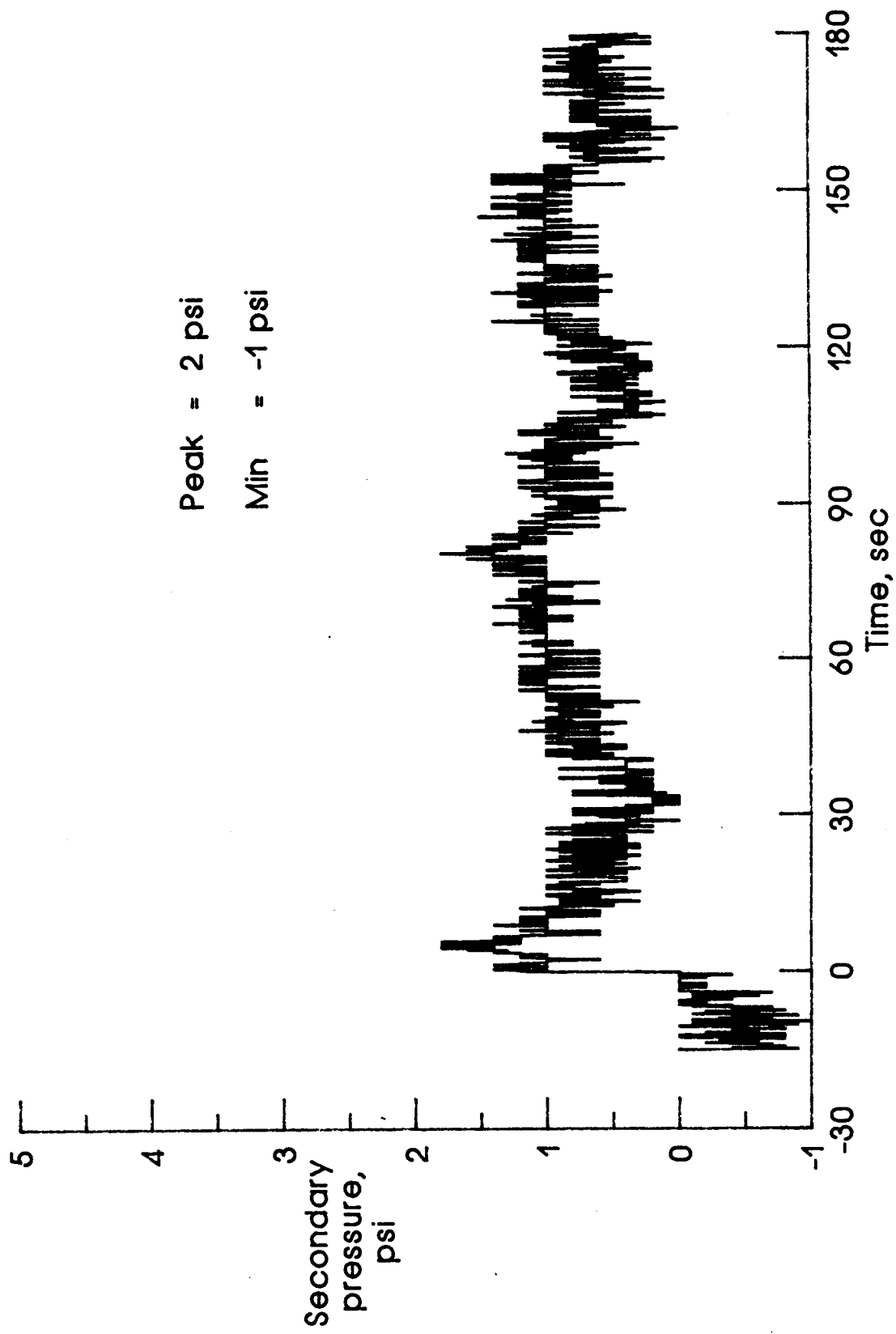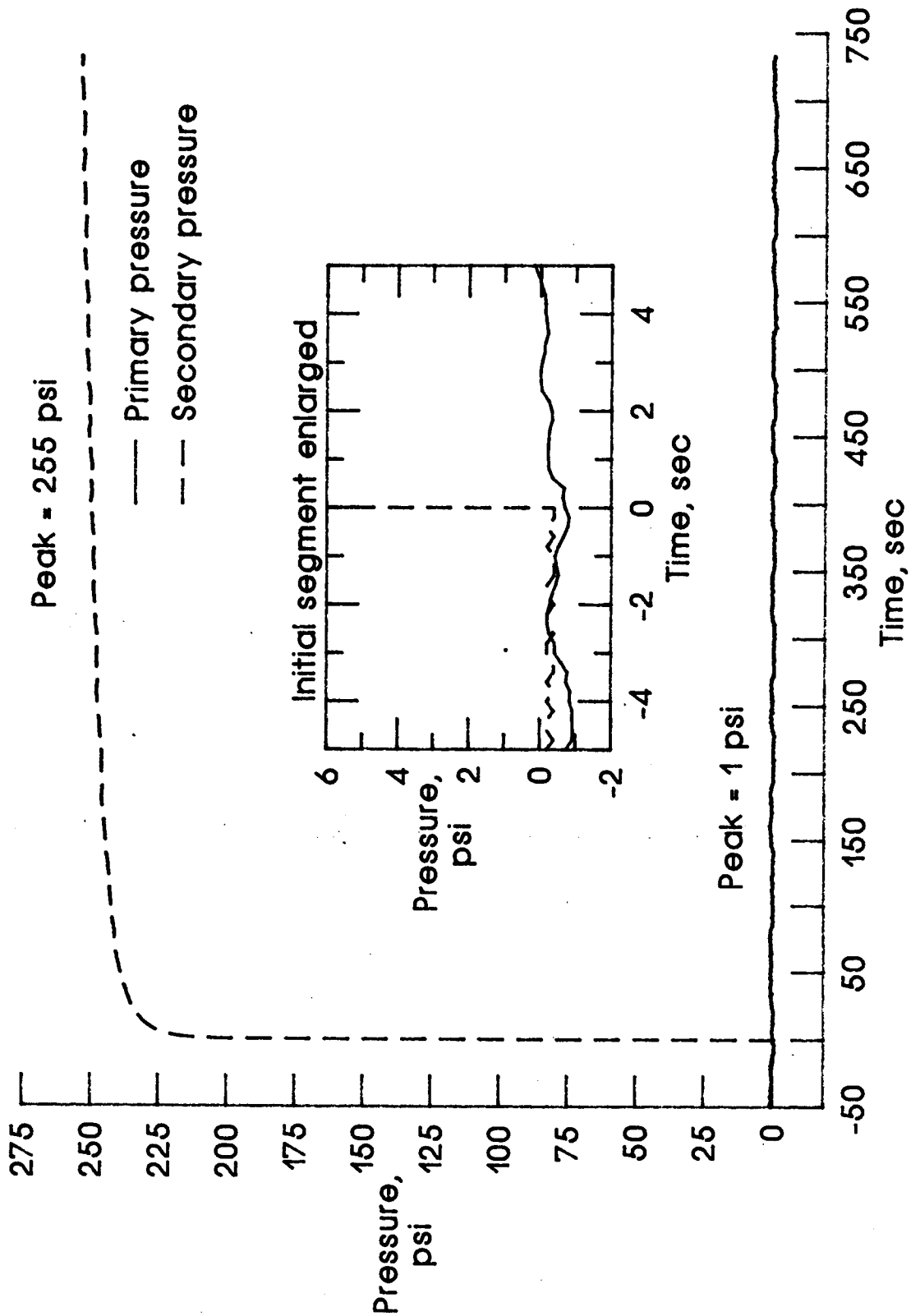
Figure 19a. 250 psi applied to the secondary chamber.

Figure 19. Pressure and displacement curves for the leak check and seal test for a successful seal at an initial squeeze of 3.5%.

MIN3-4, P/P
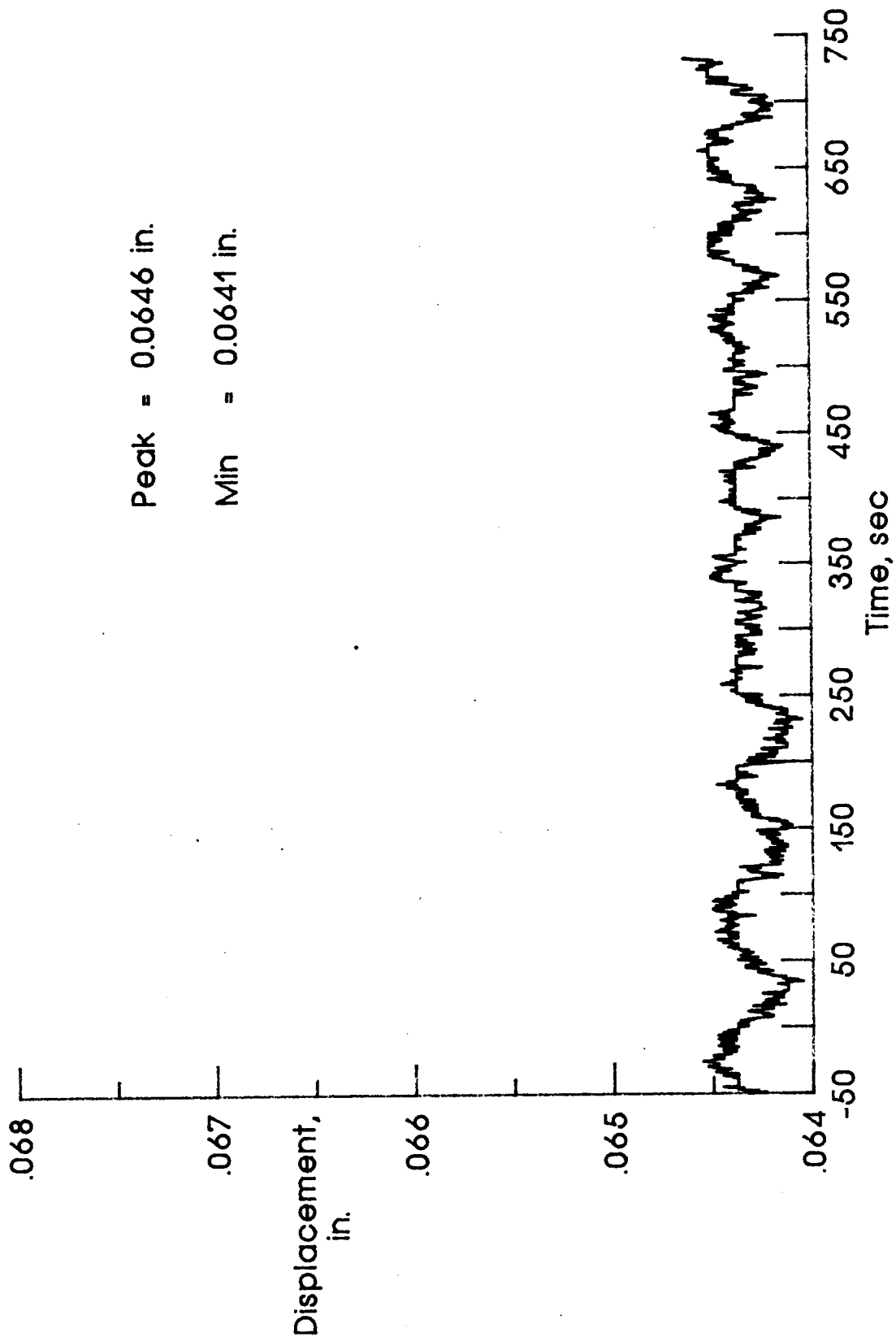
Figure 19b. 250 psi applied to the secondary chamber.

MIN3-4, Disp

62
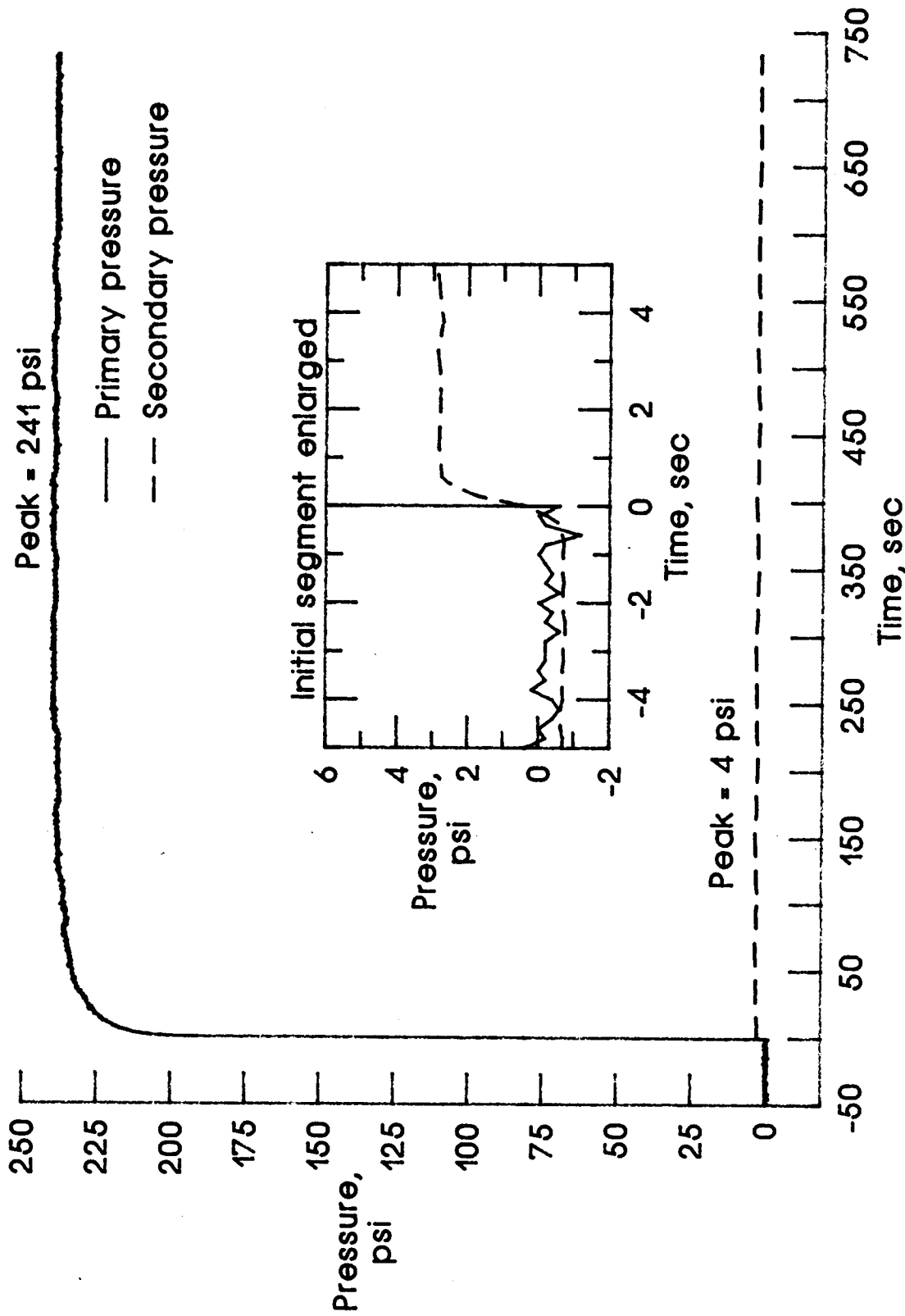
Figure 19c. 250 psi applied to the primary chamber.

63

MIN3-5, P/P

Peak = 0.0645 in.

Min = 0.0641 in.
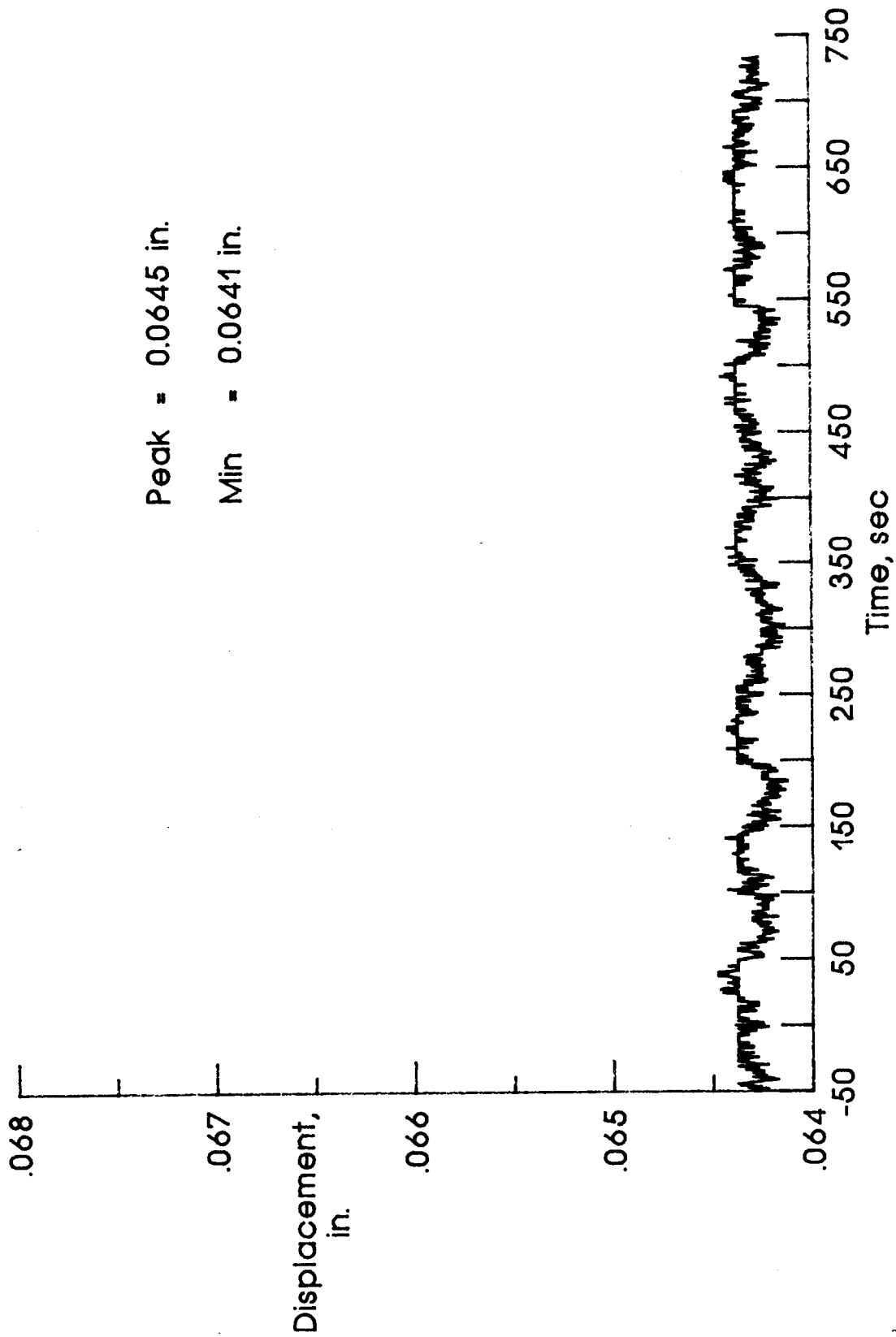
Figure 19d. 250 psi applied to the primary chamber.

64

MIN3-5, Disp
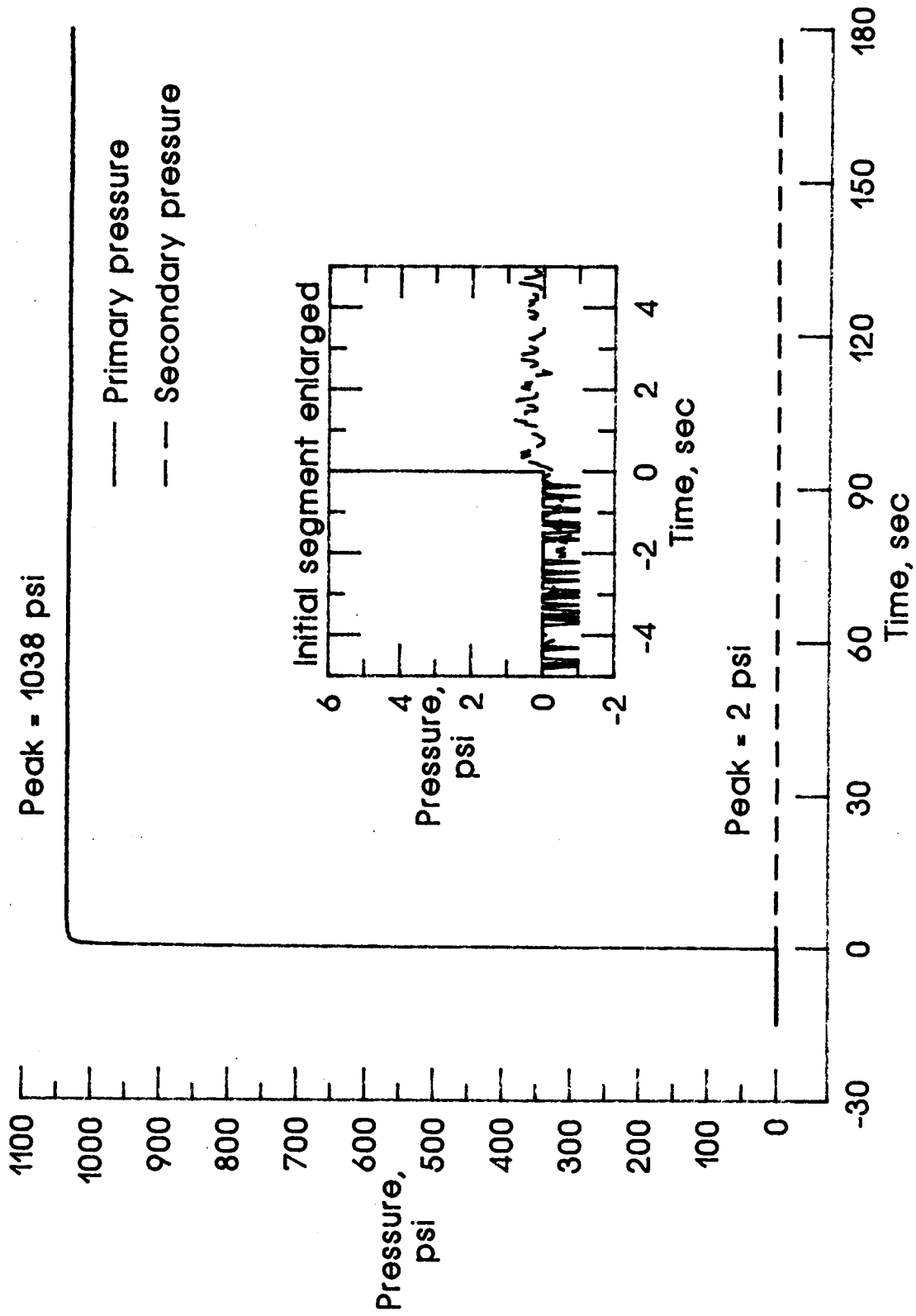
Figure 19e.   1015 psi applied to the primary chamber.

MIN3-6, P/P

65
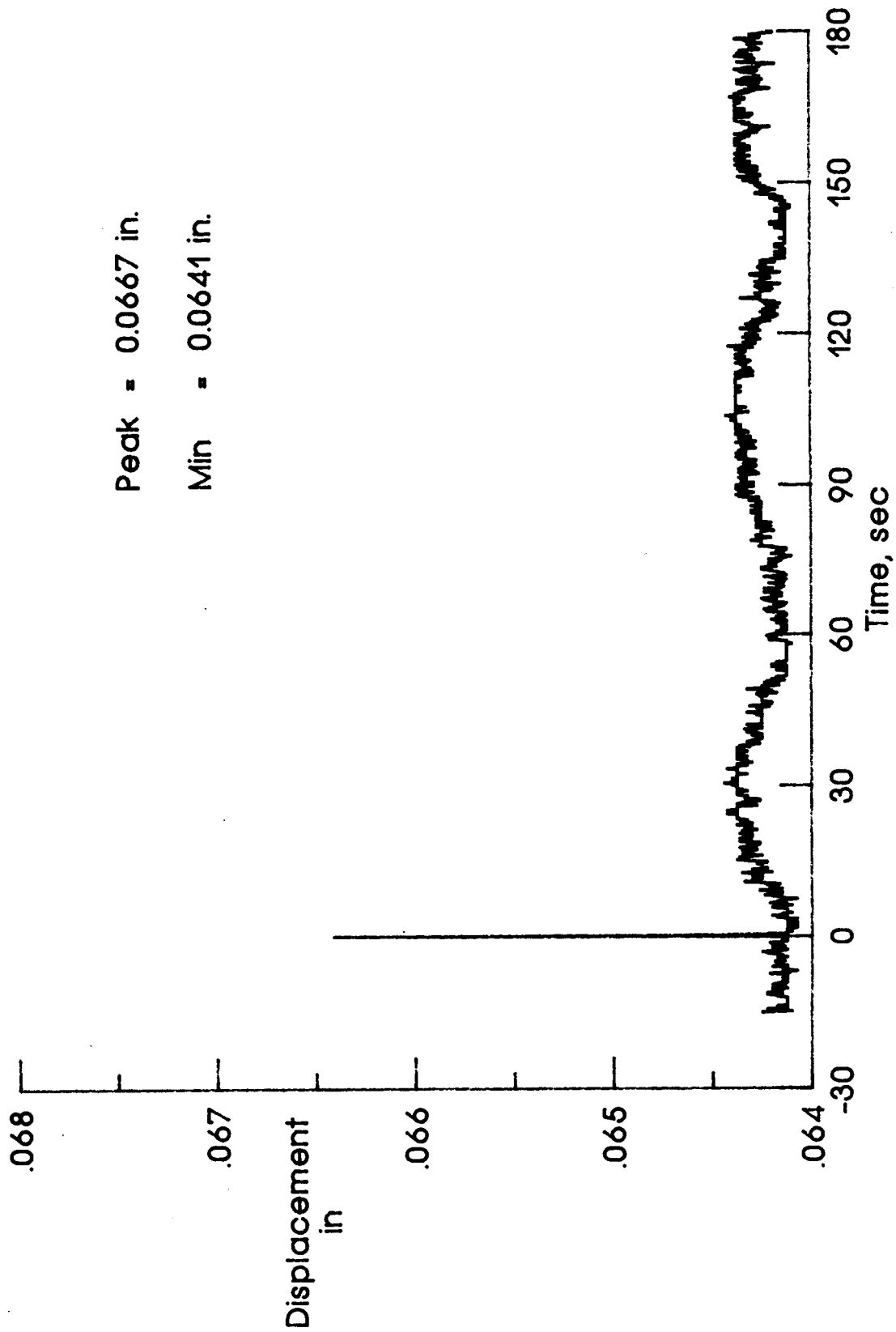
Figure 19f. 1015 psi applied to the primary chamber.

MIN3-6, Disp

66

Peak = 2 psi

Min = -1 psi
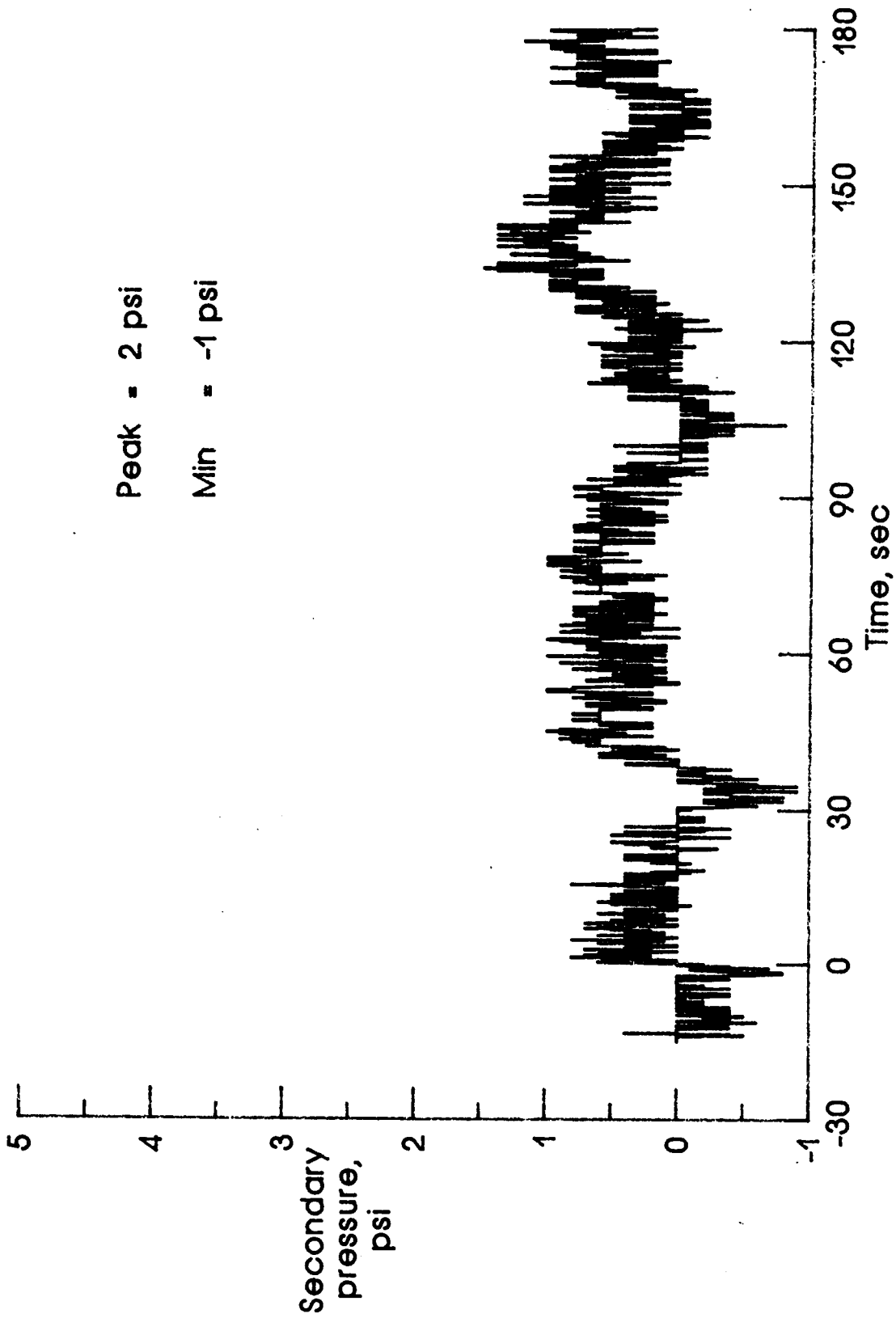
Figure 19g. 1015 psi applied to the primary chamber.

67

MIN3-6, SecPr
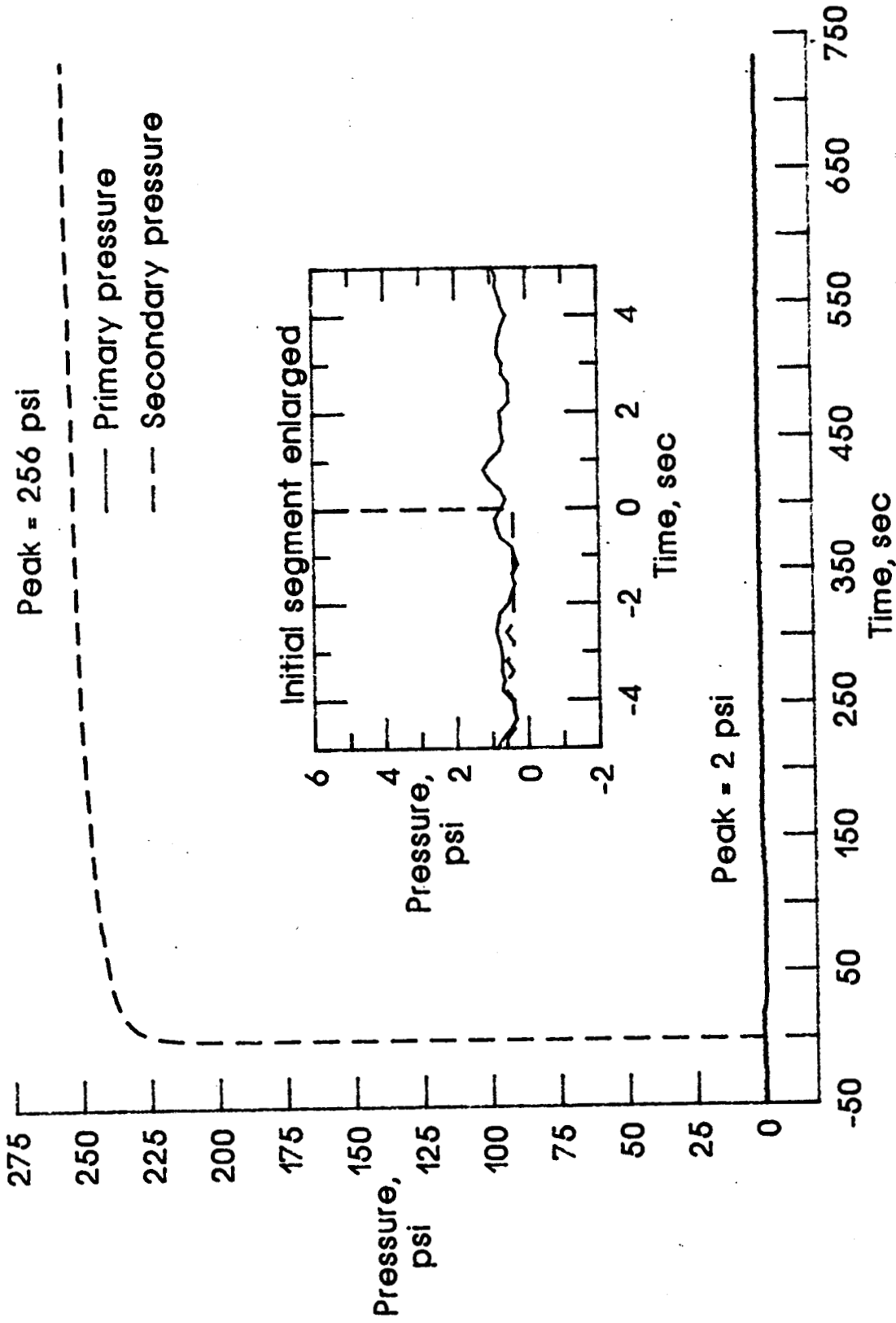
Figure 20a. 250 psi applied to the secondary chamber.

Figure 20. Pressure and displacement curves for the leak check and seal test of a successful seal at an initial squeeze of 3.5%.

MIN4-16, P/P

68

Peak = 0.0654 in.

Min = 0.0649 in.
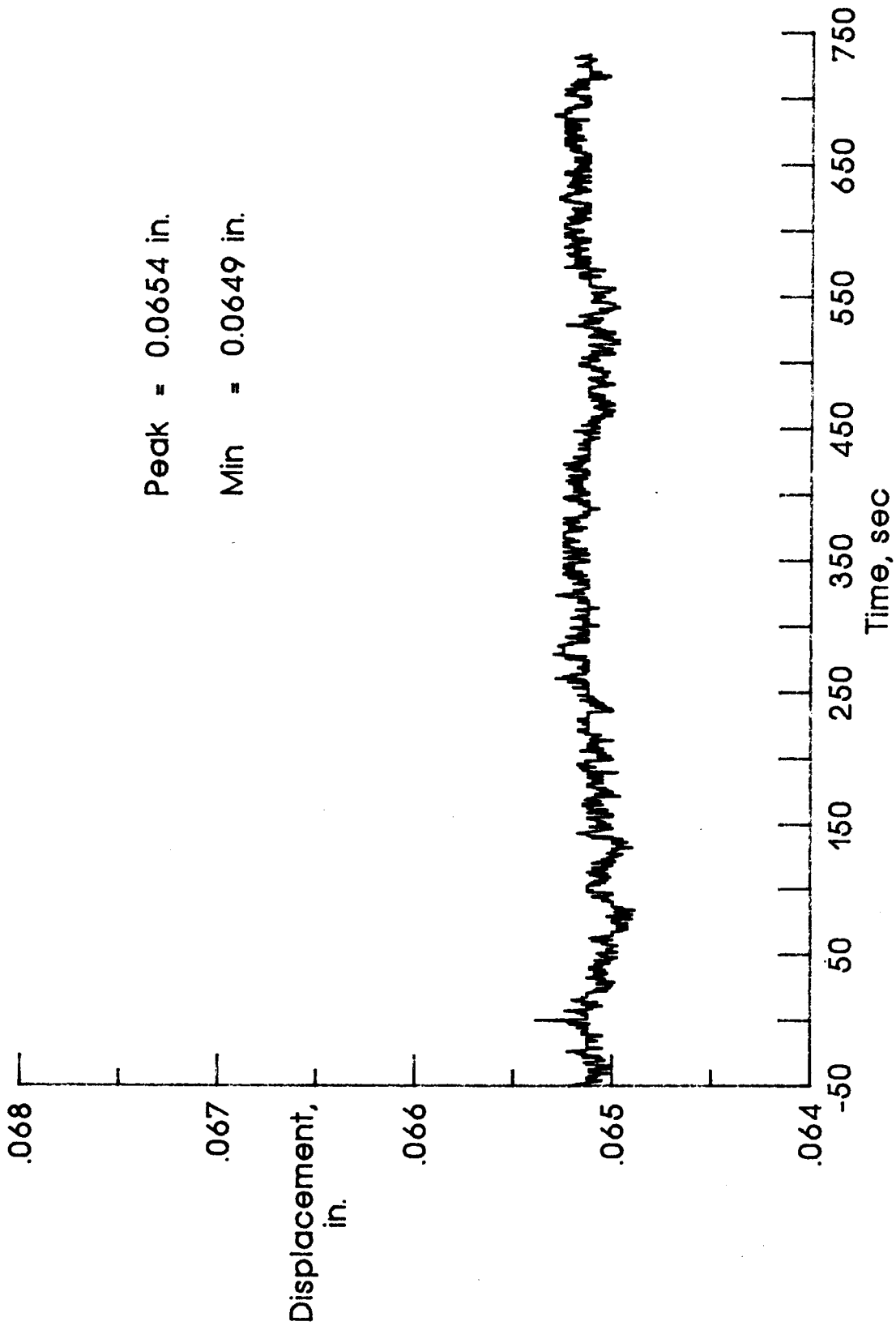
Figure 20b. 250 psi applied to the secondary chamber.

69

MIN4-16, Disp
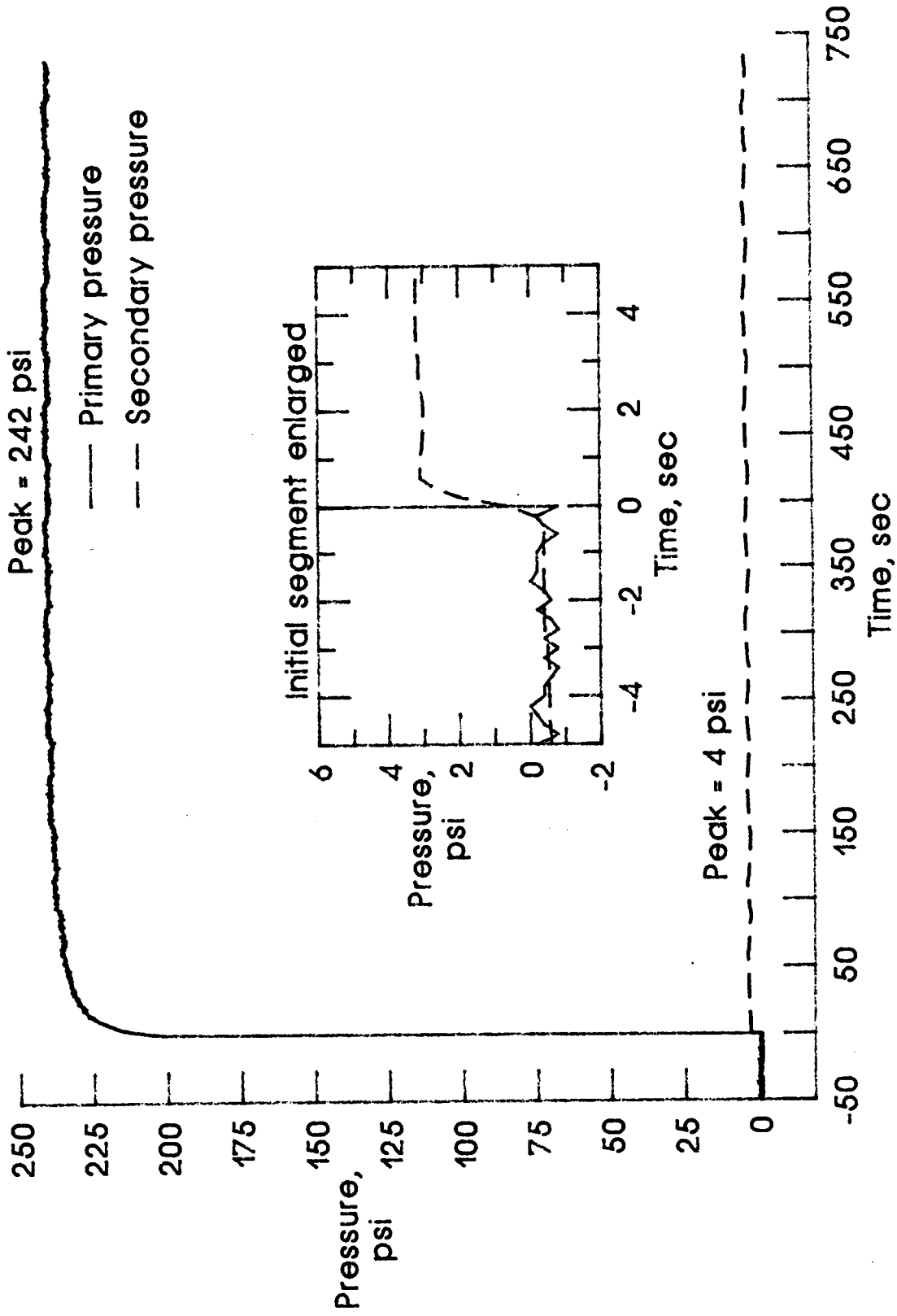
Figure 20c. 250 psi applied to the primary chamber.

70

MIN4-17, P/P

Peak = 0.0652 in.

Min = 0.0647 in.

Displacement, in.

Time, sec
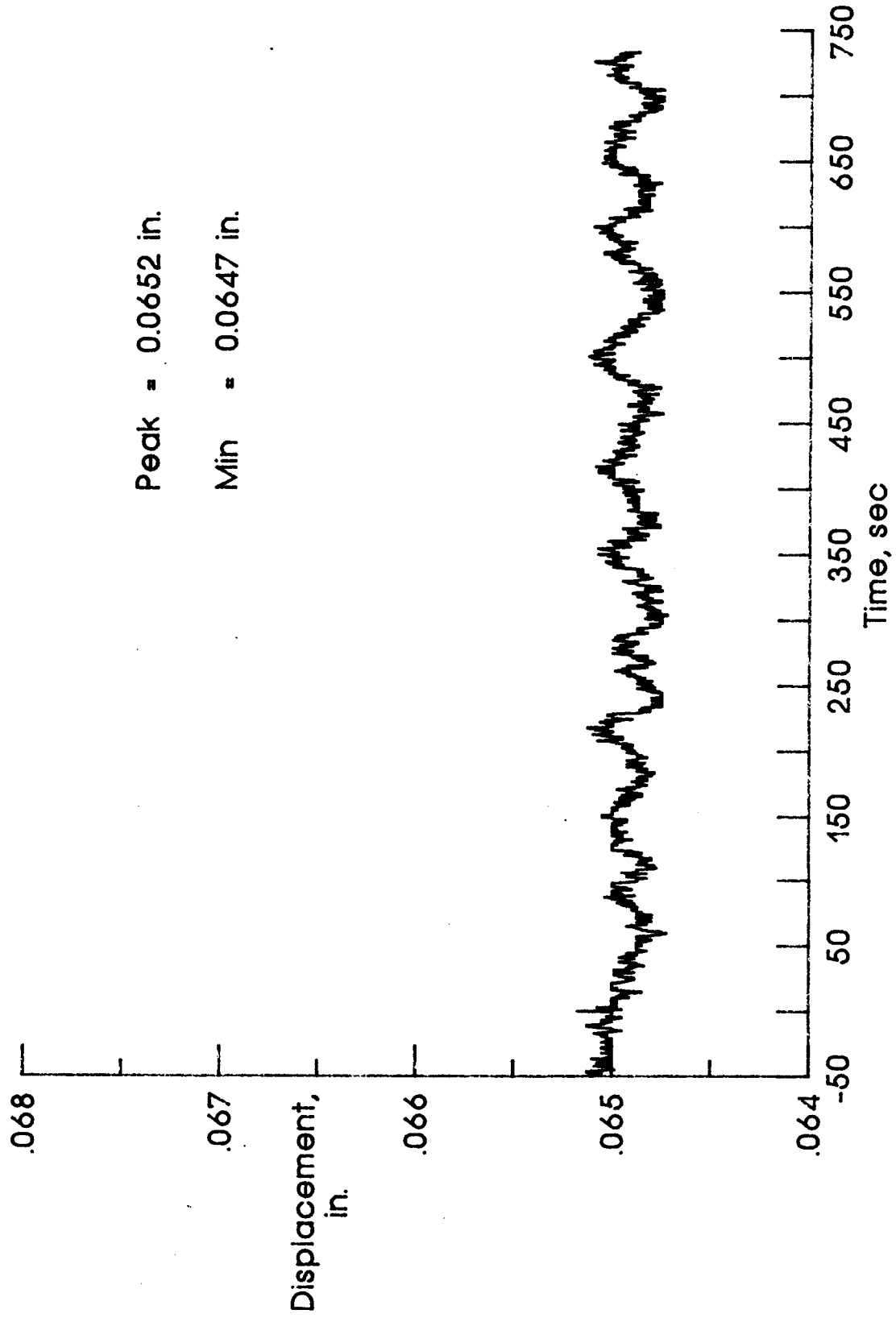
Figure 20d. 250 psi applied to the primary chamber.

71

MIN4-17, Disp
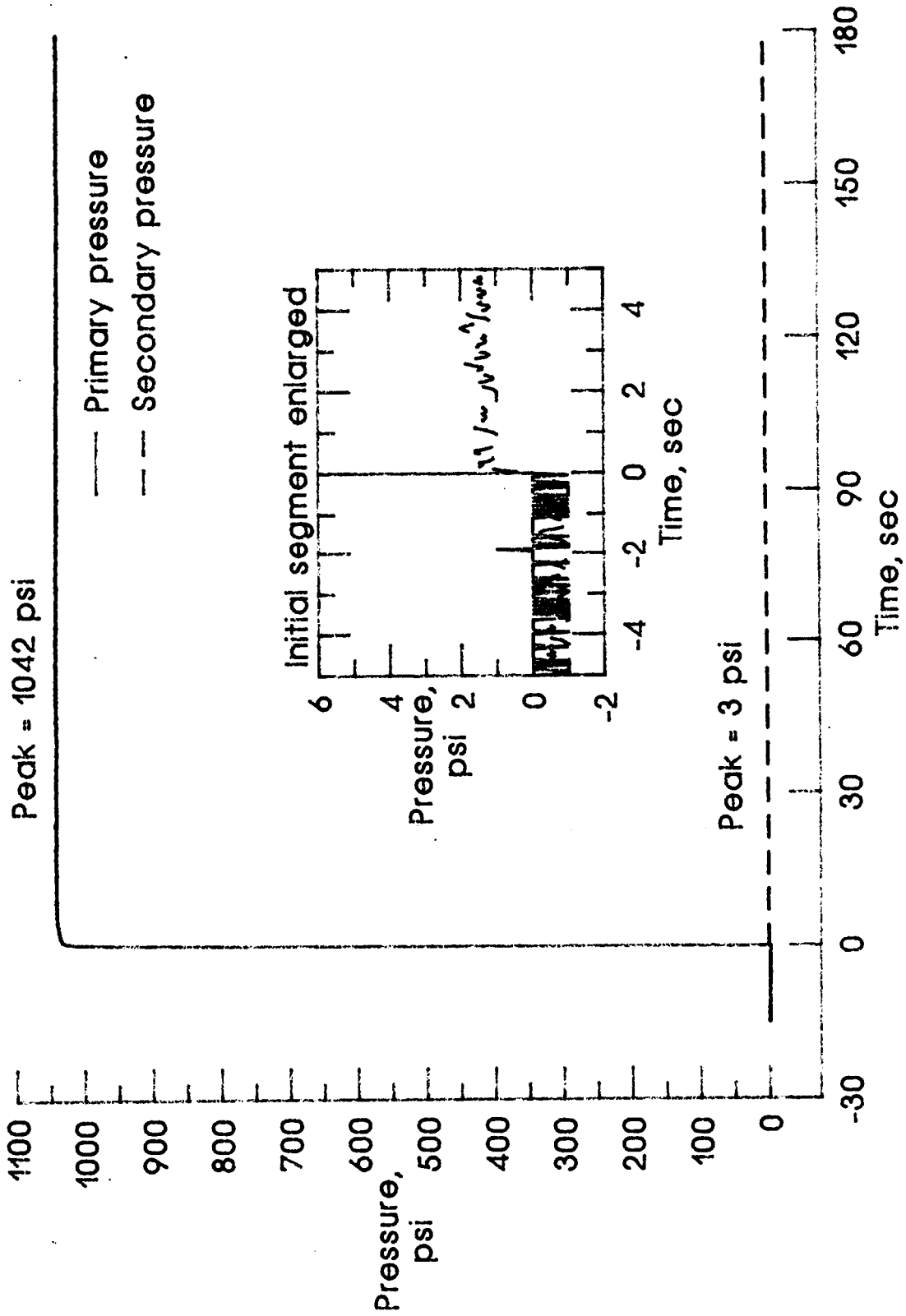
Figure 20e. 1015 psi applied to the primary chamber.

MIN4-18, P/P

72

Peak = 0.0675 in.

Min = 0.0648 in.
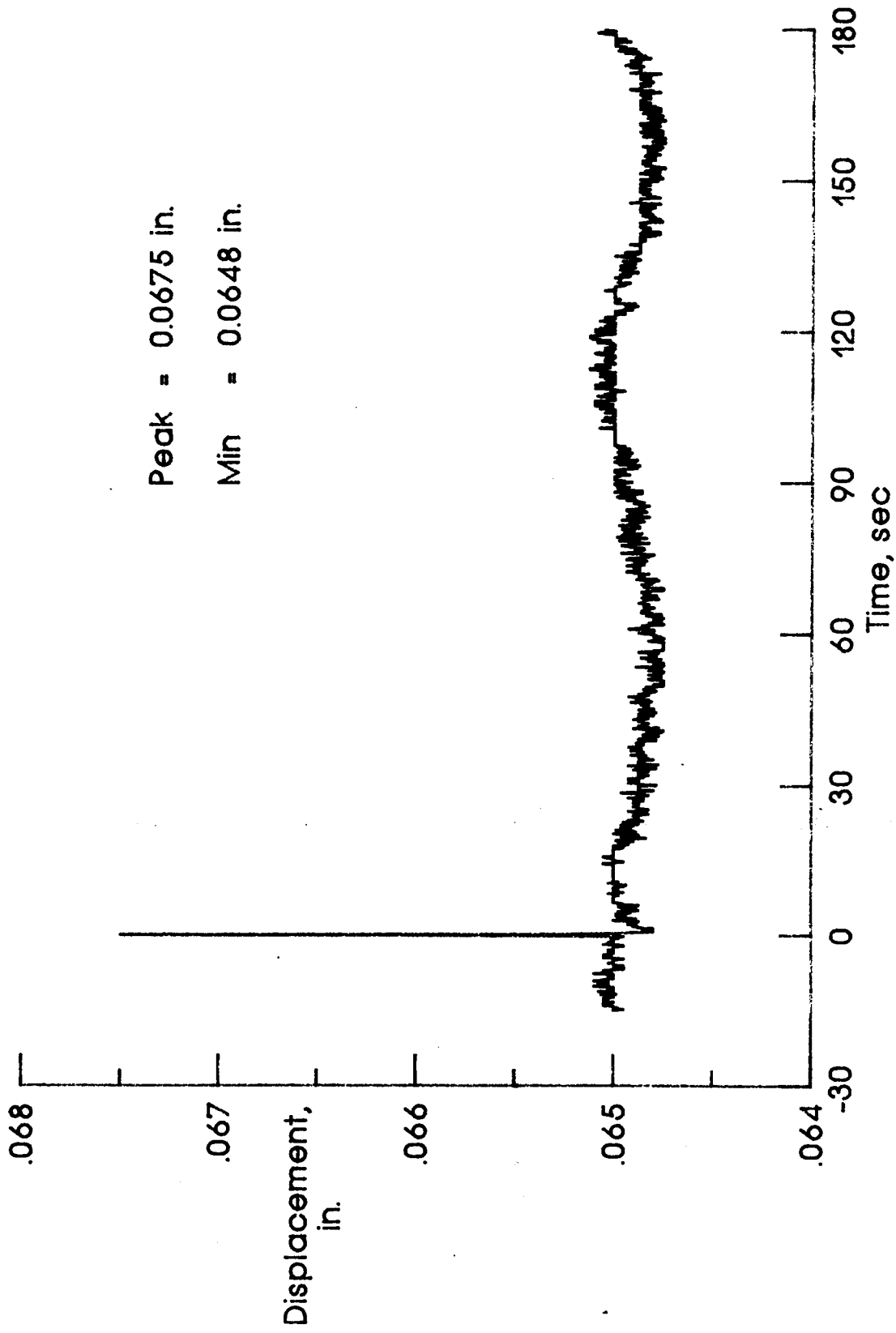
Figure 20f. 1015 psi applied to the primary chamber.

MIN4-18, Disp

73
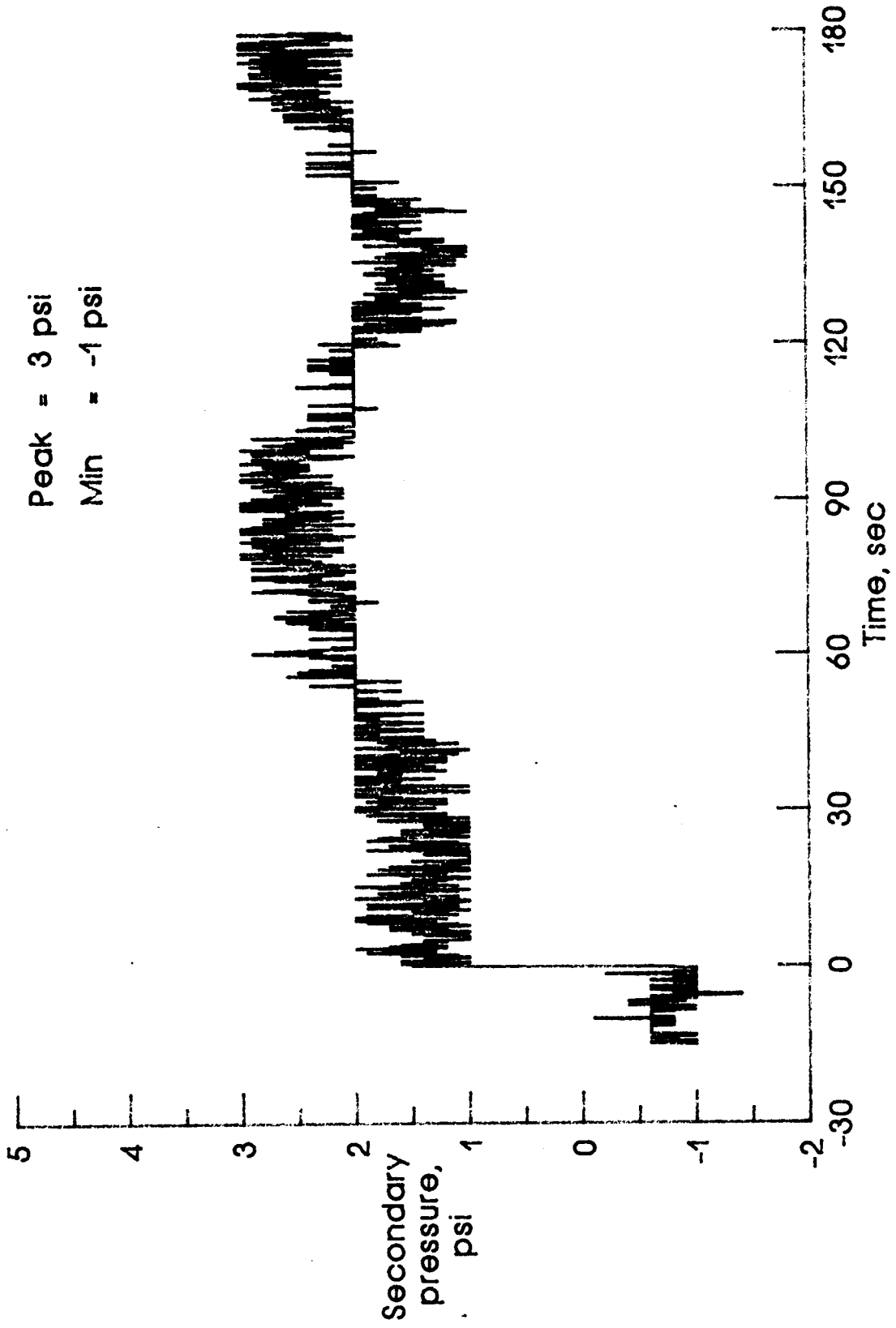
Figure 20g.   1015 psi applied to the primary chamber.

74

MIN4-18, SecPr
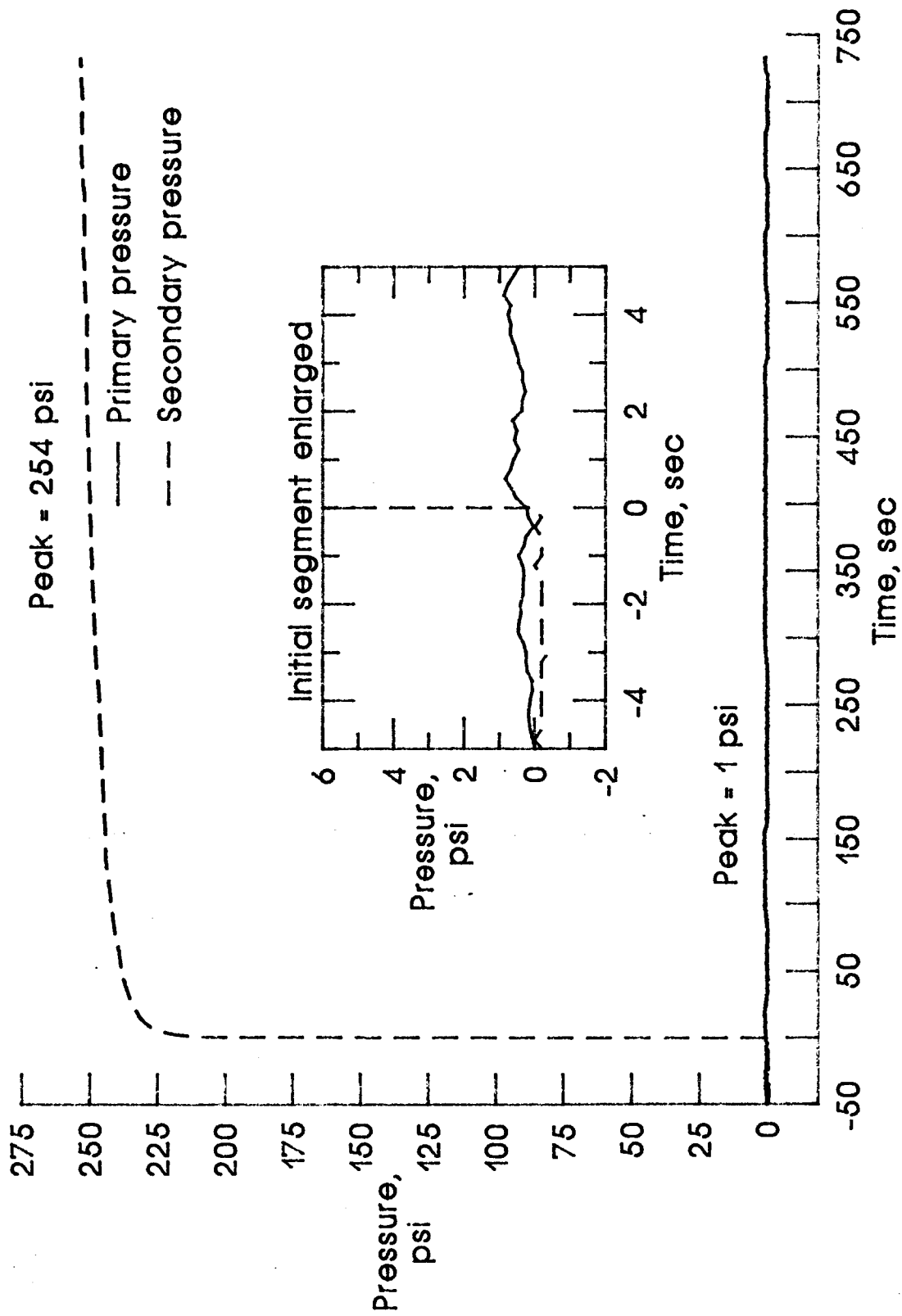
Figure 21a. 250 psi applied to the secondary chamber.

Figure 21. Pressure and displacement curves for the leak check and seal test for a successful seal at an initial squeeze of 1.7%.

MIN1-16, P/P

75
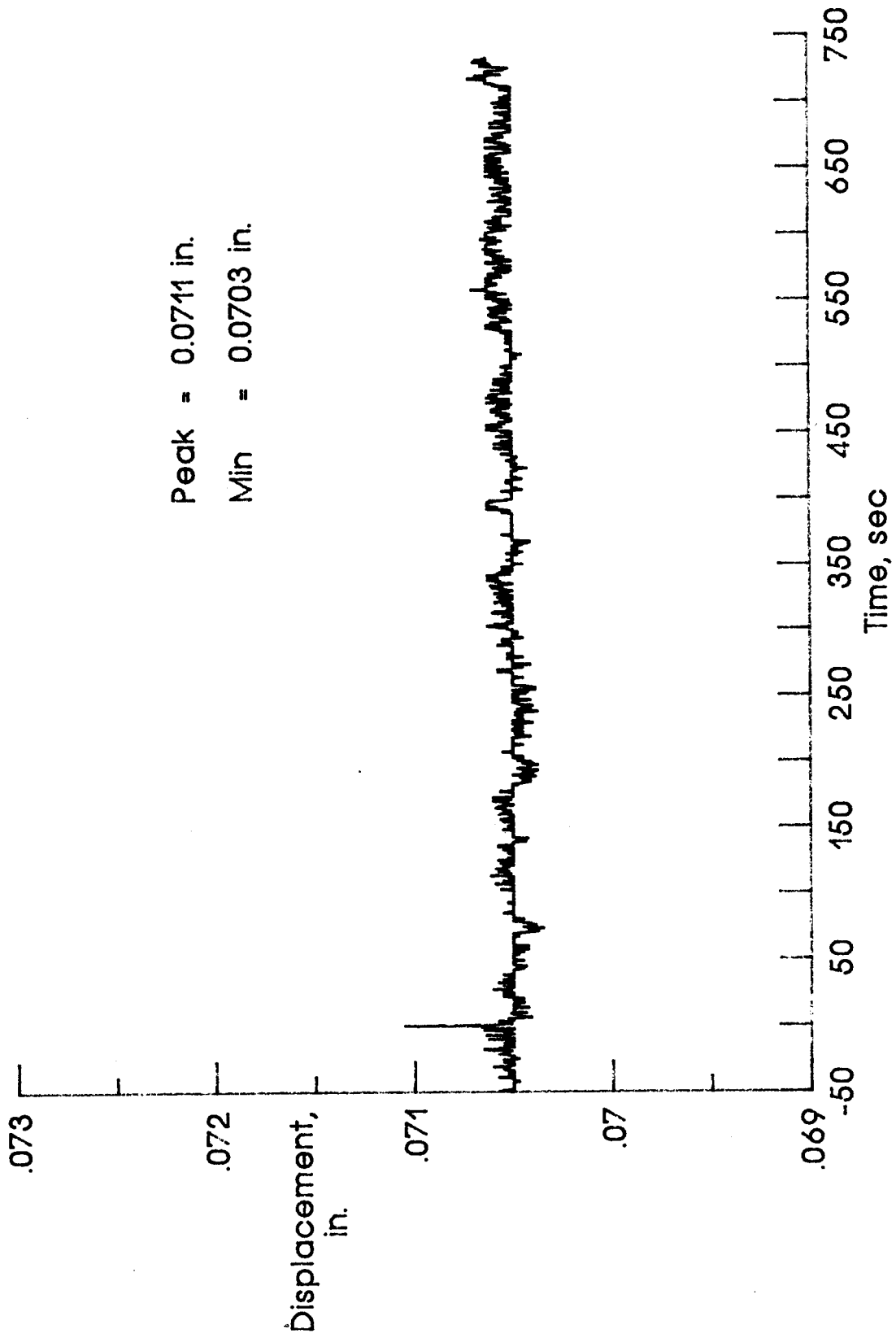
Figure 21b.   250 psi applied to the secondary chamber.

MIN1-16, Disp

76
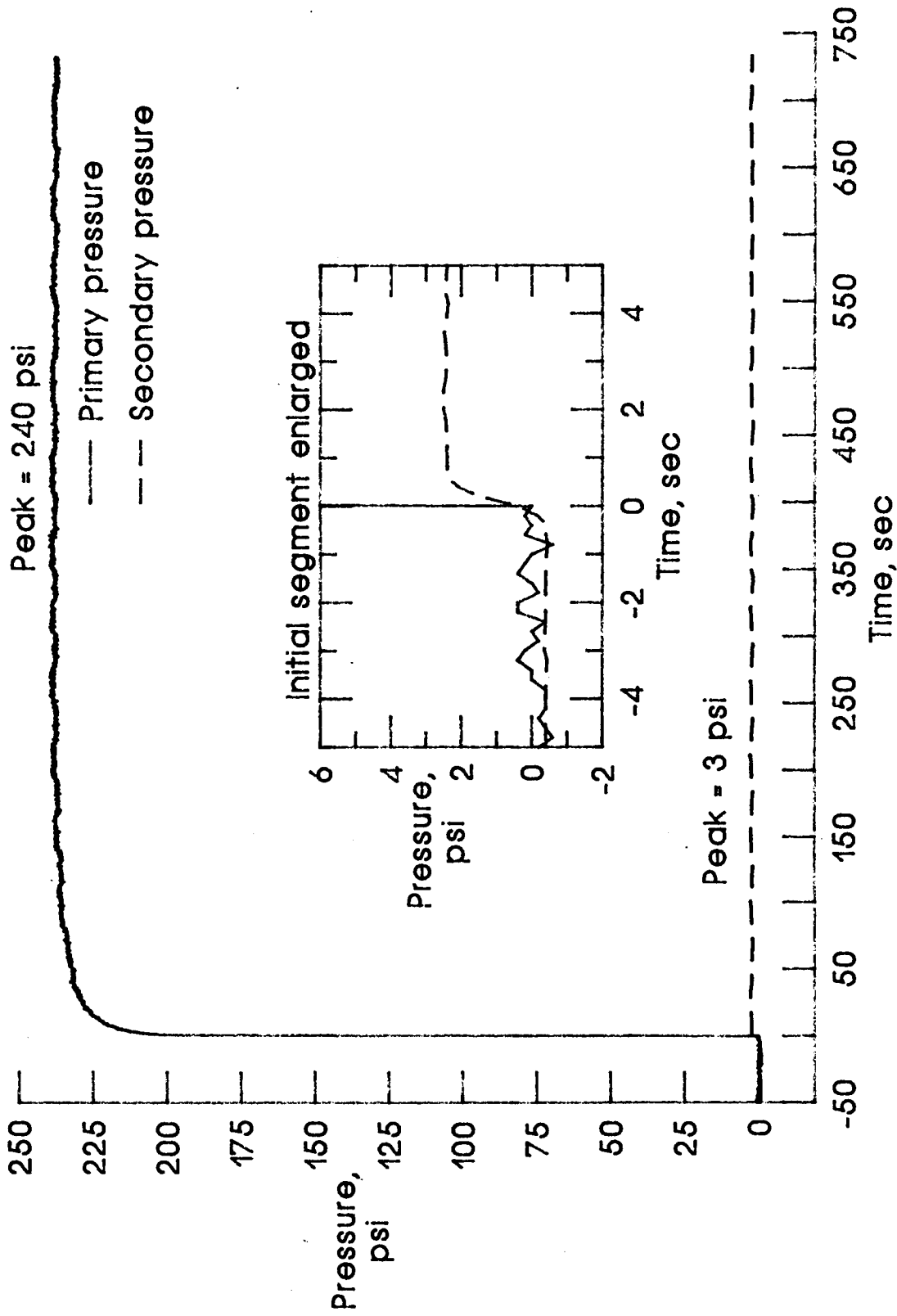
Figure 21c. 250 psi applied to the primary chamber.

MIN1-17,P/P

77
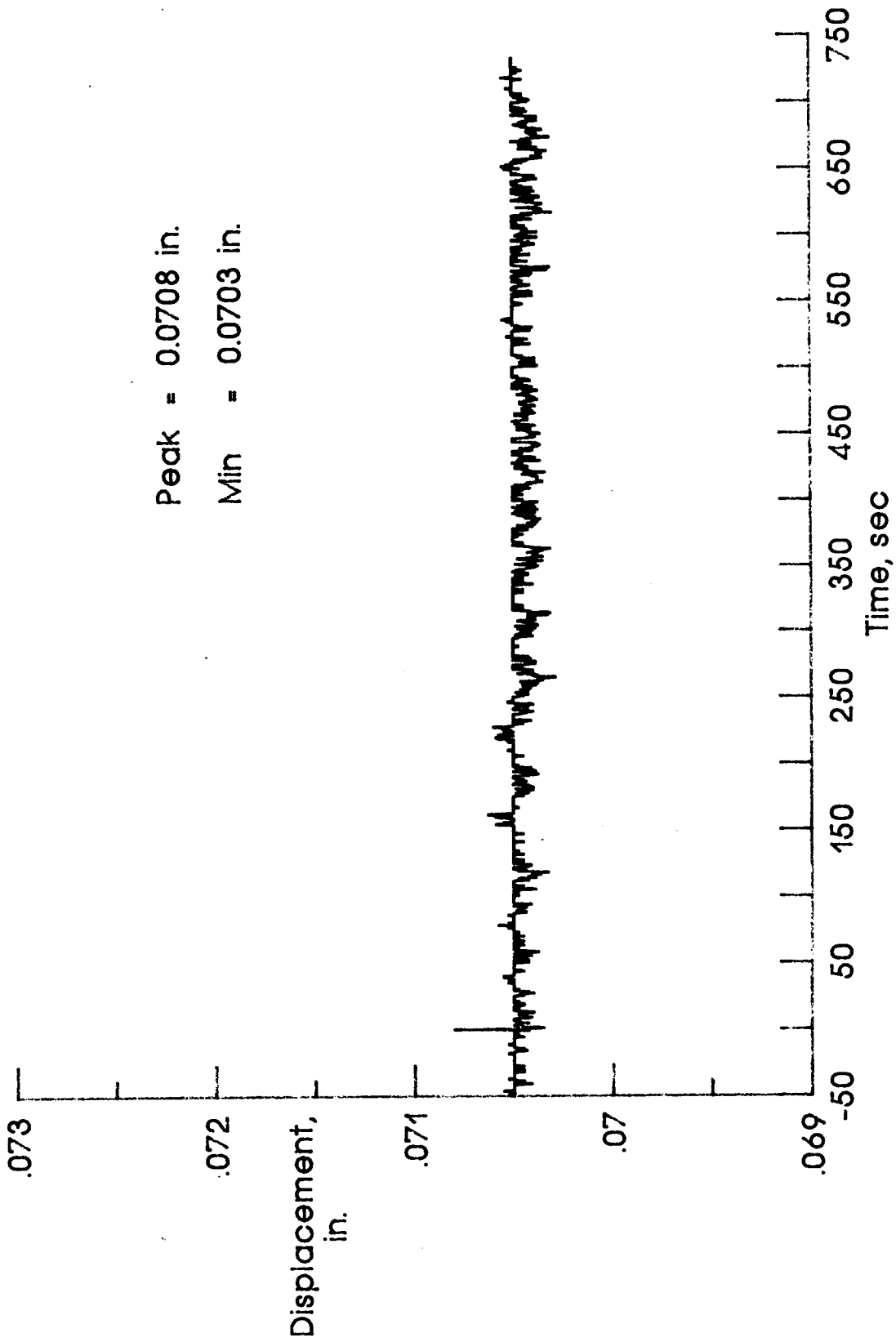
Figure 21d.   250 psi applied to the primary chamber.

MIN1-17, Disp
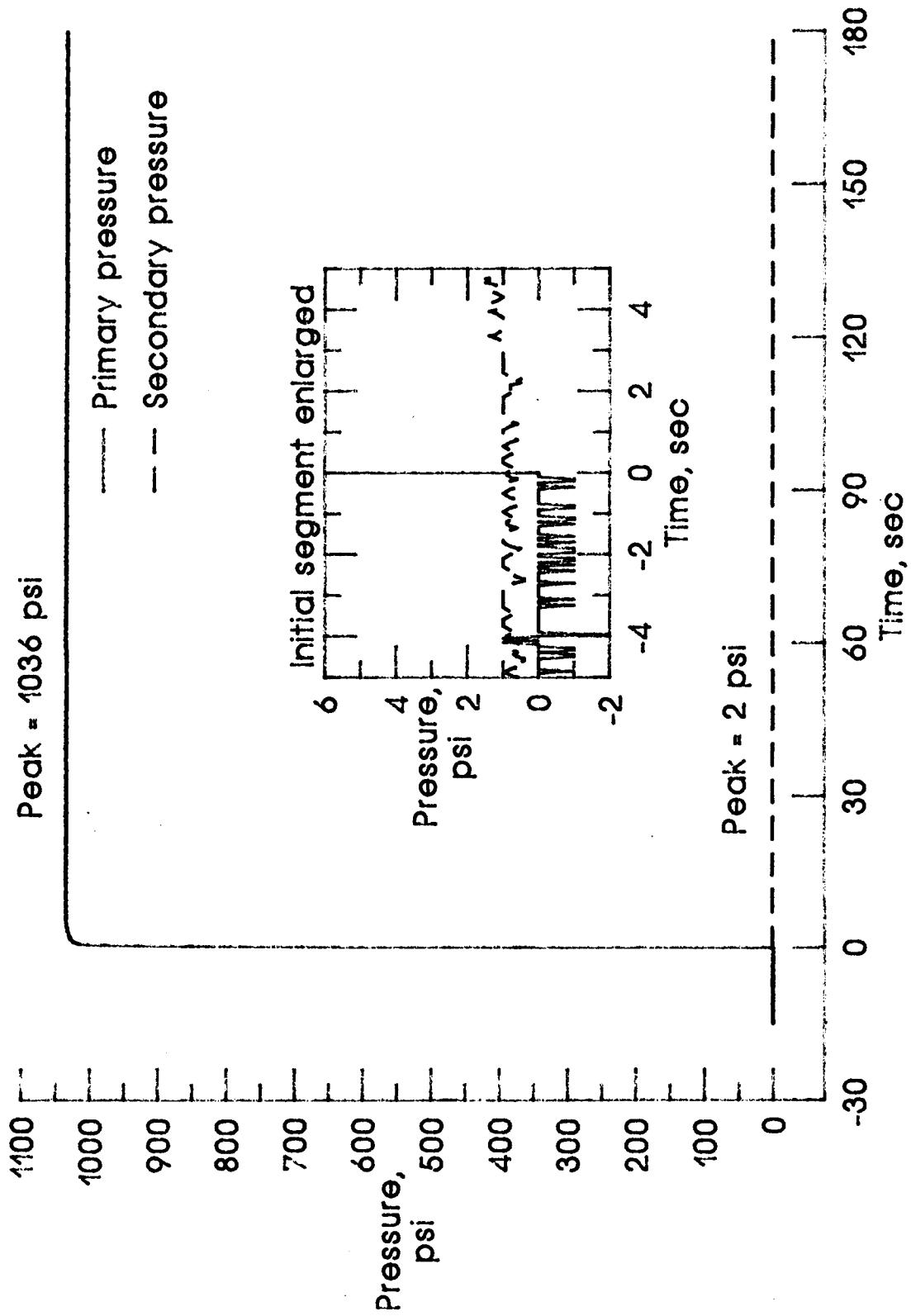
Figure 21e.   1015 psi applied to the primary chamber.

MIN1-18,P/P

79
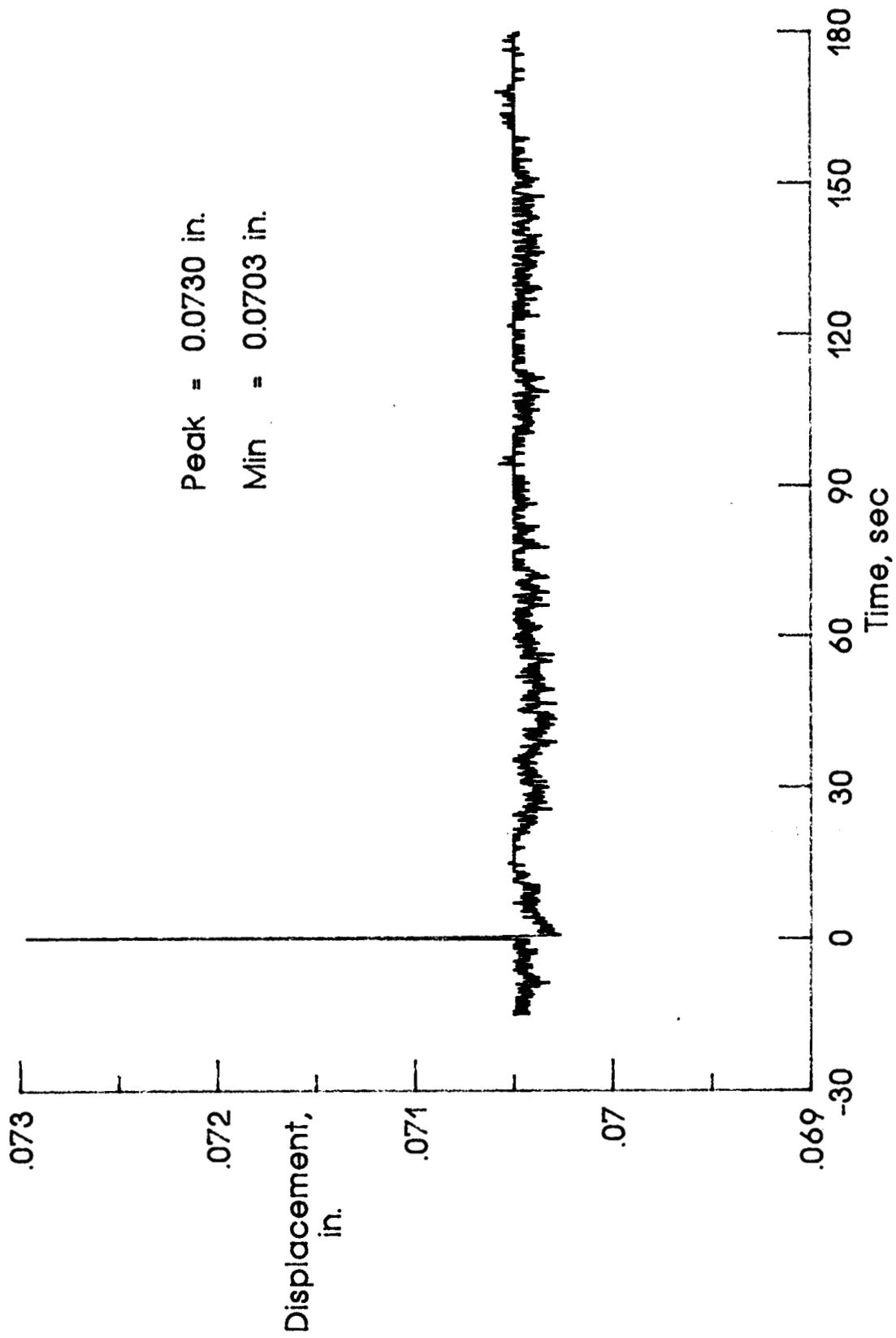
Figure 21f.   1015 psi applied to the primary chamber.

MIN1-18,Disp
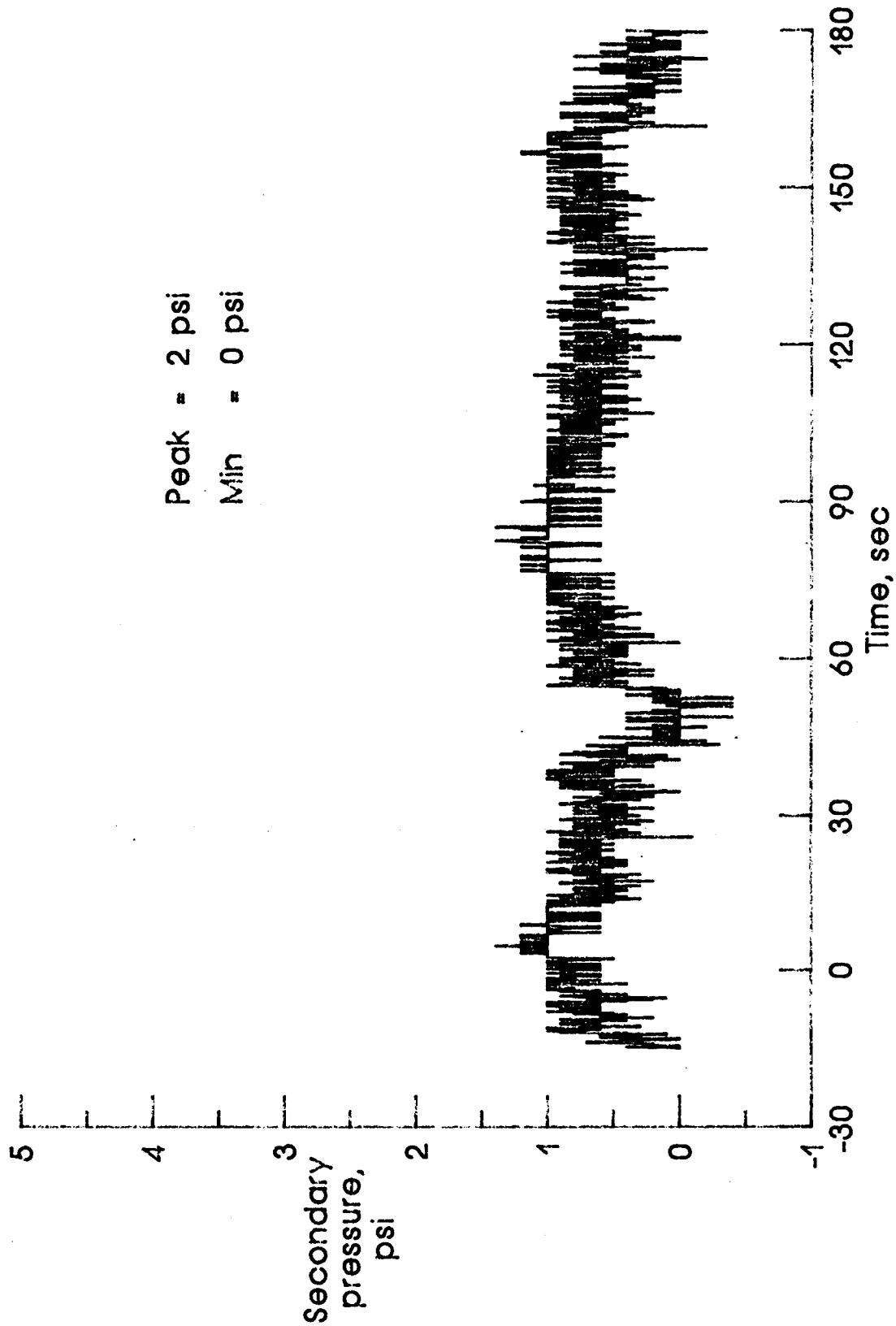
Figure 21g. 1015 psi applied to the primary chamber.

MIN1-18,SecPr
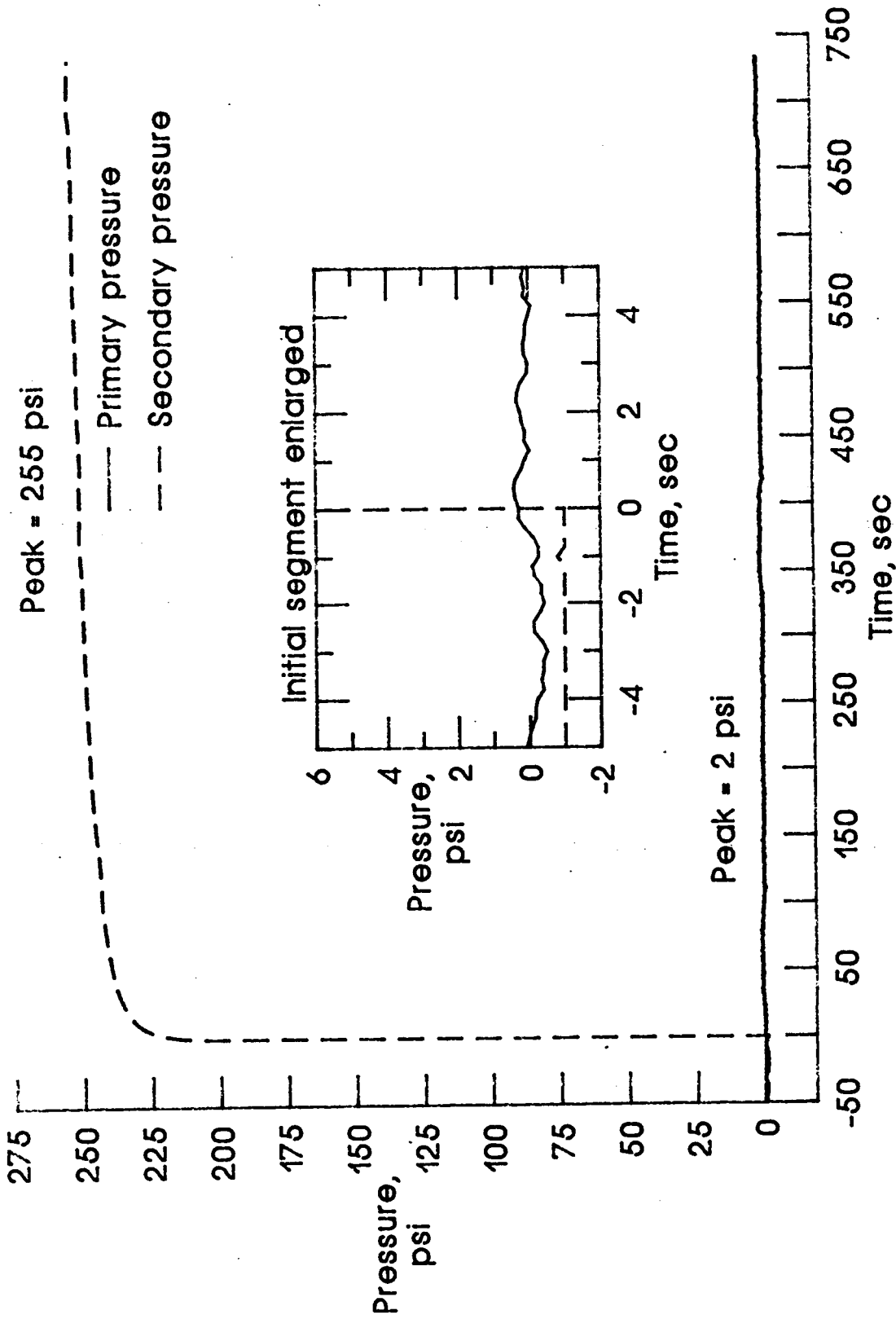
Figure 22a. 250 applied to the secondary chamber.

Figure 22. Pressure and displacement curves for the leak check and seal test
for a successful seal at an initial squeeze of 1.7%.

MIN5-4, P/P

82
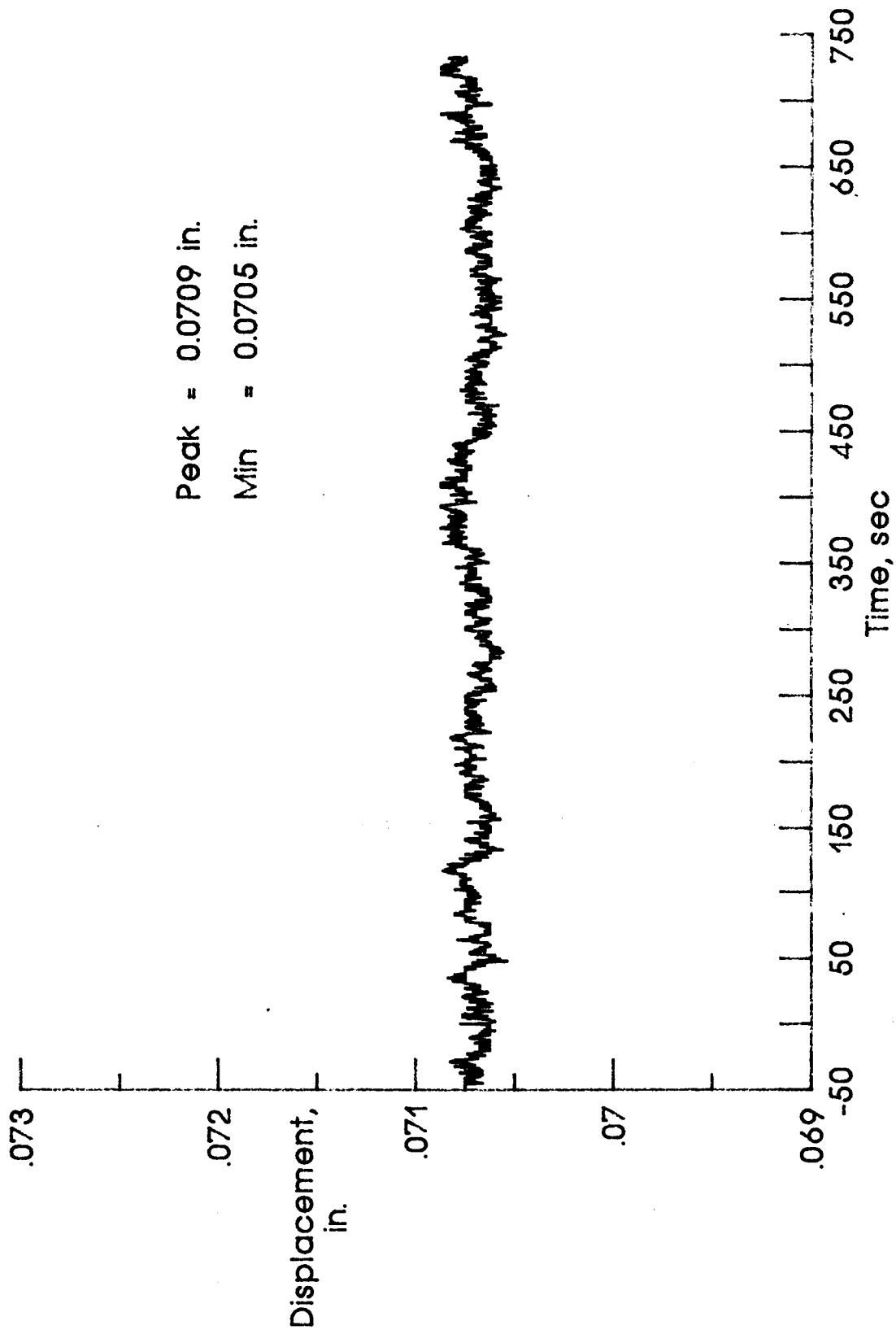
Figure 22b. 250 psi applied to the secondary chamber.

MIN5-4, Disp
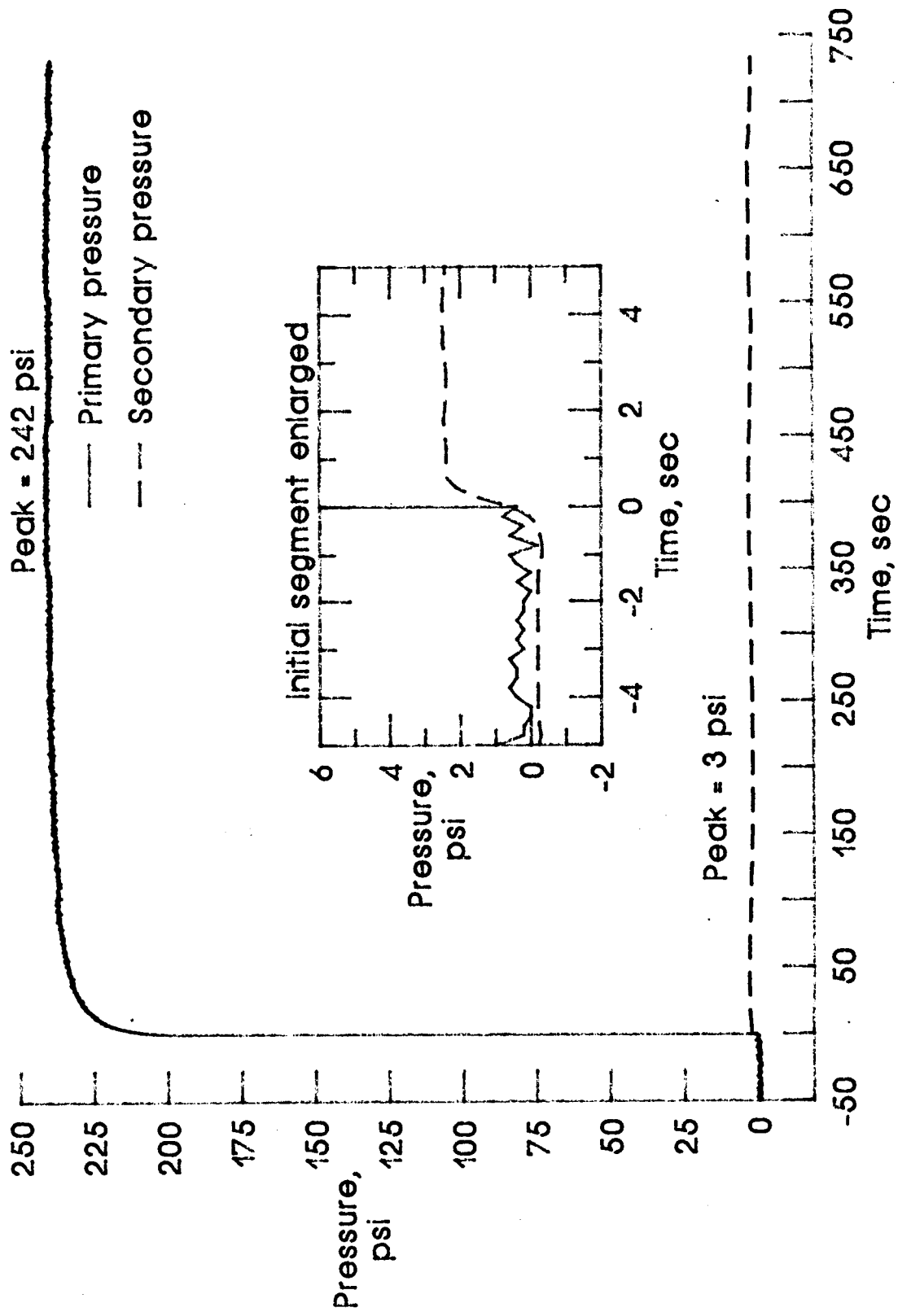
Figure 22c. 250 psi applied to the primary chamber.

MIN5-5,P/P

84

Displacement, in.

.073

.072

.071

.07

.069

Peak = 0.0710 in.

Min = 0.0704 in.

-50   50   150   250   350   450   550   650   750

Time, sec
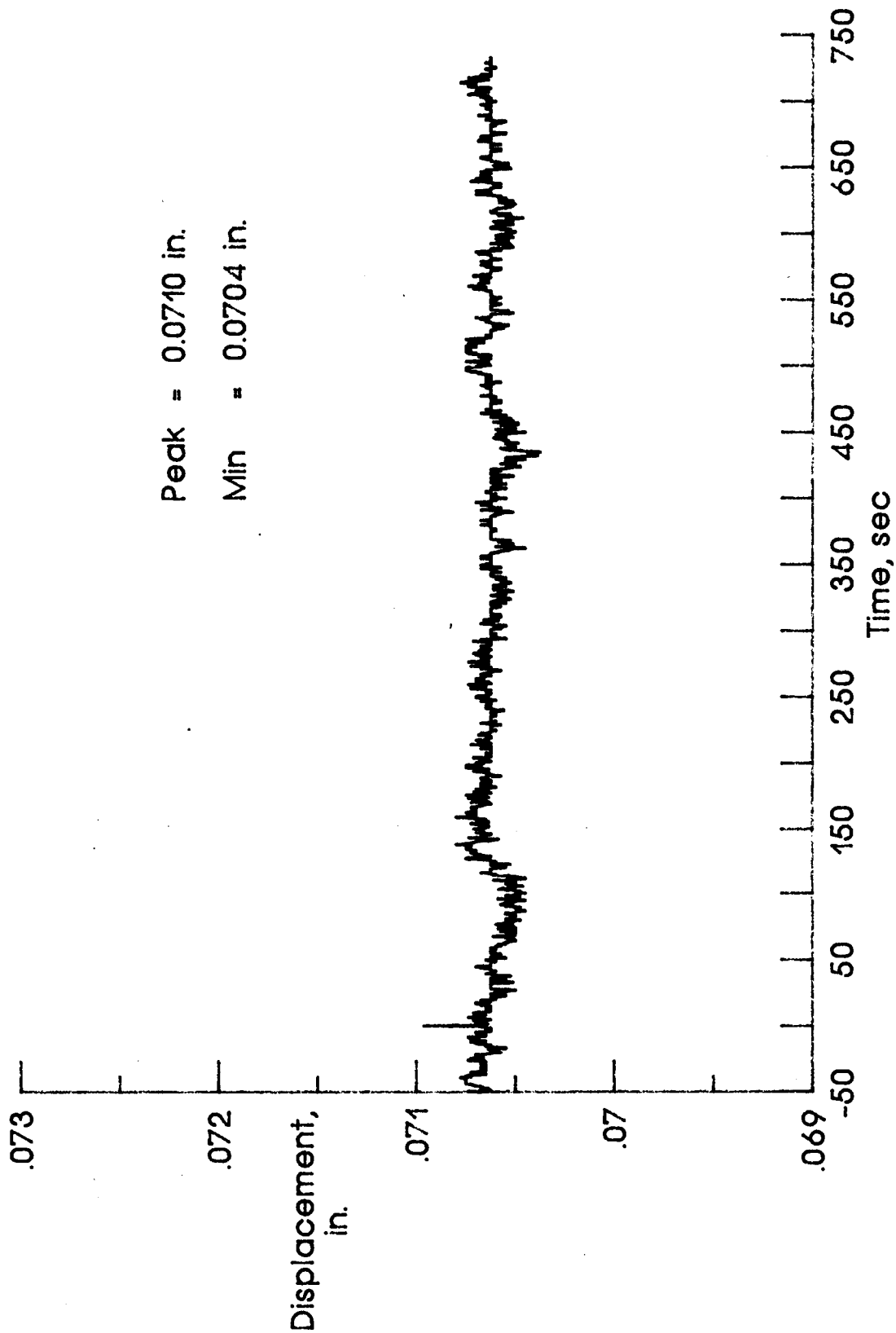
Figure 22d.   250 psi applied to the primary chamber.

MIN5-5, Disp

85
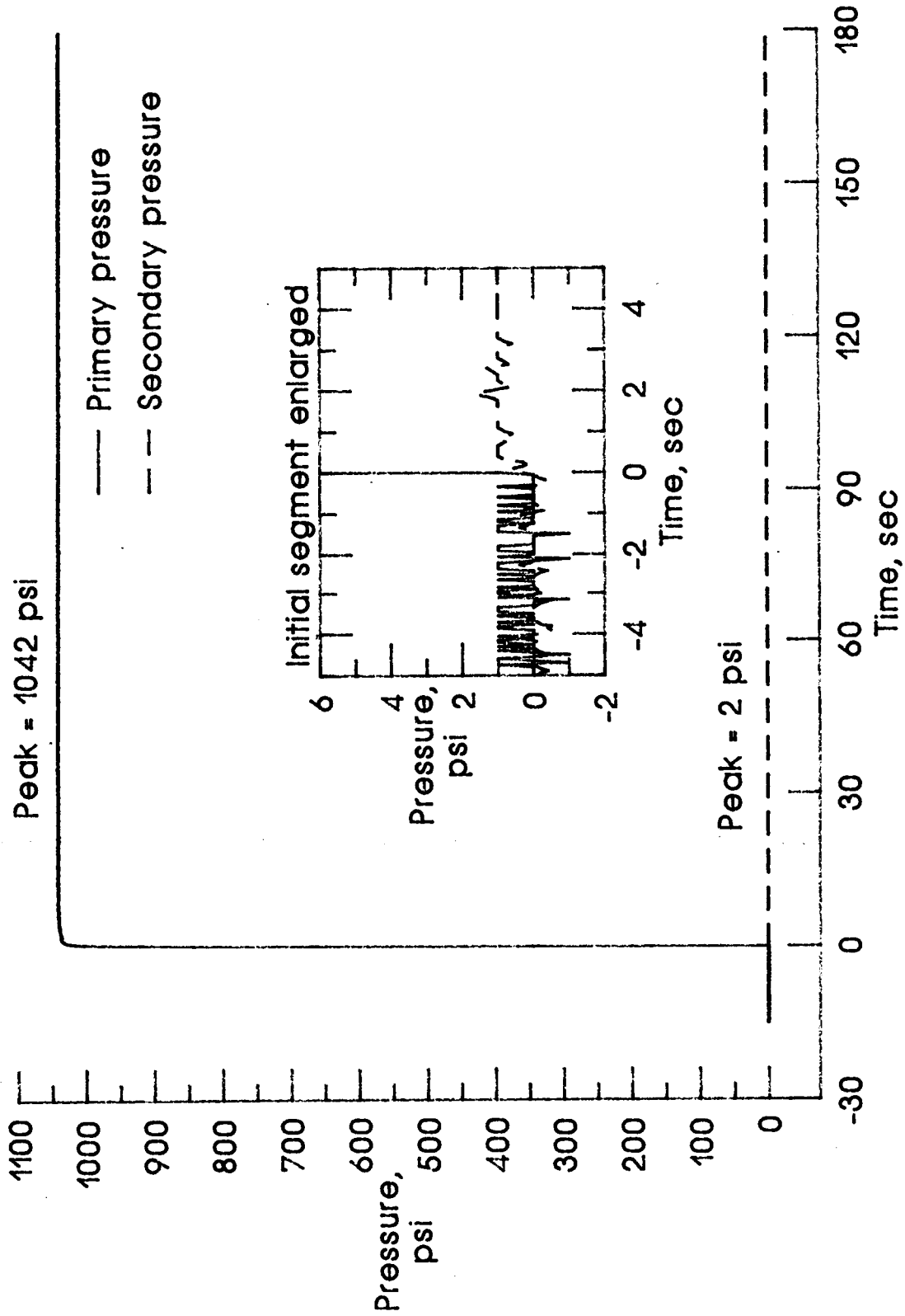
Figure 22e. 1015 psi applied to the primary chamber.

86

MIN5-6,P/P
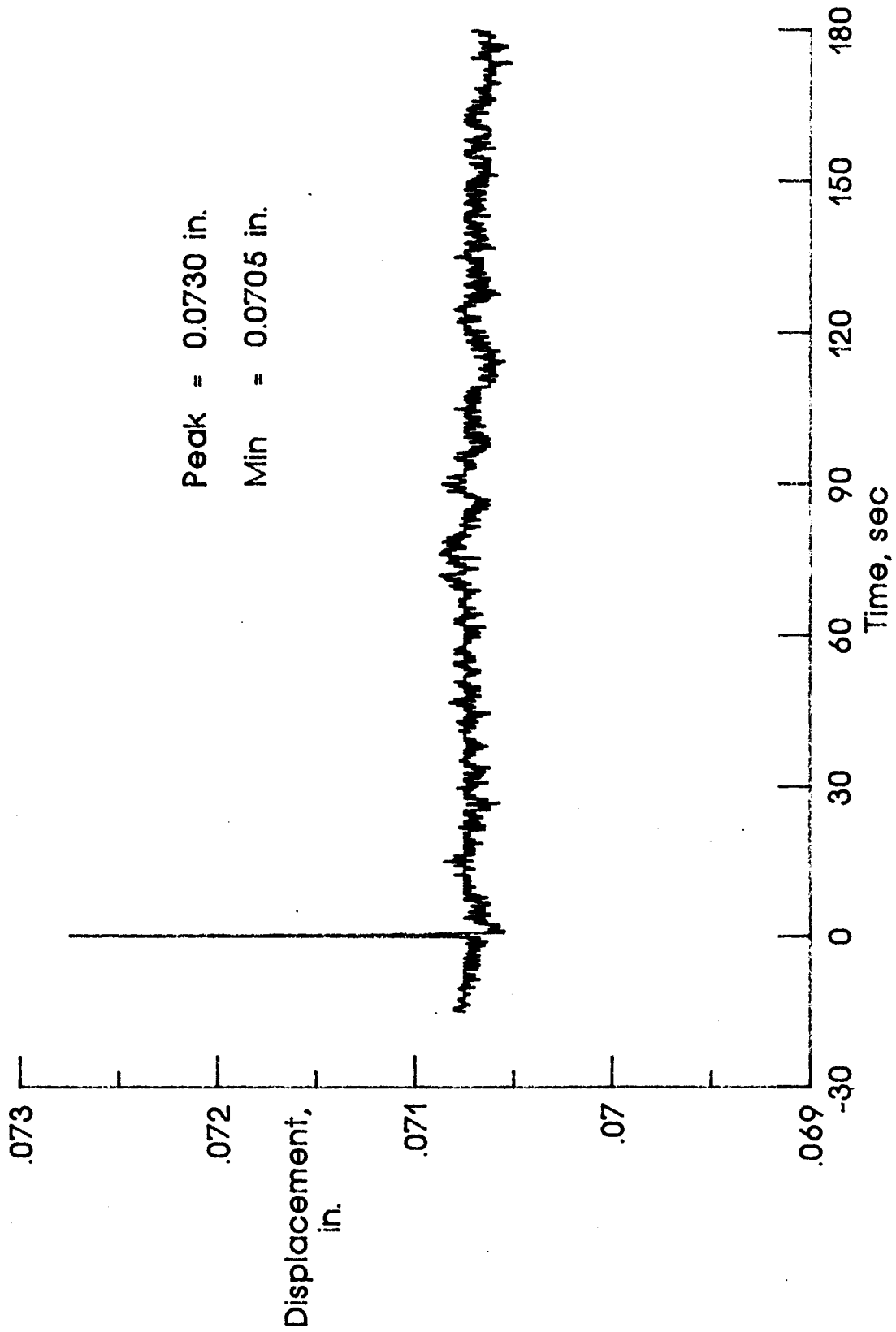
Figure 22f. 1015 psi applied to the primary chamber.

MIN5-6,Disp

87
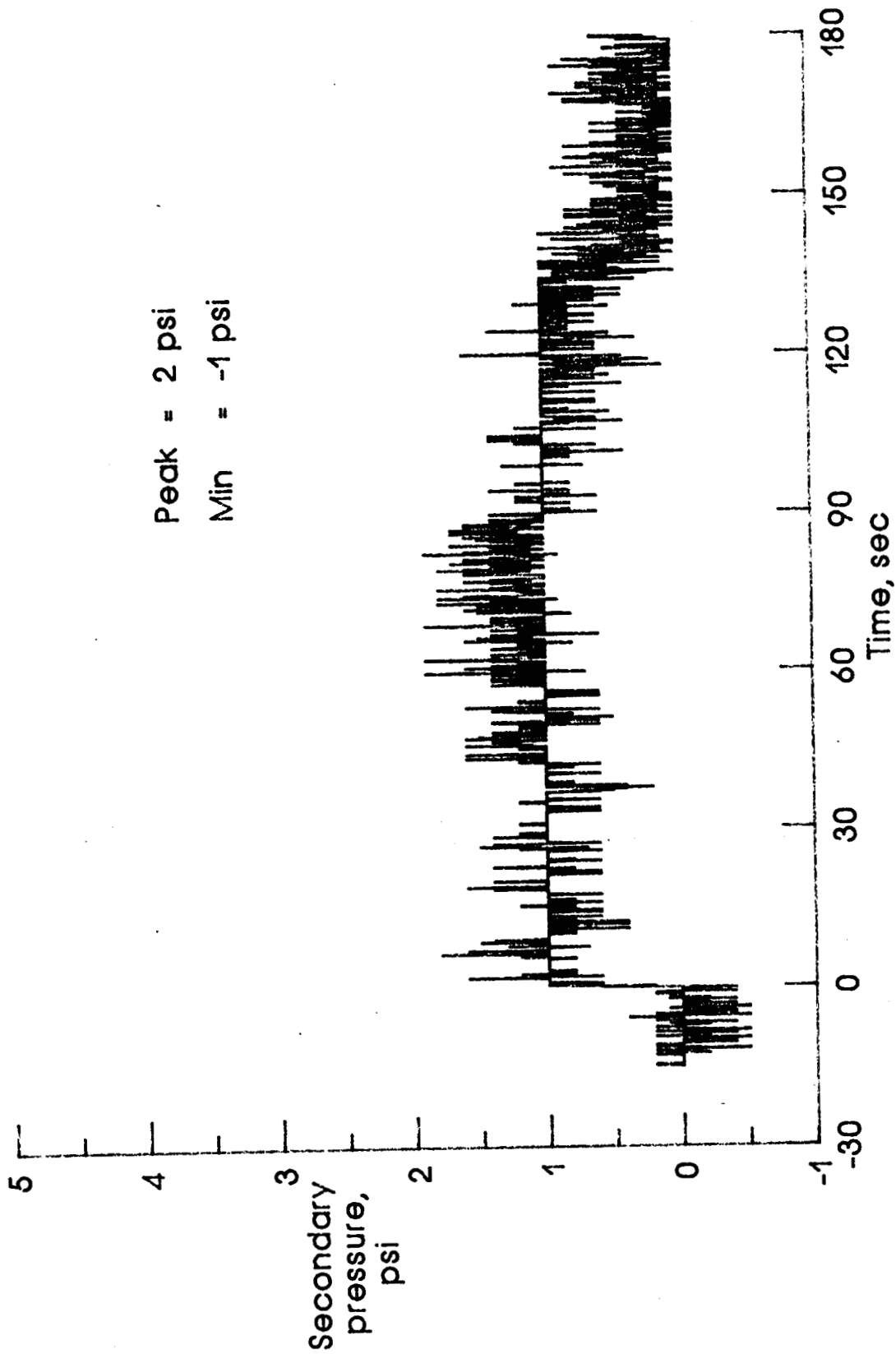
Figure 22g. 1015 psi applied to the primary chamber.

MIN5-6,SecPr
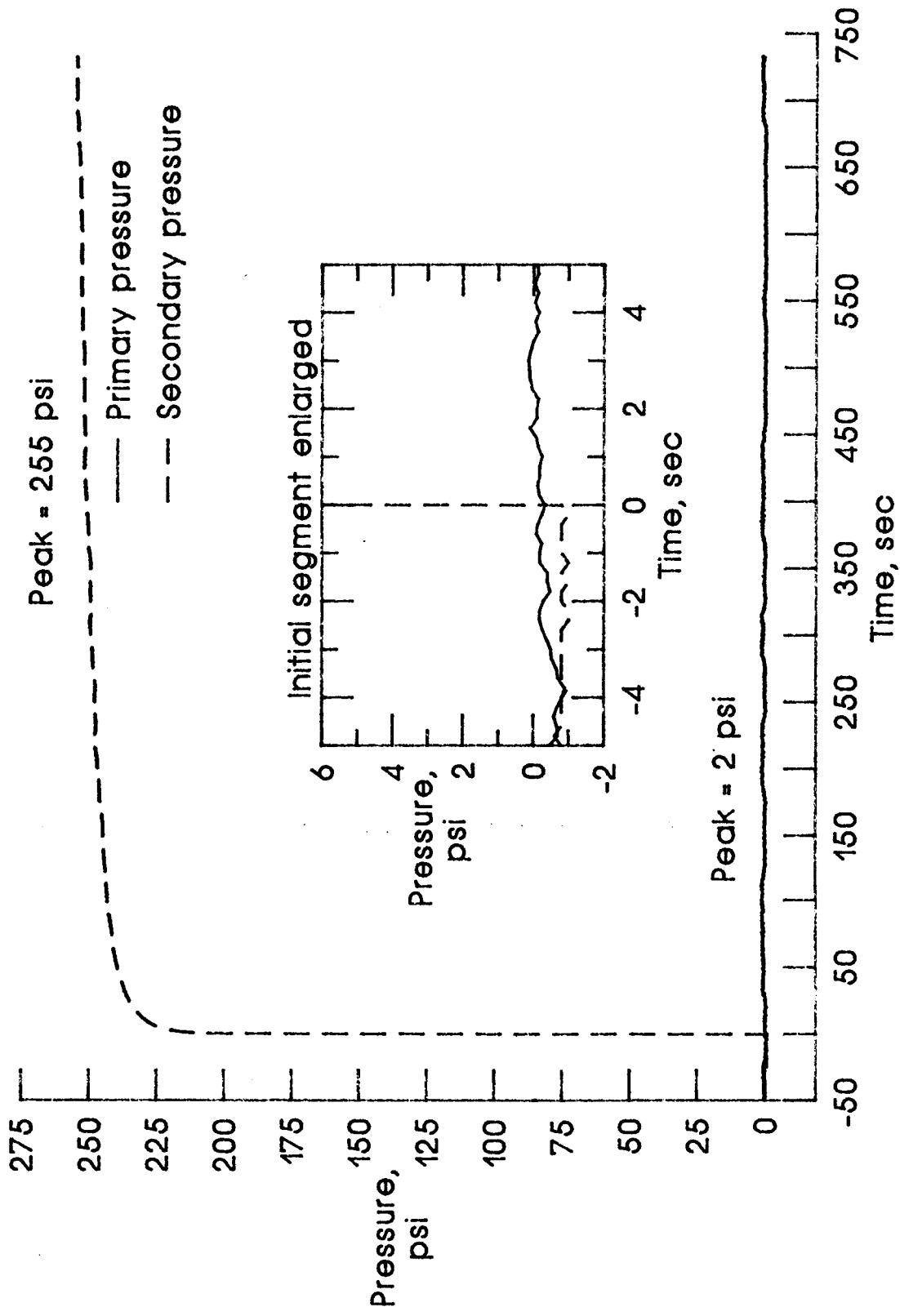
Figure 23a. 250 psi applied to the secondary chamber.

Figure 23. Pressure and displacement curves for the leak check and seal test for a successful seal at an initial squeeze of 1.7%.

MIN3-10, P/P

89
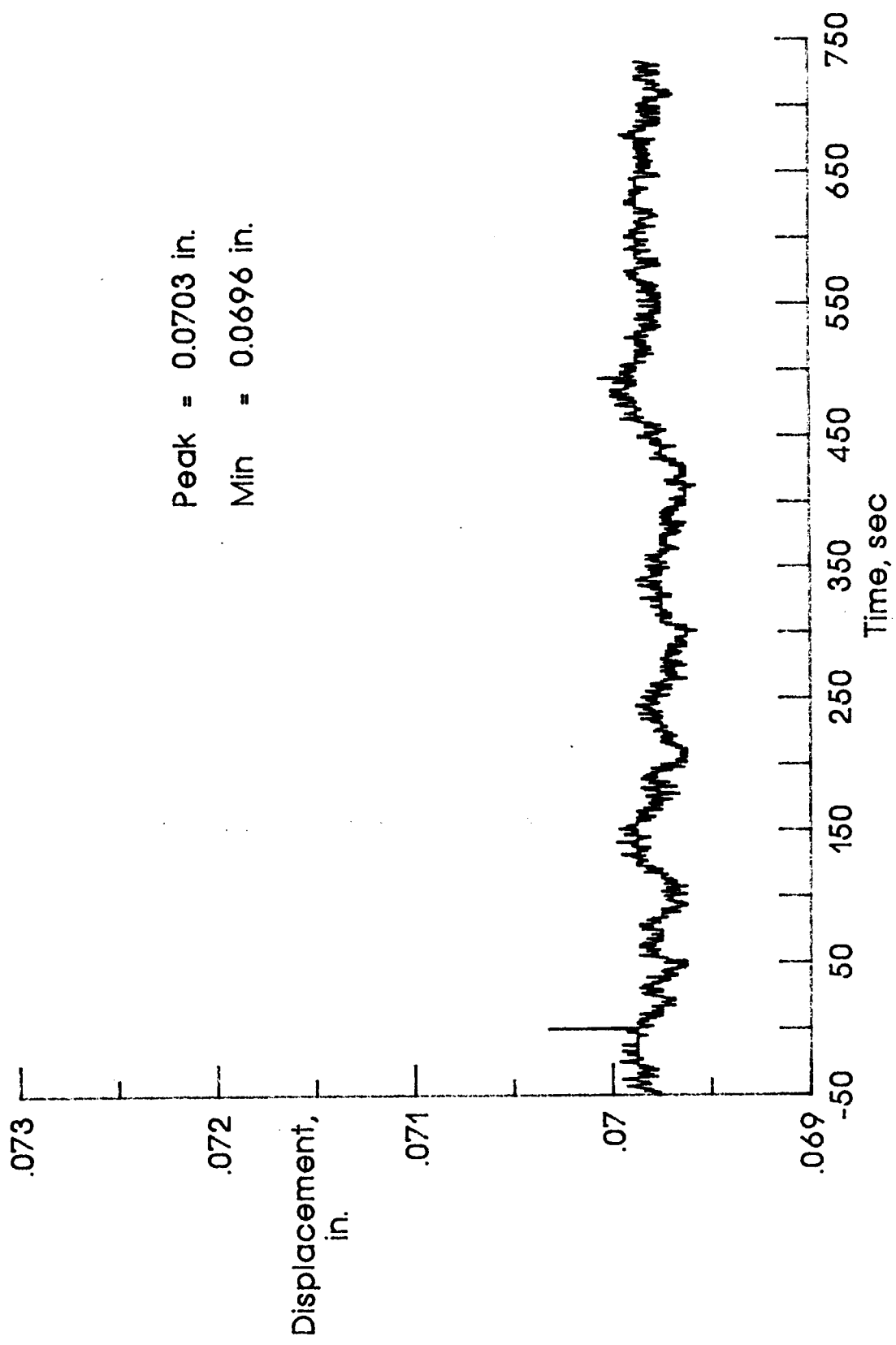
Figure 23b. 250 psi applied to the secondary chamber.

MIN3-10, Disp

90
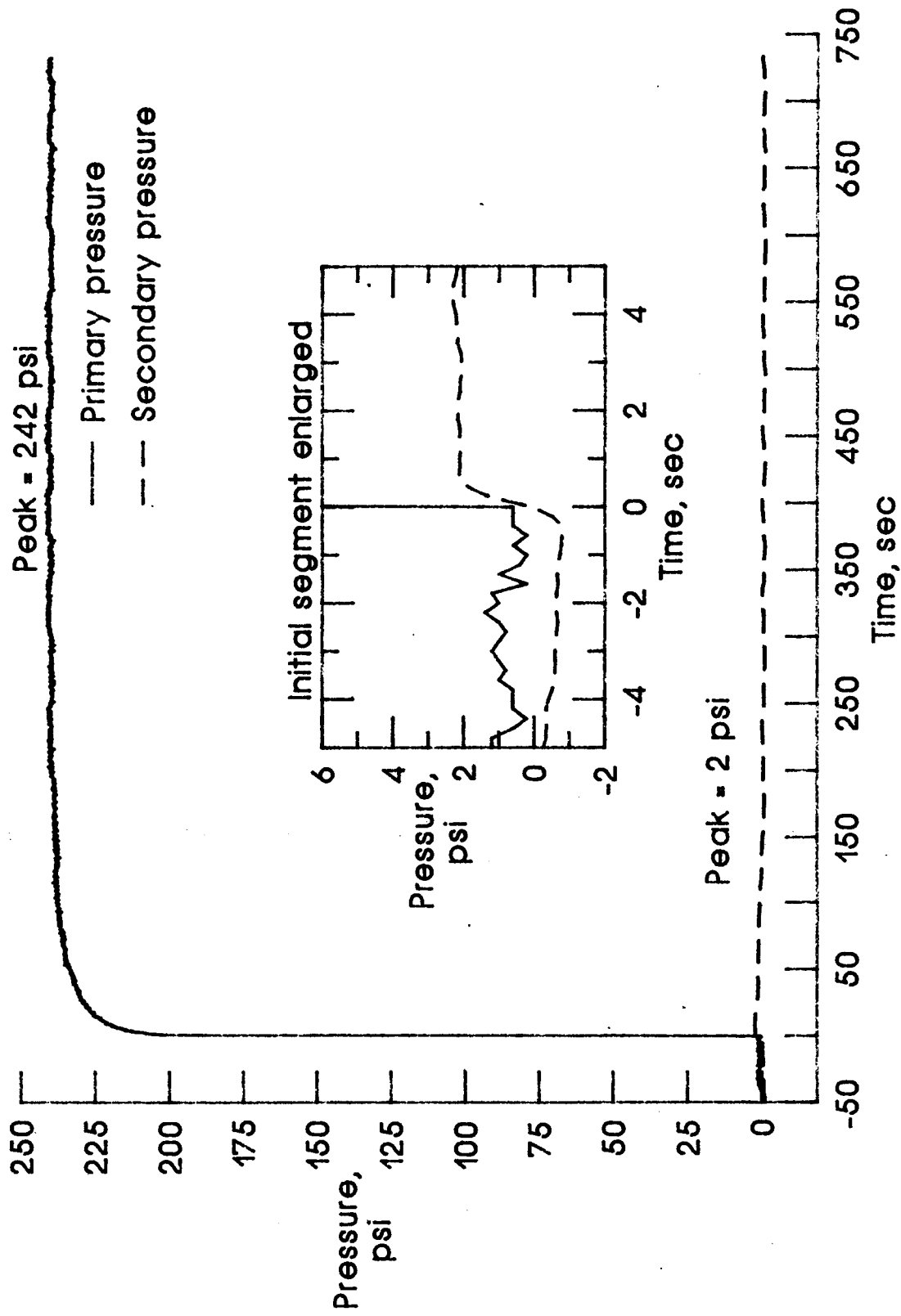
Figure 23c. 250 psi applied to the primary chamber.

91

MIN3-11,P/P

Peak = 0.0698 in.

Min = 0.0693 in.
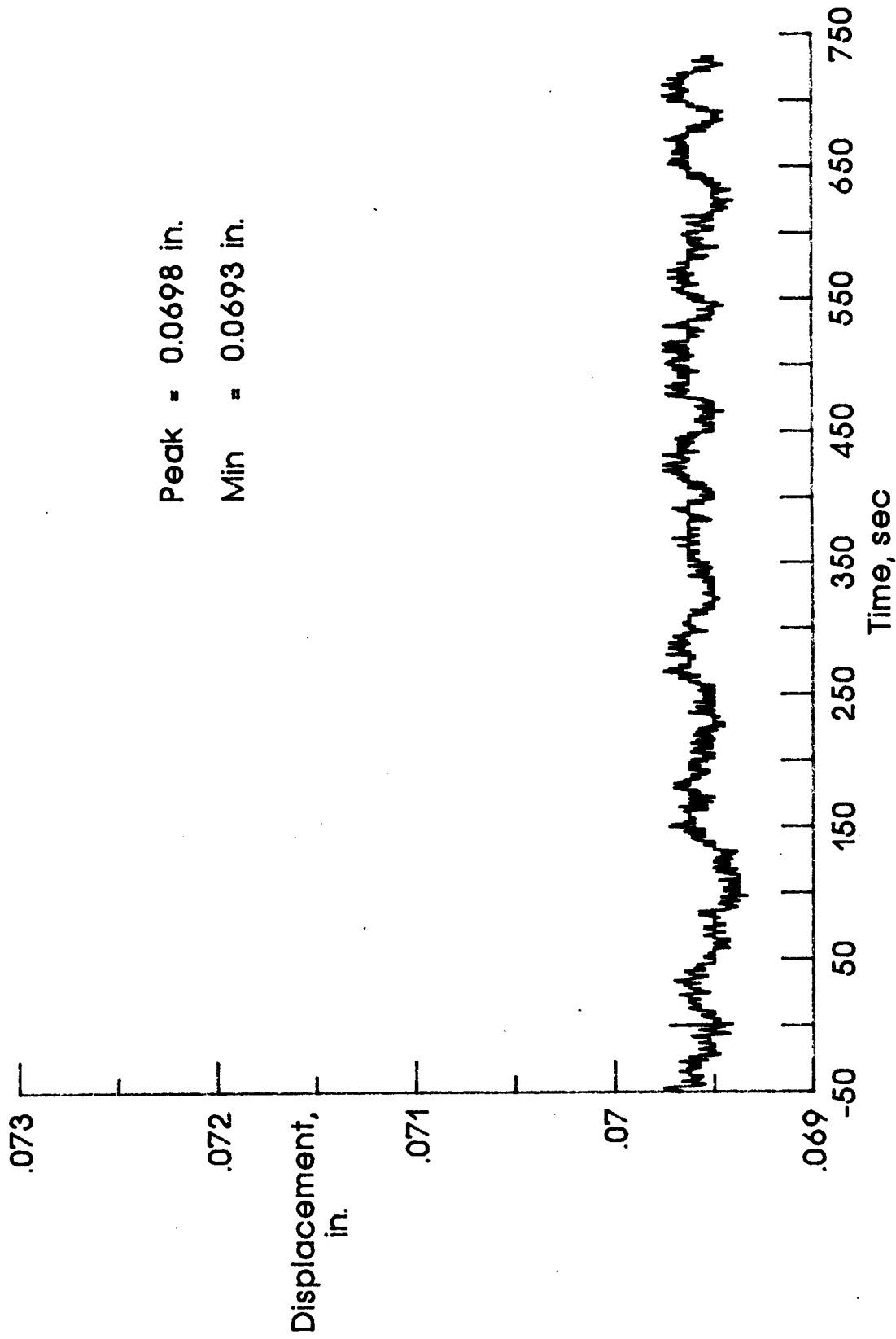
Figure 23d. 250 psi applied to the primary chamber.

MIN3-11, Disp

92
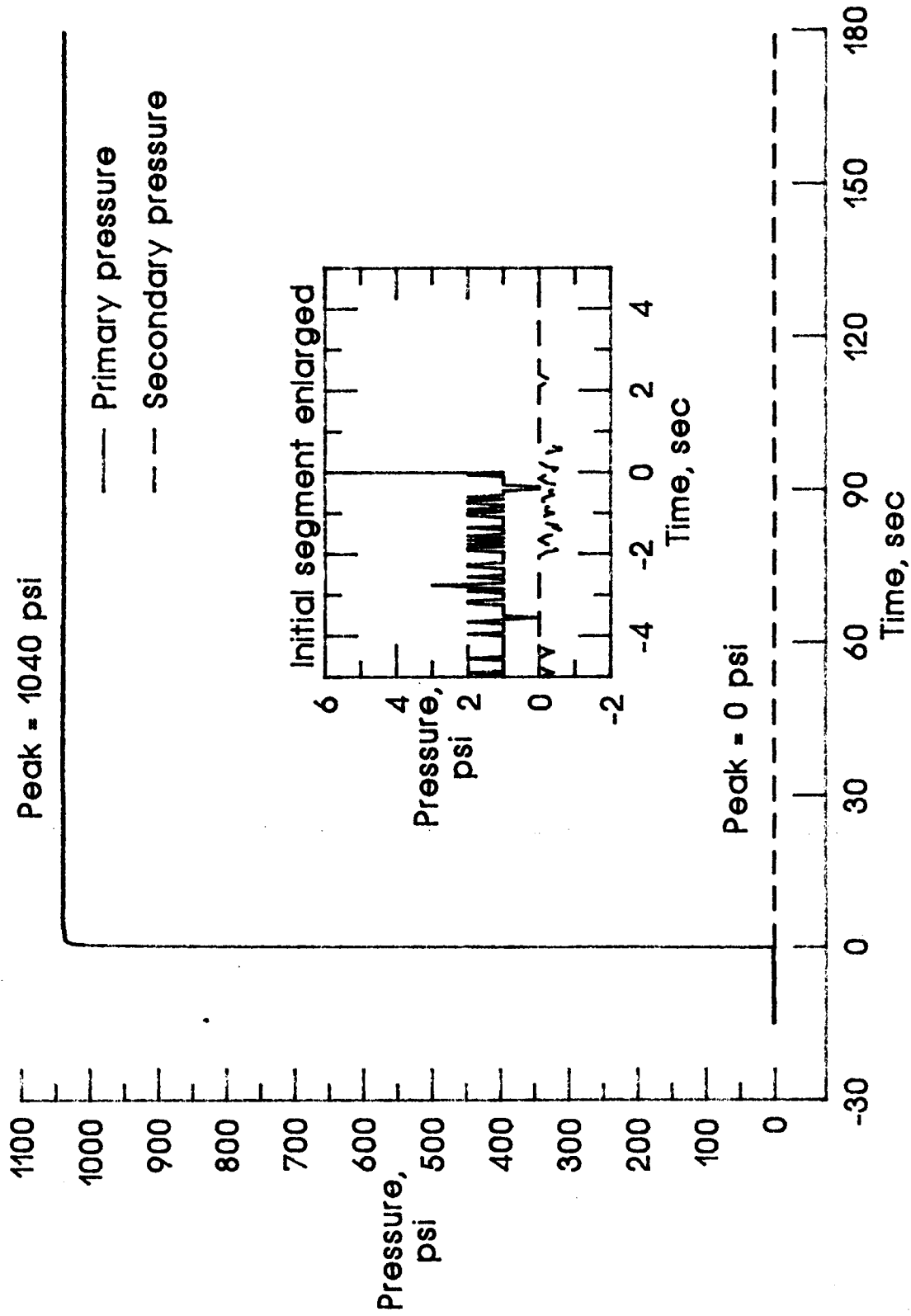
Figure 23e. 1015 psi applied to the primary chamber.

93

MIN3-12,P/P

Peak = 0.0719 in.

Min = 0.0695 in.

Displacement, in.

Time, sec
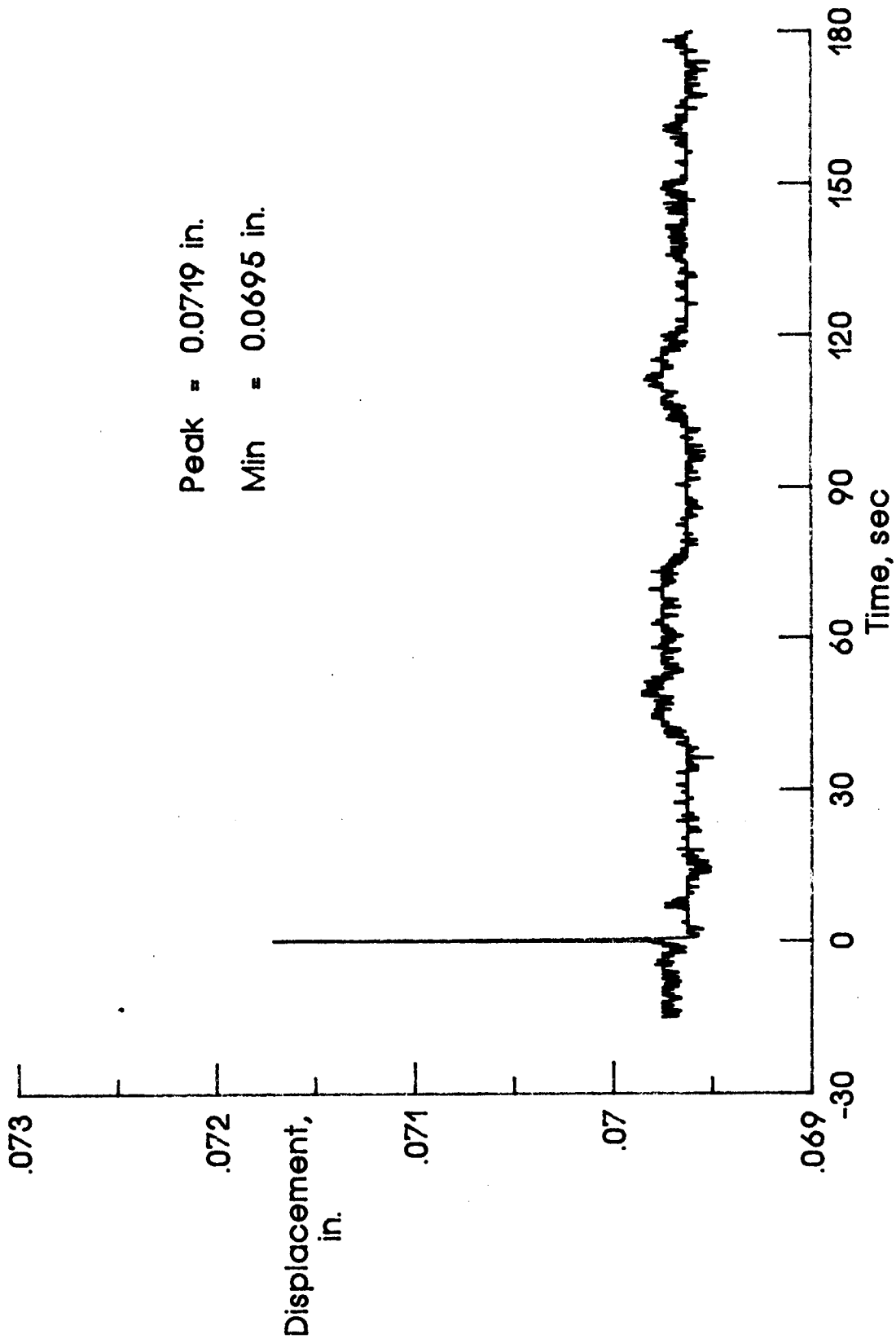
Figure 23f. 1015 psi applied to the primary chamber.

MIN3-12,Disp

94
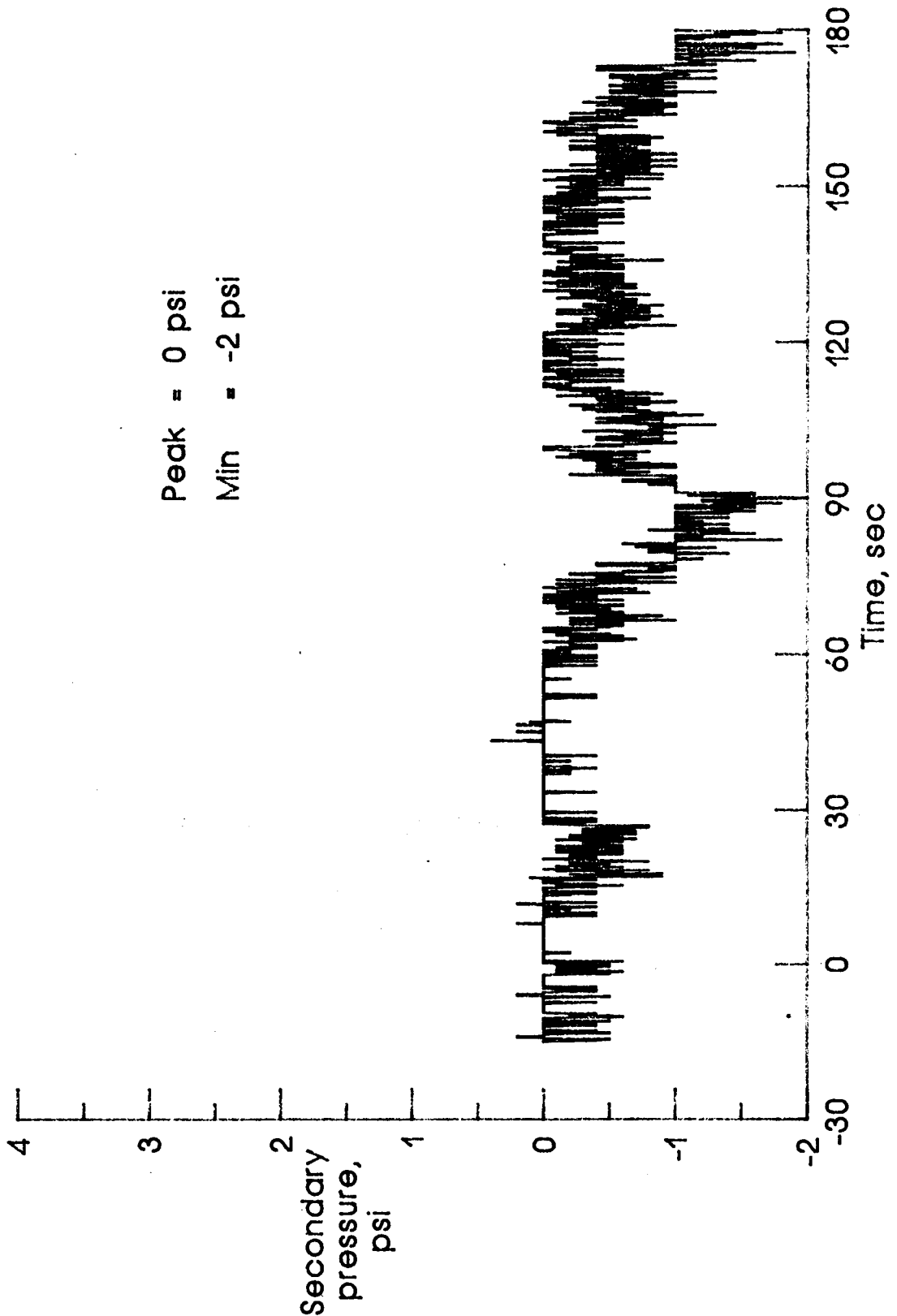
Figure 23g. 1015 psi applied to the primary chamber.

Peak = 0 psi

Min = -2 psi

MIN3-12,SecPr

95
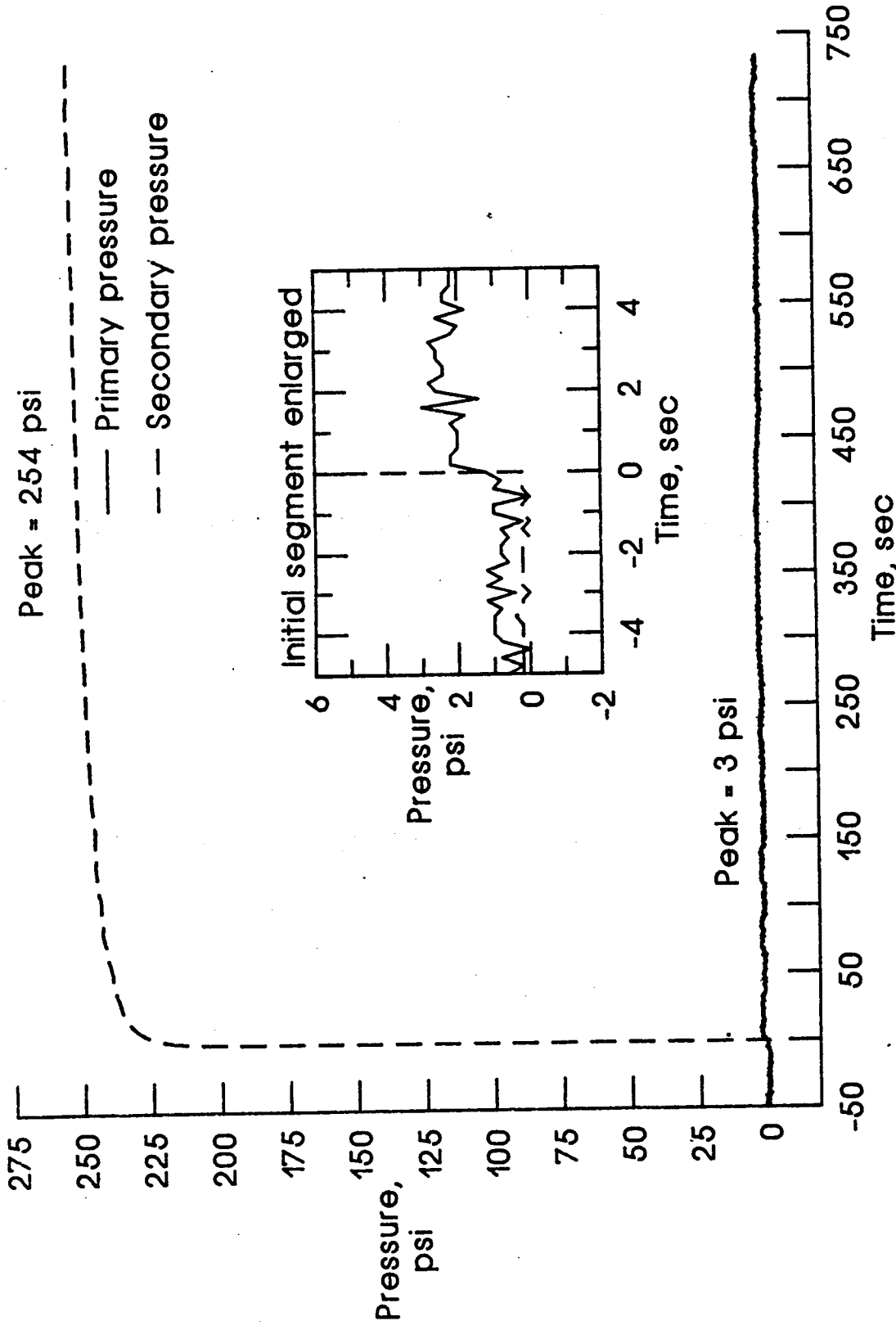
Figure 24a. 250 psi applied to the secondary chamber.

Figure 24. Pressure and displacement curves for the leak check and seal test for a successful seal at an initial squeeze of 0%.

MIN2-4, P/P

96
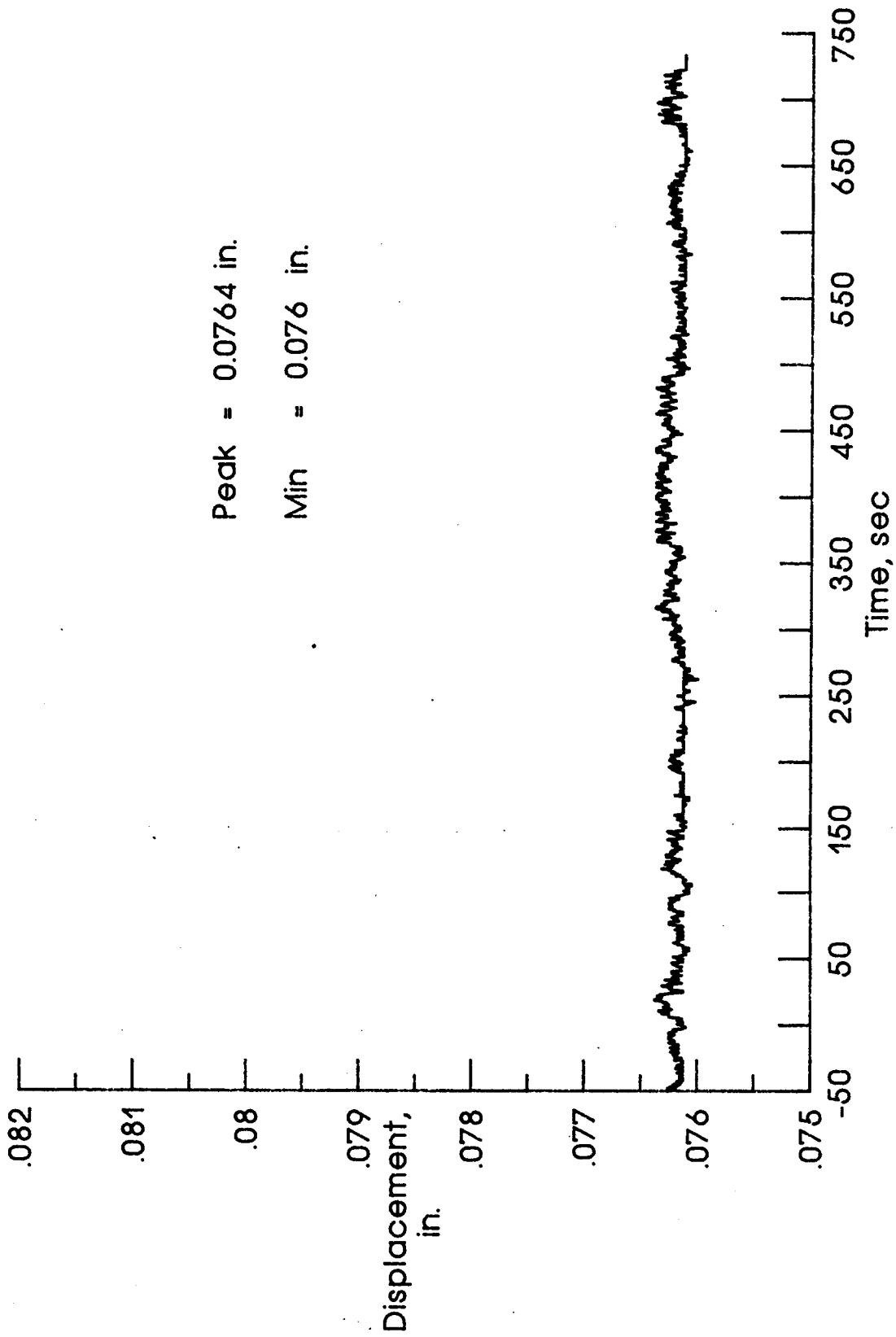
Figure 24b. 250 psi applied to the secondary chamber.

97

MIN2-4, Disp
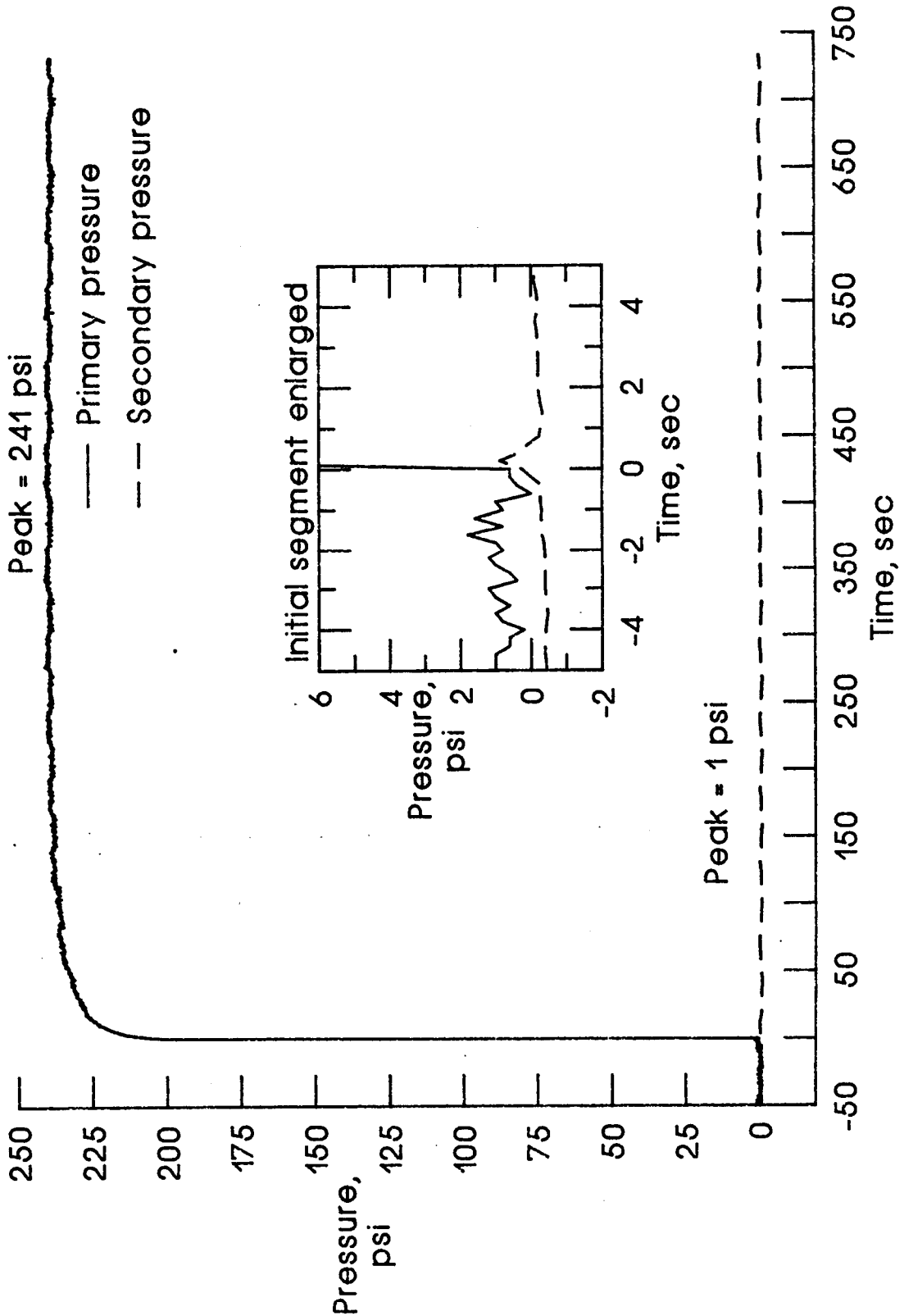
Figure 24c.   250 psi applied to the primary chamber.

MIN2-5,P/P

C-2
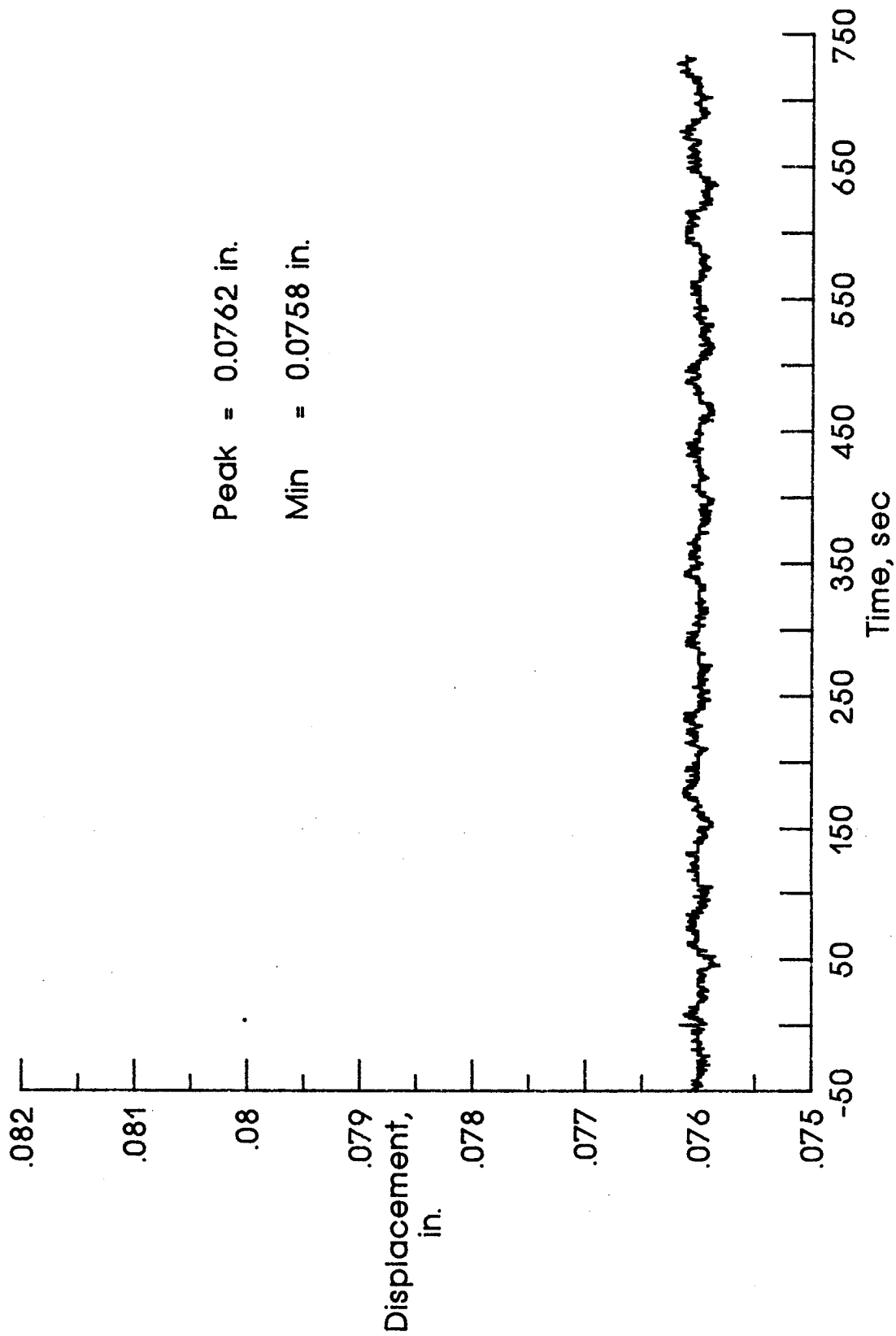
Figure 24d. 250 psi applied to the primary chamber.

MIN2-5, Disp

99
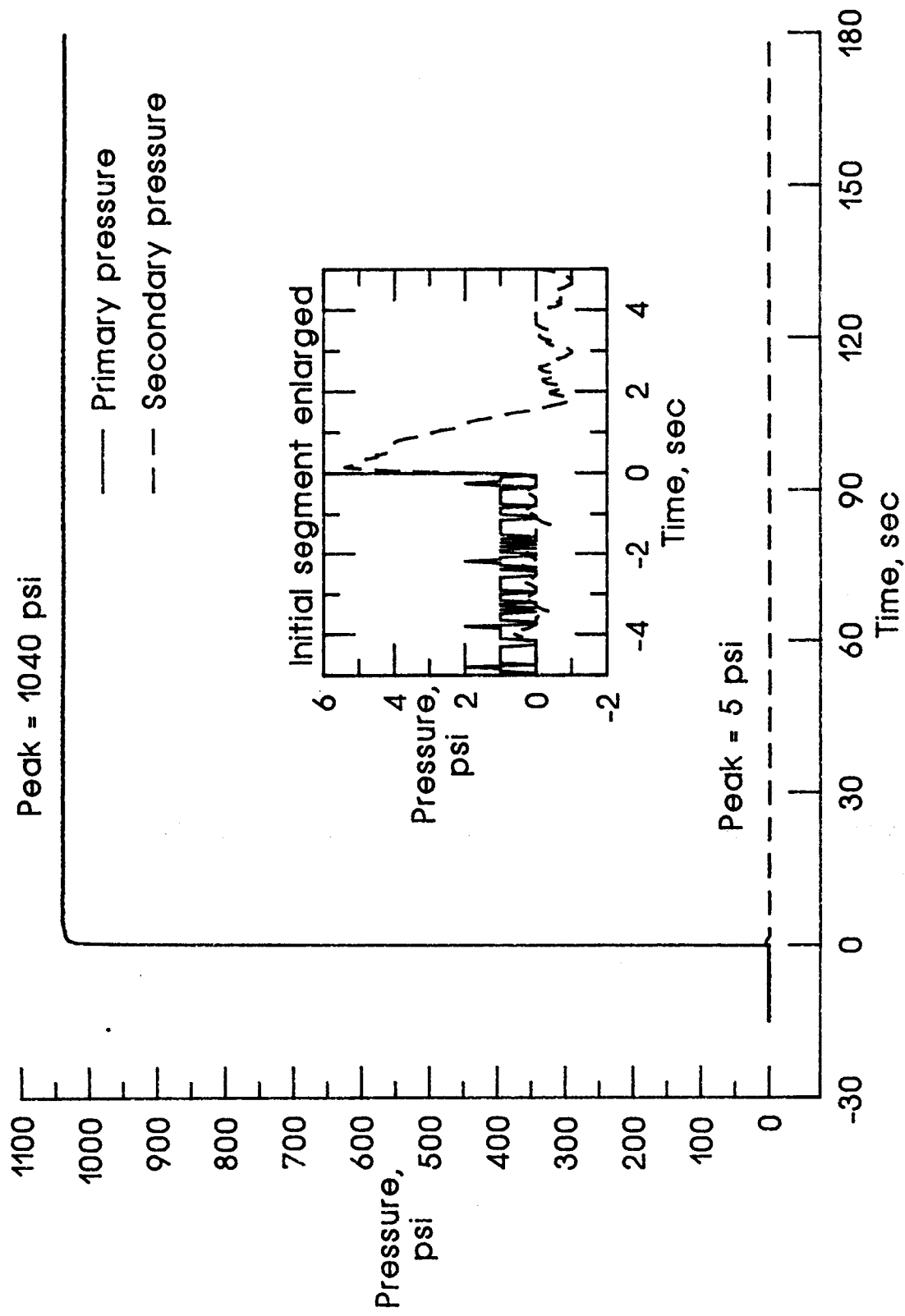
Figure 24e. 1015 psi applied to the primary chamber.

MIN2-6,P/P

100
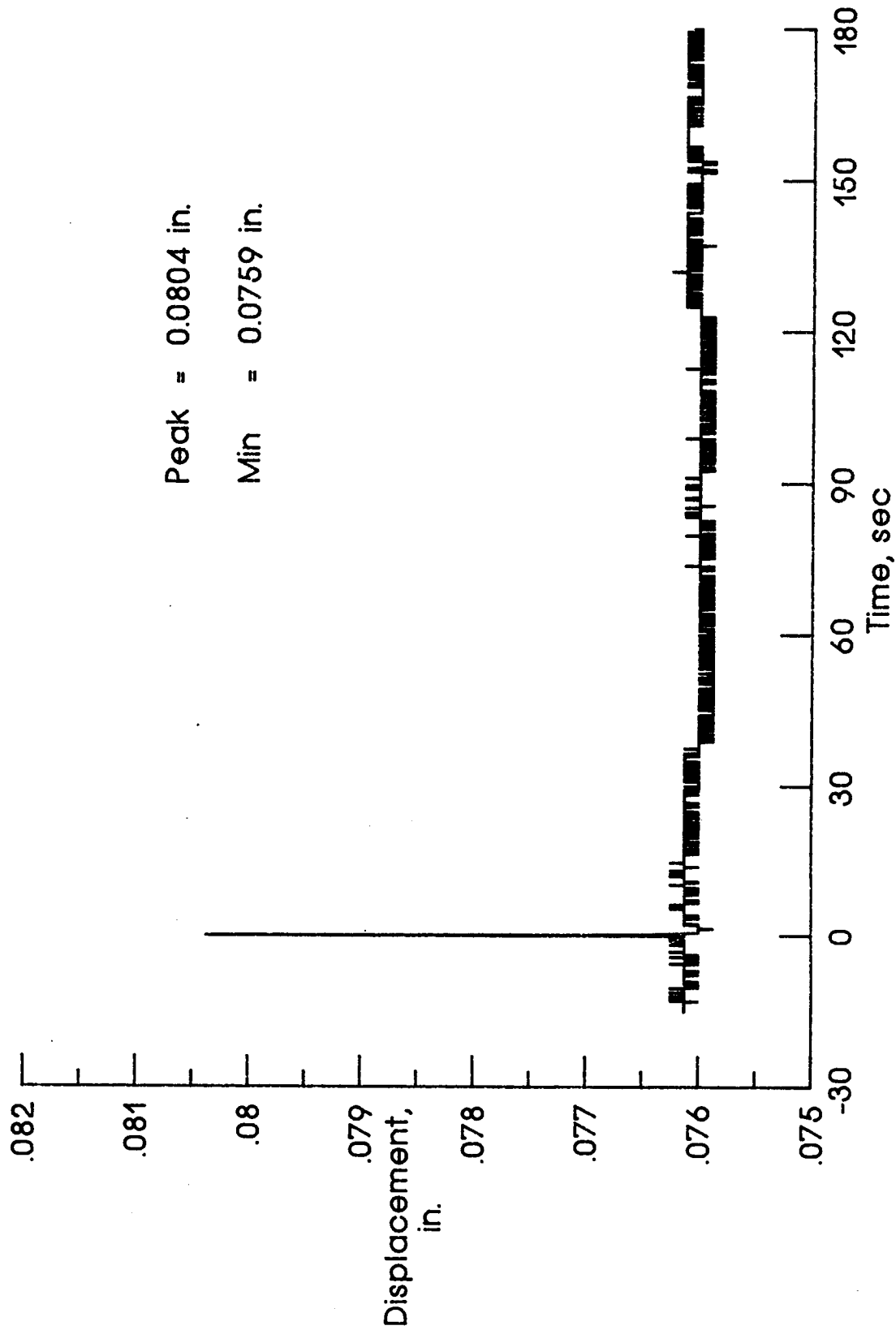
Figure 24f. 1015 psi applied to the primary chamber.

Peak = 0.0804 in.

Min = 0.0759 in.

MIN2-6,Disp

101

Figure 24g. 1015 psi applied to the primary chamber.

MIN2-6,SecPr
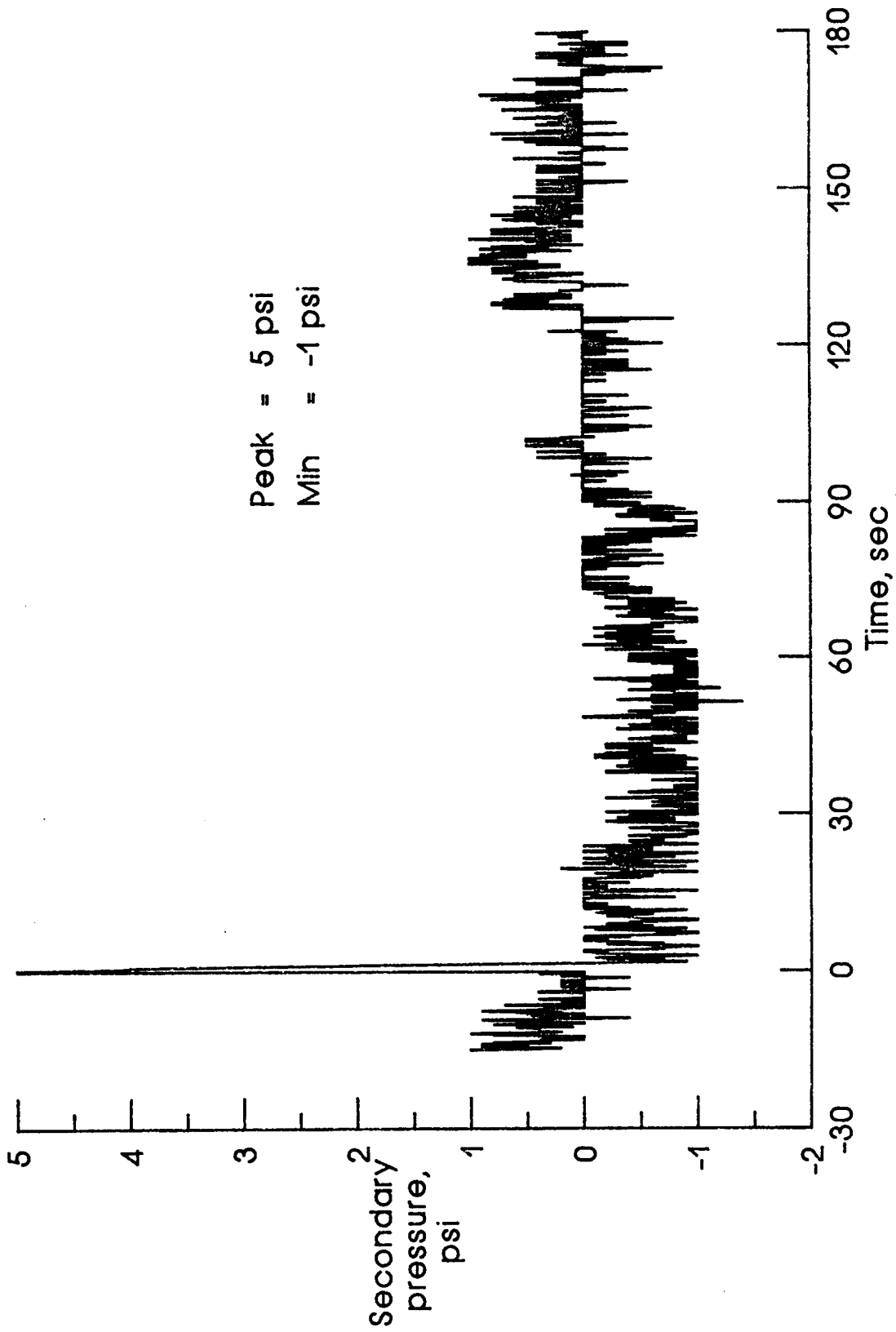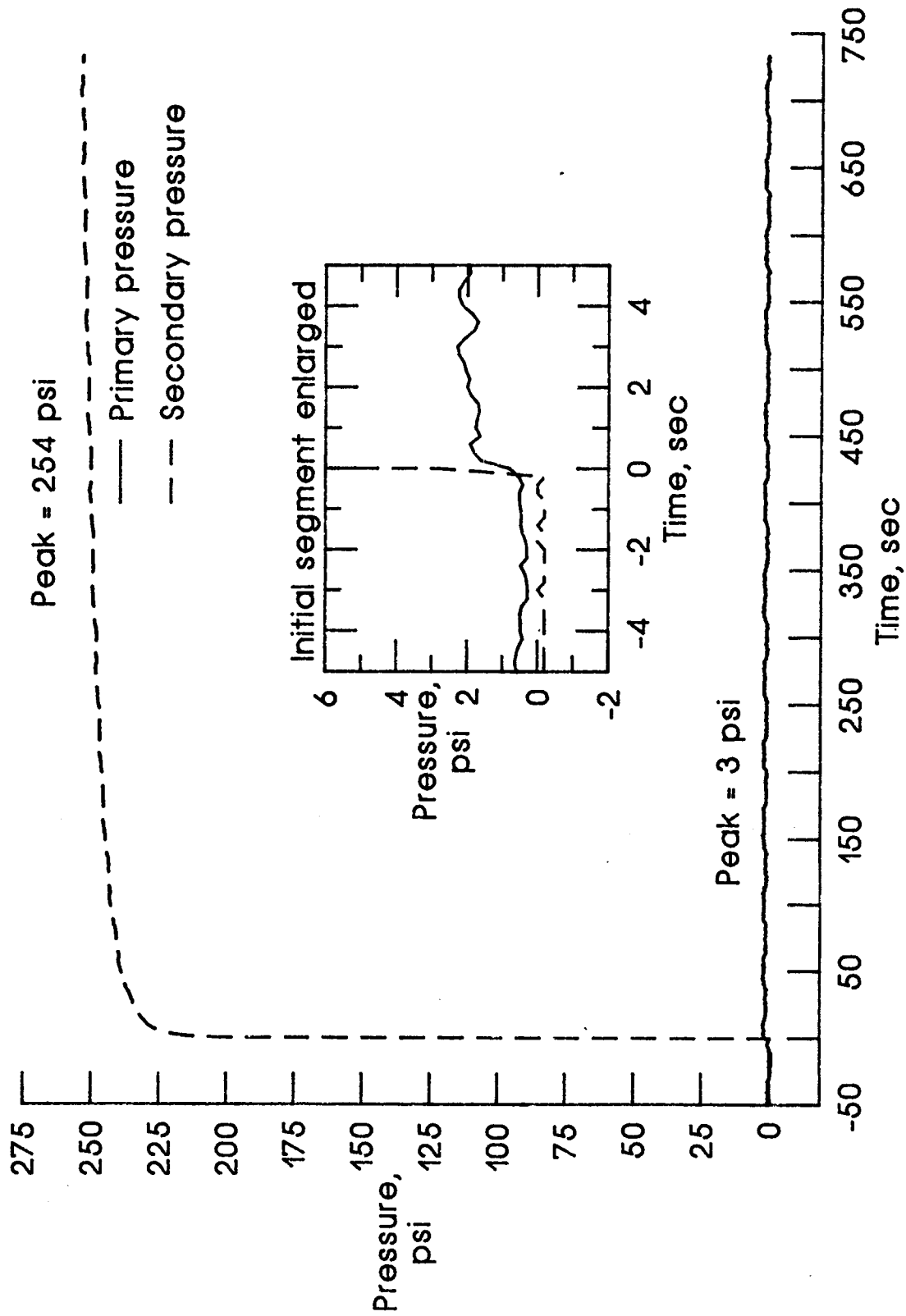
Figure 25a. 250 psi applied to the secondary chamber.

Figure 25. Pressure and displacement curves for the leak check and seal test for a delayed seal at an initial squeeze of 0%.

MIN3-16,P/P

103
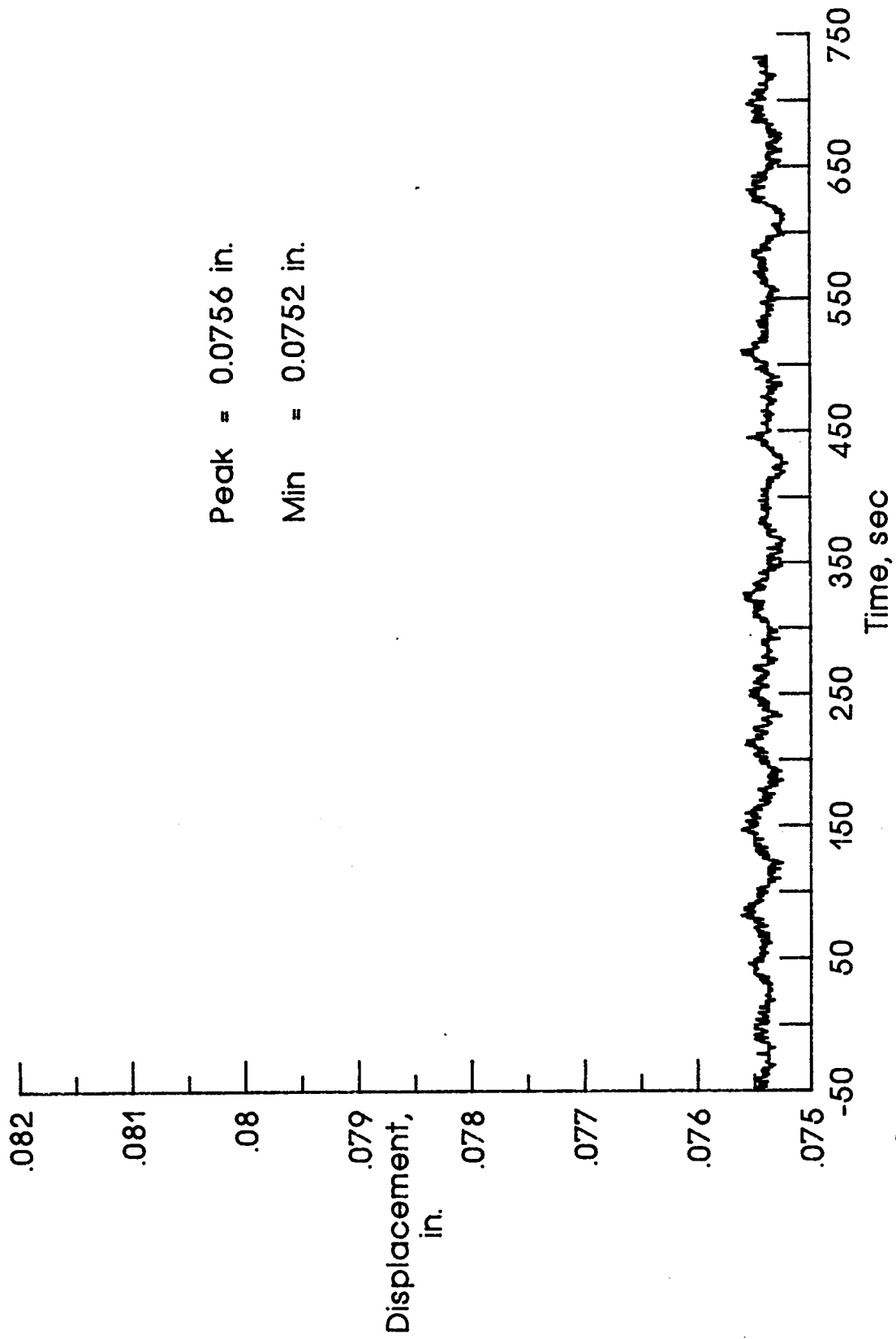
Figure 25b. 250 psi applied to the secondary chamber.

MIN3-16,Disp

104
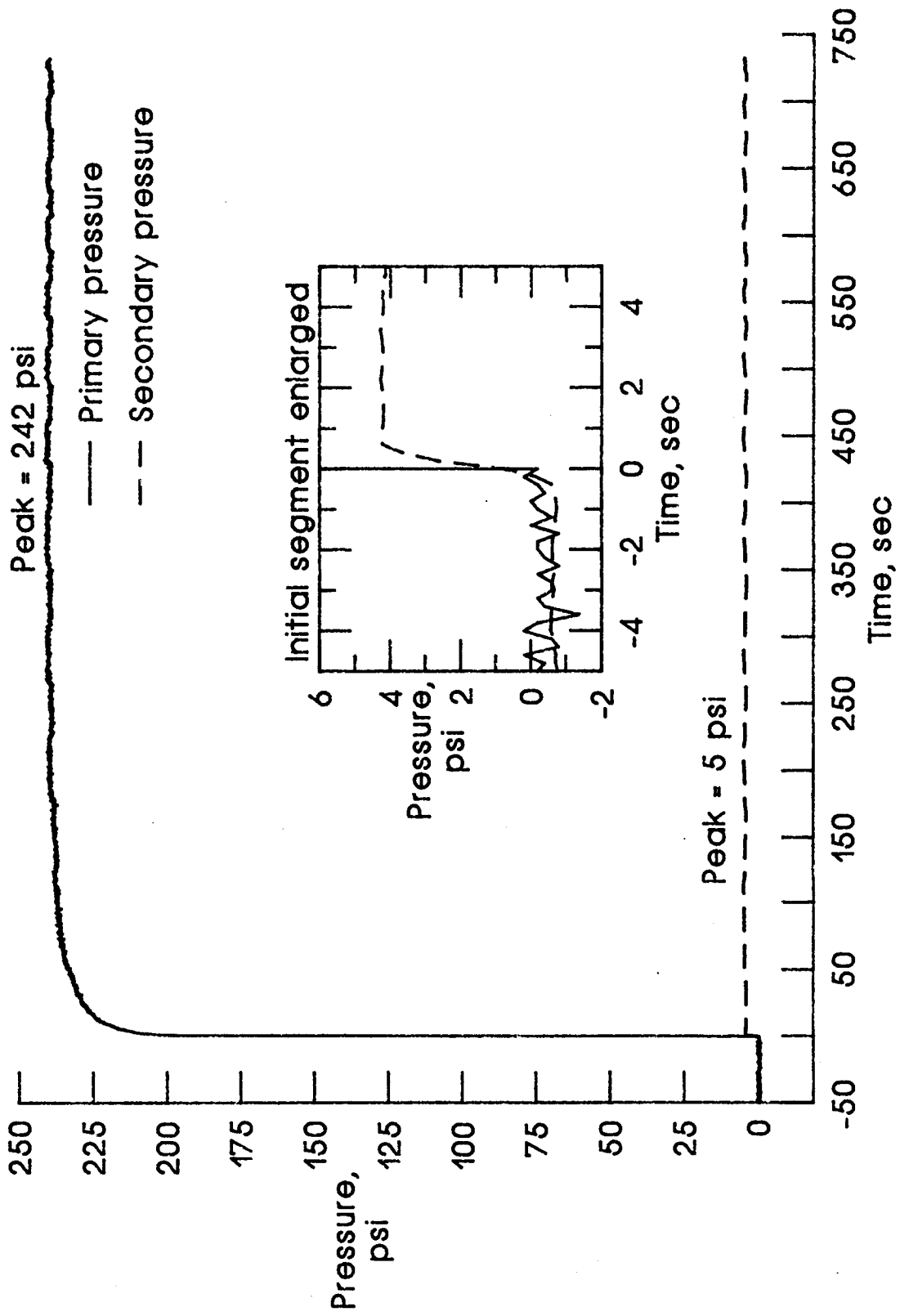
Figure 25c. 250 psi applied to the primary chamber.

MIN3-17,P/P
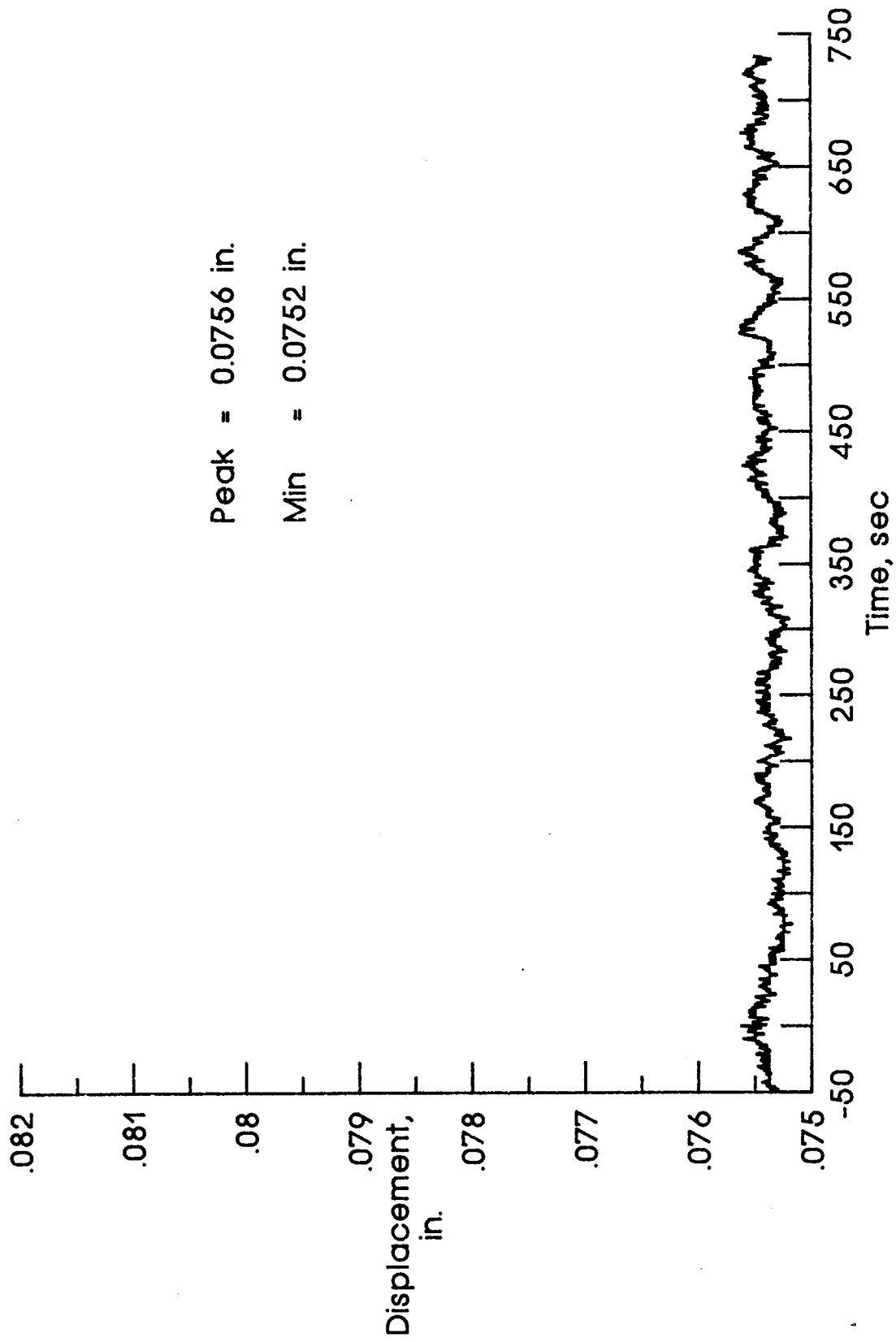
Figure 25d. 250 psi applied to the primary chamber.

Peak = 0.0756 in.

Min = 0.0752 in.

MIN3-17, Disp

106
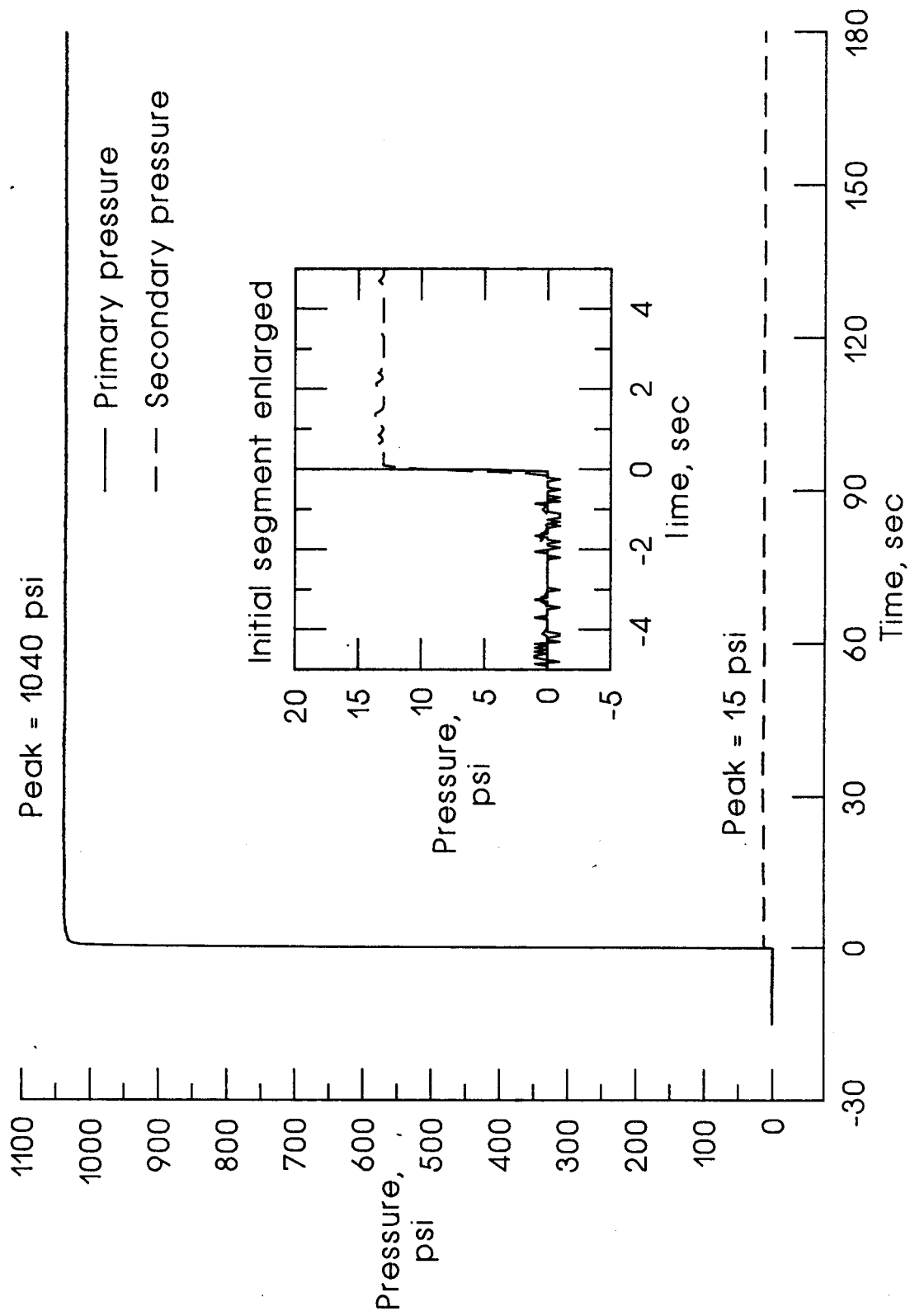
Figure 25e. 1015 psi applied to the primary chamber.

107

MIN3-18,P/P

Peak = 0.0776 in.

Min = 0.0750 in.
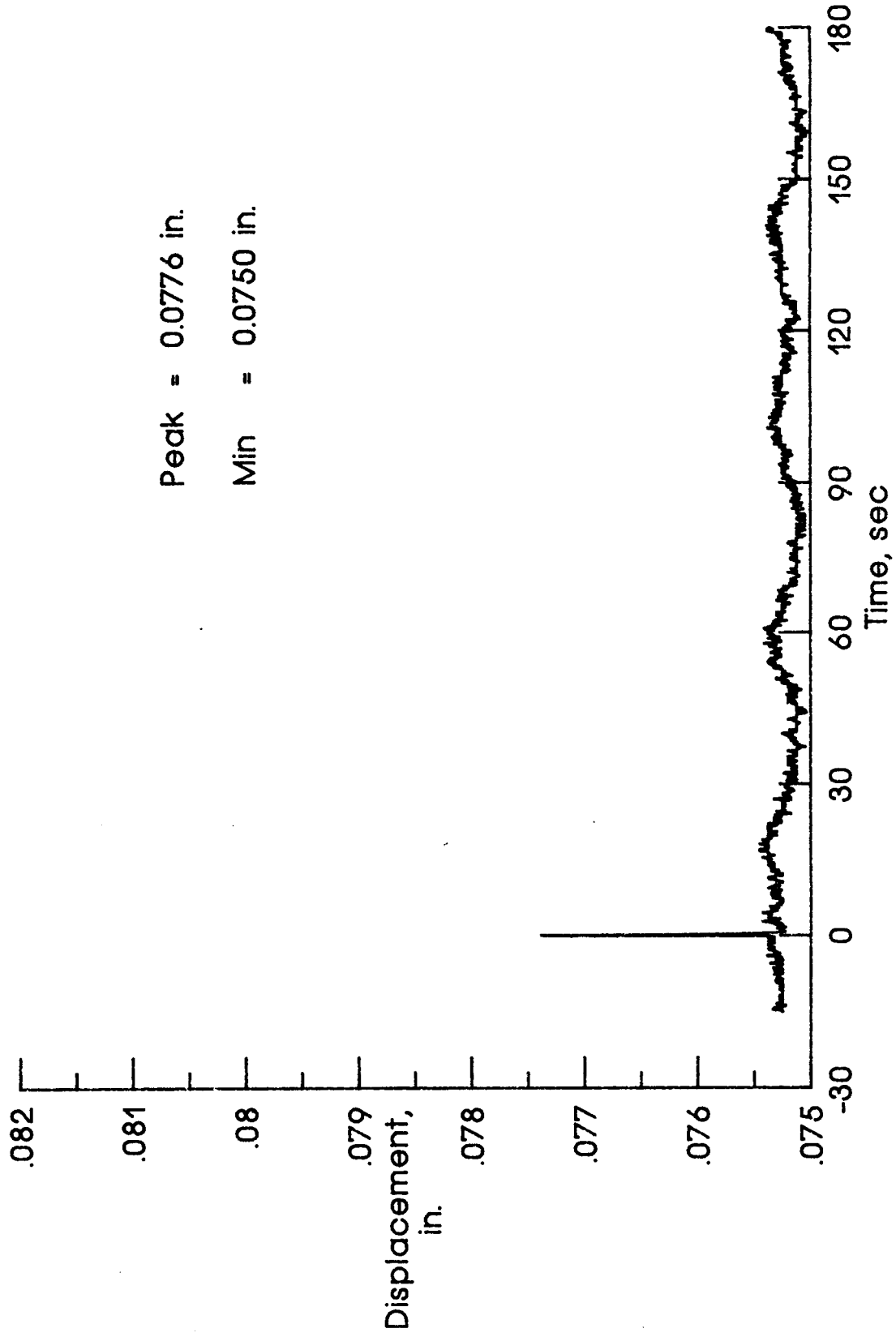
Figure 25f. 1015 psi applied to the primary chamber.

108

MIN3-18,Disp
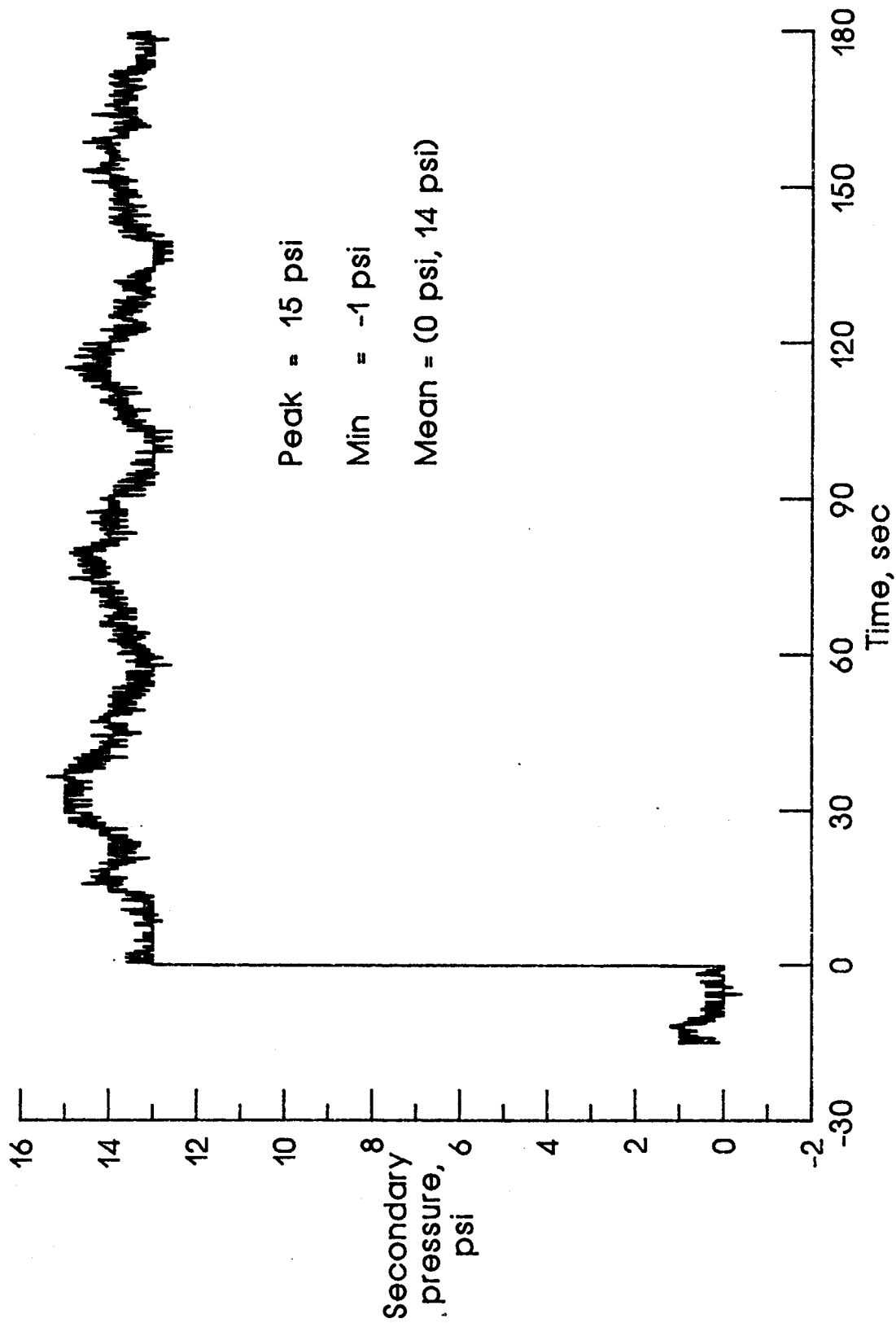
Figure 25y. 1015 psi applied to the primary chamber.

MIN3-18,SecPr

109
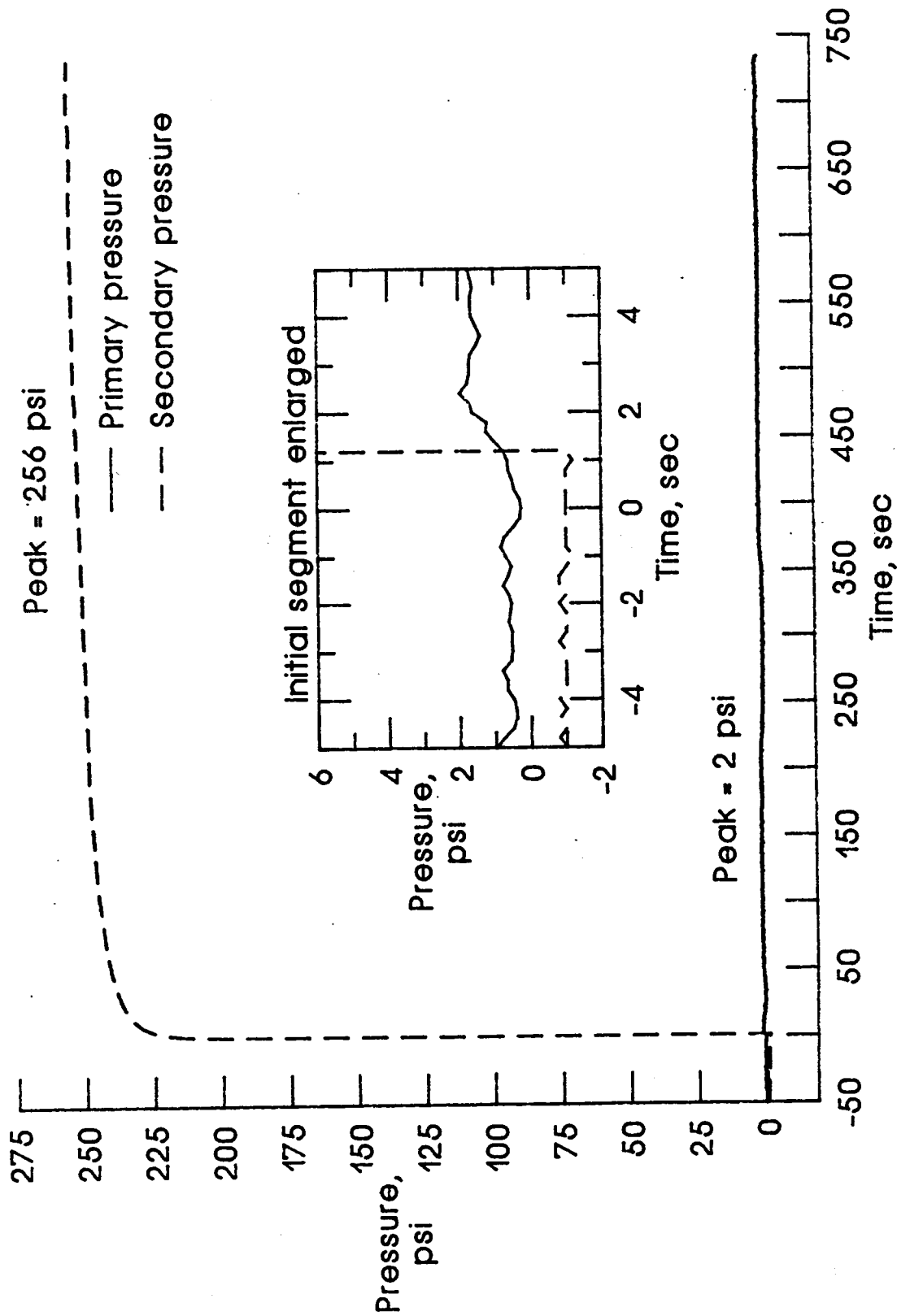
Figure 26a. 250 psi applied to the secondary chamber.

Figure 26. Pressure and displacement curves for the leak check and seal test for a delayed seal at an initial squeeze of 0%.

MIN5-10, P/P

Peak = 0.0773 in.

Min = 0.0768 in.
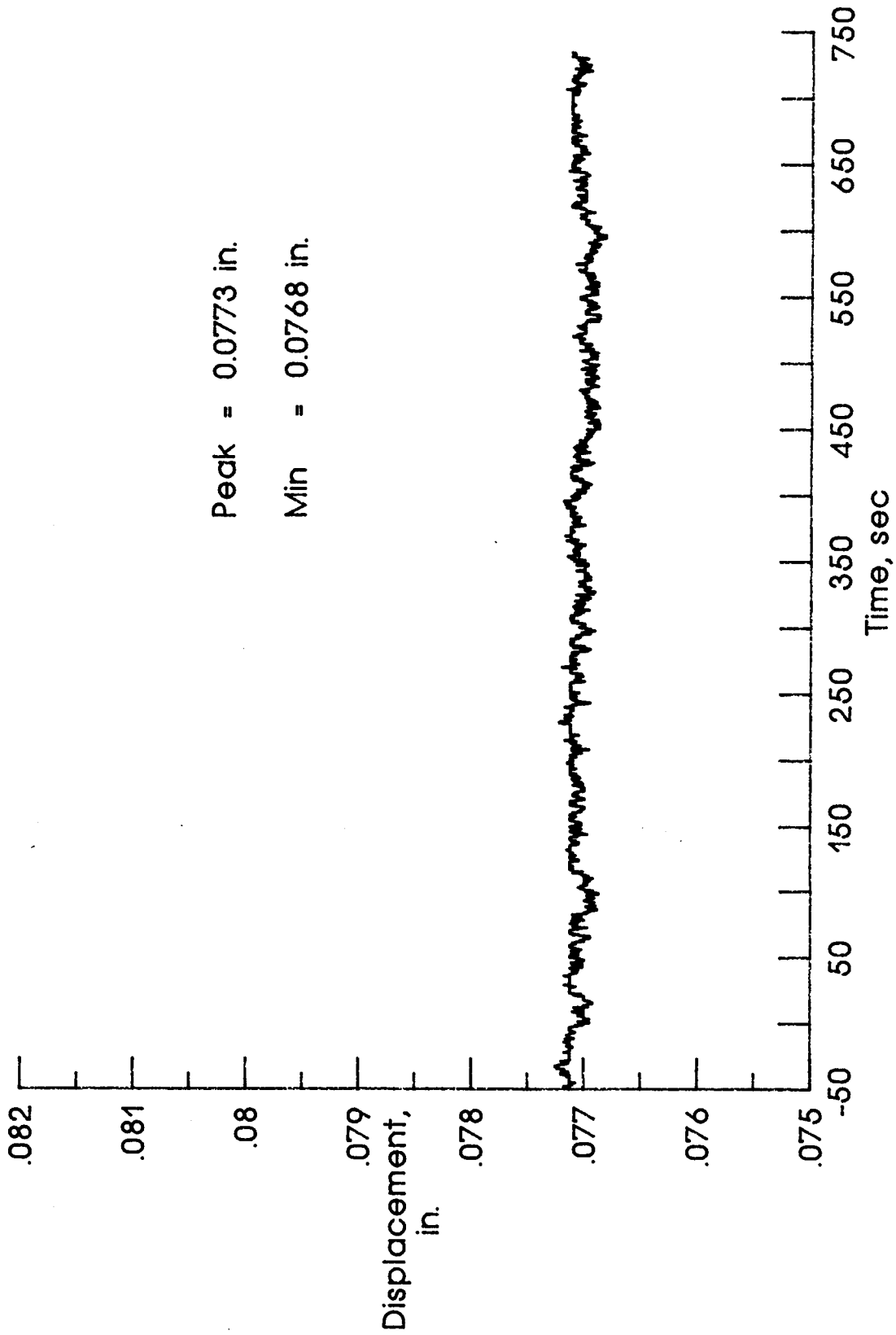
Figure 26b. 250 psi applied to the secondary chamber.

111

MIN5-10, Disp
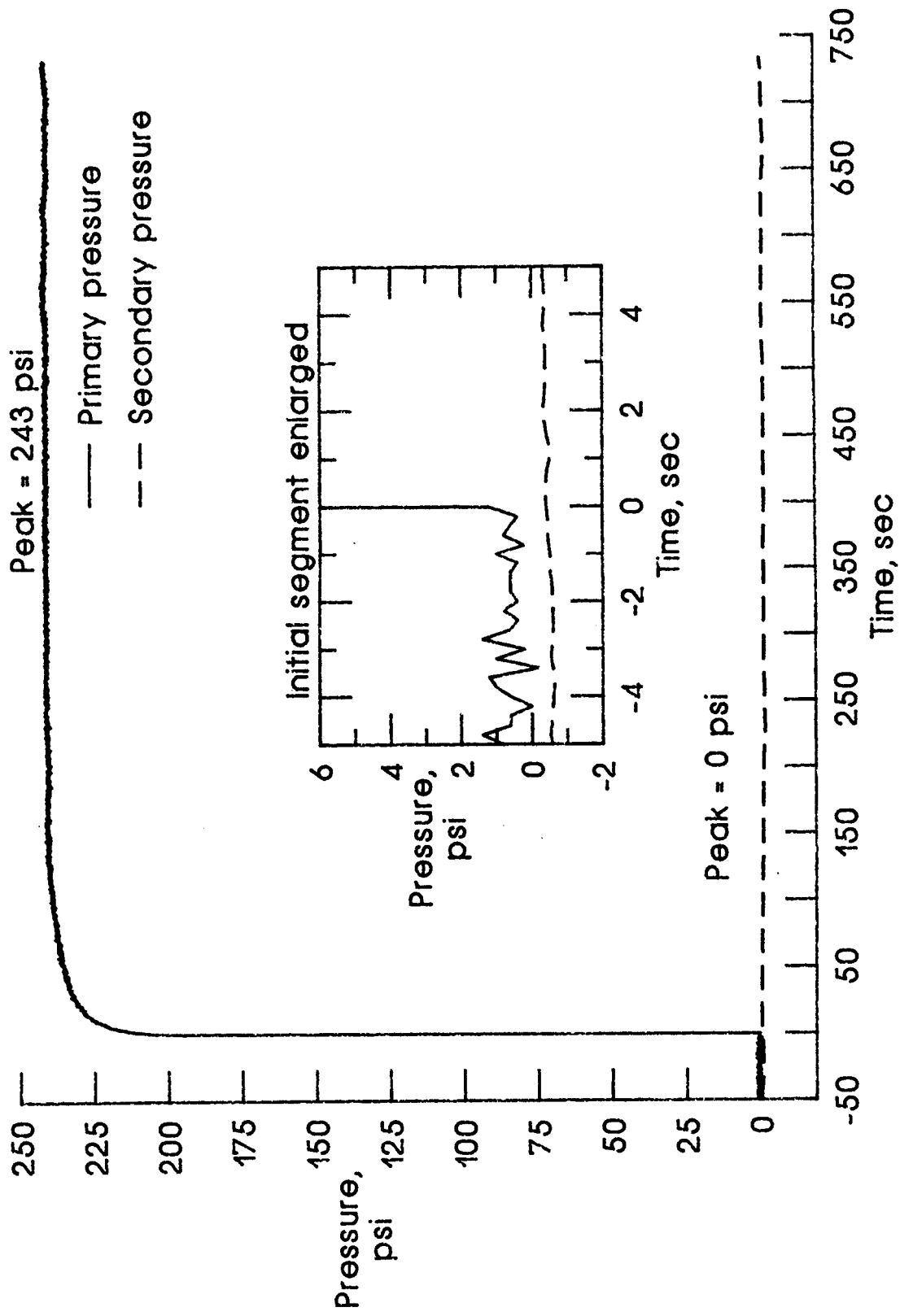
Figure 26c. 250 psi applied to the primary chamber.

112

MIN5-11,P/P

Peak = 0.0772 in.

Min = 0.0768 in.
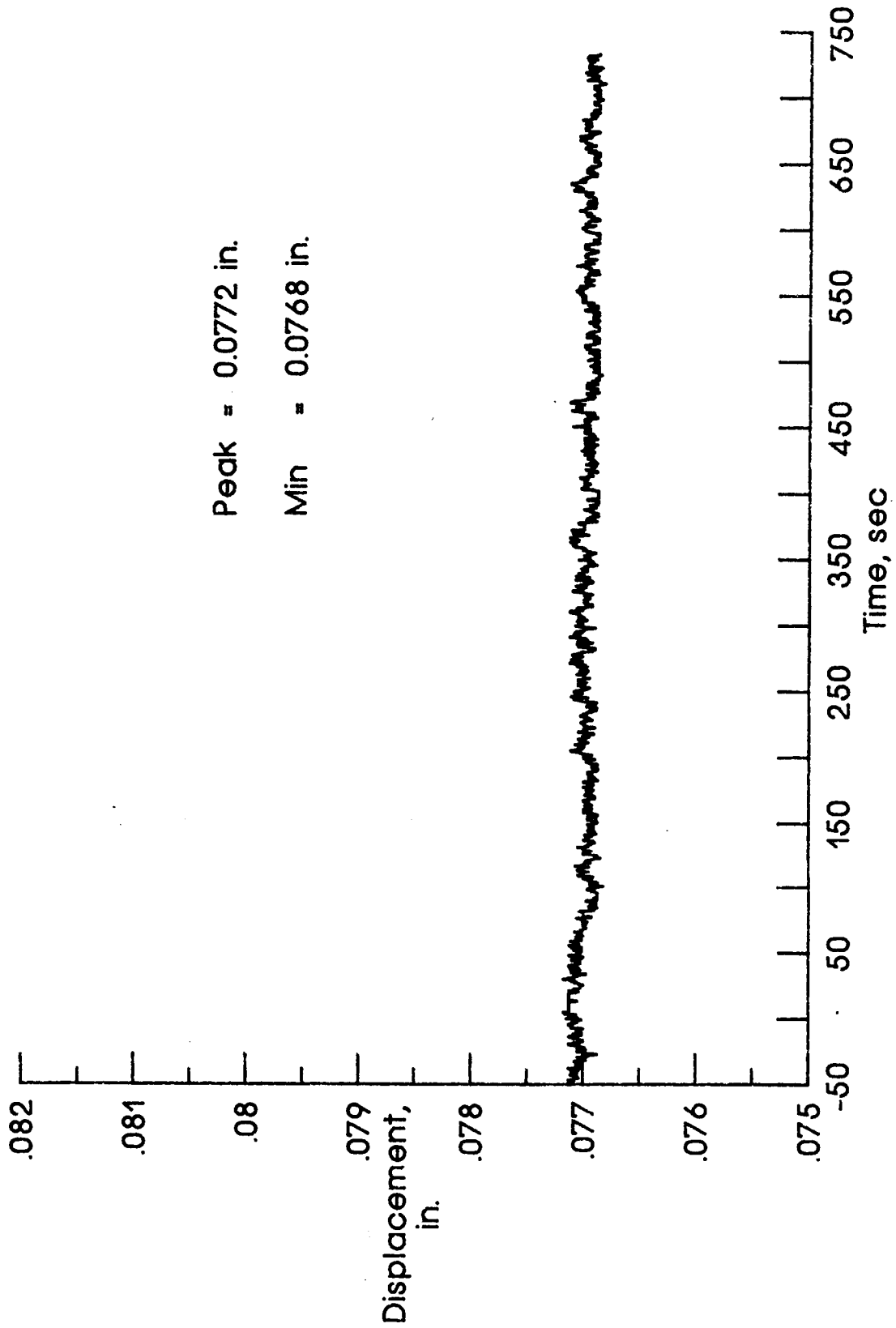
Figure 26d.   250 psi applied to the primary chamber.

113

MIN5-11, Disp
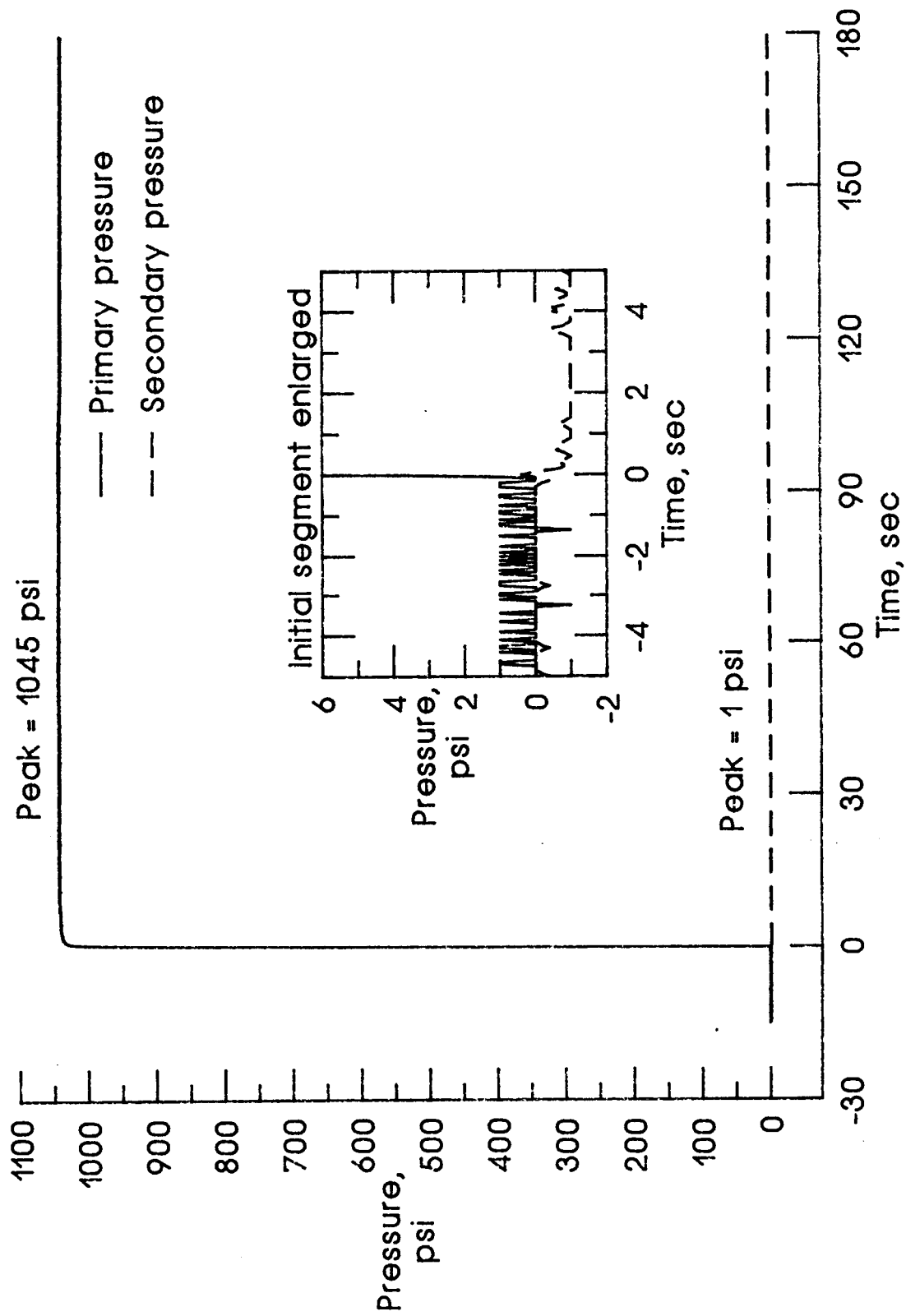
Figure 26e.   1015 psi applied to the primary chamber.

MIN5-12,P/P
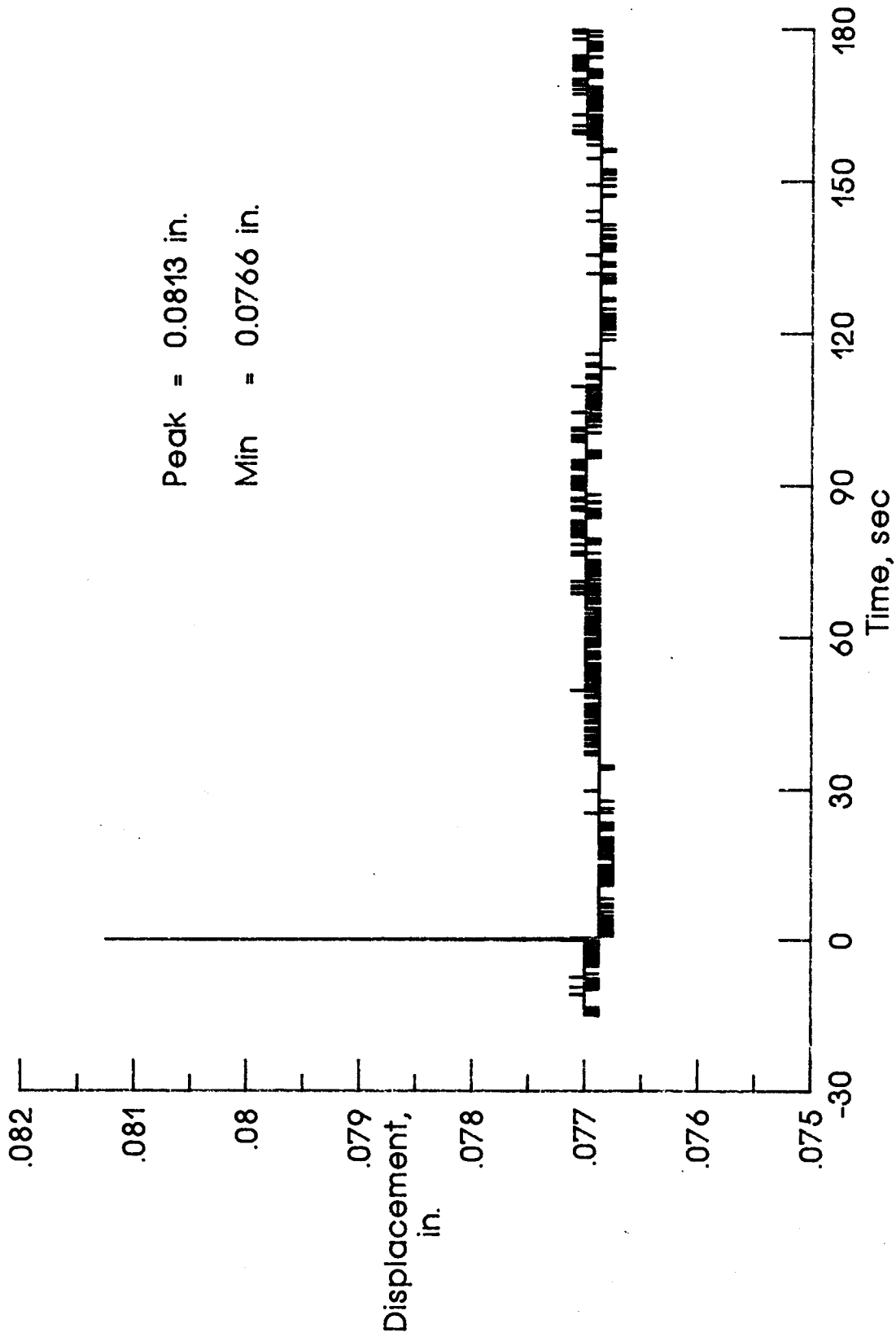
Figure 26f. 1015 psi applied to the primary chamber.

115

Figure 26q. 1015 psi applied to the primary chamber.

Peak = 1 psi

Min = -2 psi

Secondary pressure, psi

Time, sec

116
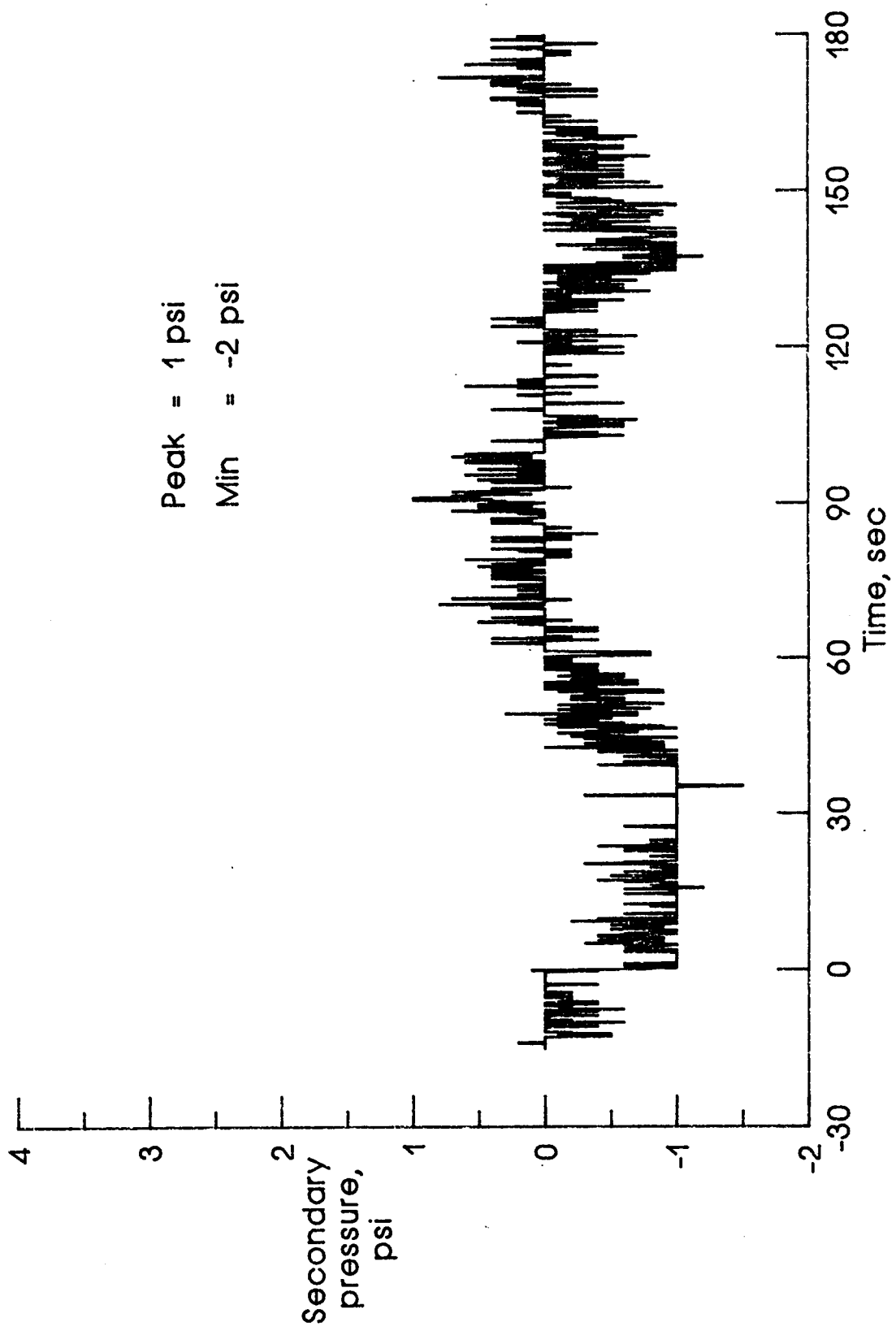
MIN5-12,SecPr

Report Documentation Page

1. Report No. NASA TM-101591	2. Government Accession No.	3. Recipient's Catalog No.
4. Title and Subtitle O-RING SEALING VERIFICATION FOR THE SPACE SHUTTLE REDESIGN SOLID ROCKET MOTOR		5. Report Date May 1989
		6. Performing Organization Code
7. Author(s) Cynthia L. Lach		8. Performing Organization Report No.
		10. Work Unit No. 505-63-01-05
9. Performing Organization Name and Address NASA Langley Research Center Hampton, VA 23665-5225		11. Contract or Grant No.
		13. Type of Report and Period Covered Technical Memorandum
12. Sponsoring Agency Name and Address National Aeronautics and Space Administration Washington, DC 20546-0001		14. Sponsoring Agency Code

15. Supplementary Notes

16. Abstract

As a part of the redesign of the Space Shuttle Solid Rocket Motor, the field and nozzle-to-case joints were redesigned to minimize the dynamic flexure caused by internal motor pressurization during ignition. The O-ring seals and glands for the joints were designed to accommodate both structural deflections and to promote pressure assistance. A test program was conducted to determine if a fluorocarbon elastomeric O-ring (V747-75) could meet this criteria in the redesigned gland. Resiliency tests were used to investigate the O-ring response to gap motion while static seal tests were used to verify design criteria of pressure assistance for sealing. All tests were conducted in face seal fixtures mounted in servo-hydraulic test machines.

The resiliency of the O-ring was found to b e extremely sensitive to the effects of temperature. The External Tank/Solid Rocket Booster attach strut loads had a negligible affect on the ability of the O-ring to track the simulated SRB field joint deflection. In the static pressure-assisted seal tests, as long as physical contact was maintained between the O-ring and the gland sealing surface, pressure assistance induced instantaneous sealing.

17. Key Words (Suggested by Author(s)) O-Ring Resiliency Solid Rocket Booster Redesign Viton Clevis-Tang Joint Face Seal Elastomer	18. Distribution Statement Unclassified - Unlimited Subject Category - 39

19. Security Classif. (of this report) Unclassified	20. Security Classif. (of this page) Unclassified	21. No. of pages 117	22. Price A06